Title
Designing a Scalable and Affordable Fluoride Removal (SAFR) Process for Groundwater Remediation in India

Author
Cherukumilli, Aruna Kirani Katyayani

Publication Date
2017

Peer reviewed|Thesis/dissertation

Designing a Scalable and Affordable Fluoride Removal (SAFR) Process for Groundwater Remediation in India

By
Aruna Kirani Katyayani Cherukumilli

A dissertation submitted in partial satisfaction of the
requirements for the degree of
Doctor of Philosophy
in
Engineering – Civil and Environmental Engineering
and the Designated Emphasis
in
Development Engineering
in the
Graduate Division
of the
University of California, Berkeley

Committee in charge:

Professor Ashok Gadgil, Chair
Professor David Sedlak
Professor Laura Lammers

Summer 2017

Abstract

Designing a Scalable and Affordable Fluoride Removal
(SAFR) Process for Groundwater Remediation in India

by

Aruna Kirani Katyayani Cherukumilli

Doctor of Philosophy in Civil and Environmental Engineering
and the Designated Emphasis in Development Engineering
University of California, Berkeley
Professor Ashok Gadgil, Chair

Globally, 200 million people are at risk of adverse health effects from drinking groundwater contaminated with geogenic fluoride concentrations exceeding the World Health Organization's maximum contaminant limit (WHO-MCL = 1.5 mg F^-/L). Although many defluoridation technologies have been demonstrated to work in lab, most have proven inappropriate for developing countries because they are cost-prohibitive, require skilled labor, or are difficult to scale. Activated alumina (AA) column filters are widely used by the upper middle class but production of AA remains costly in terms of money, energy, and greenhouse gas emissions. Eliminating these energy-intensive steps in refining bauxite, a ubiquitous aluminum-rich ore ($30/tonne), to AA ($1500/tonne), has the potential to reduce the annual per-capita material cost of treated water significantly.

The purpose of this dissertation is to ascertain the use of bauxite as a potentially inexpensive defluoridation technology through experimental studies characterizing globally diverse bauxite ores and tradeoffs associated with mild processing steps to enhance fluoride removal performance. Chapter 1 presents an overview of fluoride as a geogenic groundwater contaminant worldwide and in India, the health effects of excess fluoride consumption, and existing treatment technologies. **Chapter 2** establishes proof of concept that mildly processed bauxite can effectively remediate field-relevant fluoride concentrations to below the WHO-MCL in synthetic and real groundwater matrices at comparable kinetics and significantly lower cost than AA. This chapter also characterizes intrinsic features of globally diverse bauxite ores (from Guinea, Ghana, USA, and India) to identify factors predicting bauxite's performance. **Chapter 3** utilizes insights on underlying molecular mechanisms and proposes thermal activation and groundwater pH adjustment as two processing methods to optimize the fluoride removal performance of bauxite. **Chapter 4** discusses some remaining practical challenges and unknowns for implementing our scalable and affordable fluoride removal (SAFR) process in the field. **Chapter 5** concludes this dissertation by discussing the implications of the research findings and by suggesting additional future studies needed before field implementation of the proposed SAFR groundwater treatment technology.

To children like Rajitha and Sachita,
who deserve to have access to
clean drinking water
as a fundamental human right
for health, dignity, and prosperity.

Table of Contents

Chapter 1. Introduction…….… 1

1.1. Groundwater Fluoride Contamination: An Overview

1.1.1. Global Distribution of Geogenic Fluoride

1.1.2. Impacts of Excess Fluoride Intake on Health

1.1.3. Indian Context: Nalgonda District, Telangana

1.2. Existing Defluoridation Technologies

1.2.1. Overview

1.2.2. Membrane-Based Solutions

1.2.3. Precipitation Methods

1.2.4. Adsorbents

1.3. Outline of Remaining Chapters

Chapter 2. Factors Governing the Performance of Bauxite for Fluoride Remediation of Groundwater……...…….. 15

2.1. Background

2.2. Methods

2.2.1. Adsorbents Preparation and Characterization

2.2.2. Preparation of Synthetic Groundwater

2.2.3. Batch Adsorption Experiments

2.2.4. Calculating Minimum Required Dose

2.2.5. Adsorption Isotherms and Adsorption Envelopes

2.2.6. Investigation of Removal Mechanisms

2.2.7. Estimating Treatment Costs

2.3. Results and Discussion

2.3.1. Differences in Bauxite Ore Performance

2.3.2. Chemical Characterization of Bauxite Ores

2.3.3. Effect of Initial Fluoride Concentration and Solution pH on Fluoride Removal

2.3.4. Influence of Equilibrium pH on Fluoride Removal

2.3.5. Fluoride Adsorption Mechanism

2.3.6. Comparison between Activated Alumina and Guinea Bauxite

2.3.7. Implications for Groundwater Treatment

Chapter 3. Effective Groundwater Fluoride Remediation Using Inexpensively Processed Indian Bauxite……...…….. 32

3.1. Background

3.2. Methods

3.2.1. Indian Bauxite Preparation and Characterization

3.2.2. Batch Adsorption Experiments

3.2.3. Estimation of Combinatorial Treatment Costs
3.3. Results and Discussion
3.3.1. Characterization of Thermally Activated Bauxite
3.3.2. Effect of Thermal Activation of Bauxite on Fluoride Removal
3.3.3. Effect of Groundwater Acidification on Defluoridation and Leaching of Metals
3.3.4. Comparing Combinatorial Treatment Scenarios
3.3.5. Implications for Groundwater Treatment

Chapter 4. Remaining Practical Challenges and Unknowns……..45
4.1. Background
4.2. Methods
4.2.1. Testing Fluoride Removal With Coarser Bauxite Powders
4.2.2. Settling Experiments
4.2.3. Stokes Law Calculations
4.2.4. Desorption Experiments
4.3. Results and Discussion
4.3.1. Effect of Particle Size on Fluoride Removal
4.3.2. Effect of Particle Size on Settling
4.3.3. Application of Stokes Law
4.3.4. Fluoride Desorption During Settling

Chapter 5. Conclusion…….....55
5.1. Lab Studies: Fluoride Remediation Using Bauxite
5.1.1. Summary of Results
5.1.2. Future Work: Surface Complexation Modeling
5.1.3. Future Work: Spectroscopic Studies
5.1.4. Future Work: Variations in Bauxite Composition
5.2. Practical Considerations for Field Implementation
5.2.1. Summary of Results
5.2.2. Future Work: Field Reactor Design
5.2.3. Future Work: Resource Recovery and Detailed Cost Analysis
5.2.4. Future Work: Technology Adoption and User Behavior

REFERENCES……..…63

List of Tables

Table 1-1. Mineral sources of fluoride found in sedimentary and igneous rocks

Table 1-2. Health effects of fluoride consumption

Table 1-3. Limitations of existing defluoridation technologies

---

Table 2-1. Chemical composition of synthetic and real groundwater matrices used in Chapter 2

Table 2-2. Detailed summary of experimental conditions in Chapter 2

Table 2-3. Characterization of a suspension in equilibrium with bauxite ores in terms of pH, dissolved calcium, and dissolved inorganic carbon

Table 2-4. Calculation of equilibrium solution pH in open system with dissolution of calcium carbonate

---

Table 3-1. Chemical composition of synthetic Sri Lankan groundwater matrix used in Chapter 3

Table 3-2. Concentrations (in ppb) of metals of concern in product water of batch experiments in Figure 3-7

Table 3-3. Treatment costs (in $ per person per year) of combinatorial treatment scenarios

List of Figures

Figure 1-1: Probability of groundwater fluoride concentrations exceeding the WHO-MCL (1.5 mg F^-/L)

Figure 1-2: Photographs of dental and skeletal fluorosis patients in Nalgonda District, Telangana

Figure 1-3: Map of countries with reported endemic fluorosis resulting from reliance on fluoride contaminated groundwater

Figure 1-4: Map of countries with over 40% of the total population living in rural areas

Figure 1-5: Photograph of Reverse Osmosis (RO) plant at CSIR-IICT in Hyderabad, Telangana, India

Figure 1-6: Photograph of the National Environmental Engineering Research Institute's household filters in Chichkavtha village, Nagpur District, Maharashtra, India

Figure 1-7: Photograph of the bone char plant in Nakuru, Kenya

Figure 1-8: Photograph of the National Environmental Engineering Research Institute's Electrolytic Defluoridation (EDF) plant

---

Figure 2-1: Flow diagram demonstrating cost savings associated with using raw bauxite as opposed to activated alumina for defluoridation

Figure 2-2: Geographical origin of bauxite samples used in Chapter 2

Figure 2-3: Images of raw bauxite ores shown after ball milling and at 8K magnification using an SEM

Figure 2-4: Determination of minimum required adsorbent dose using linear regression

Figure 2-5: Minimum bauxite doses required to remediate 10 mg F^-/L to below the WHO-MCL in synthetic Sri Lankan groundwater

Figure 2-6: Characterization of globally diverse bauxite ores in terms of points of zero charge, elemental composition, and mineralogy

Figure 2-7: Adsorption isotherms and adsorption envelopes of bauxite ores from India, Guinea, Ghana, and USA

Figure 2-8: Investigation of fluoride removal mechanisms through HATR-FTIR and ionic strength studies

Figure 2-9: Diagram demonstrating the ion exchange removal mechanism of fluoride on gibbsite
Figure 2-10: Comparison of minimum required doses and annual per capita material costs for fluoride removal using milled Guinea bauxite and unmodified AA
Figure 2-11: Fluoride concentration as a function of contact time for Activated Alumina and Guinea bauxite in synthetic Sri Lankan groundwater

---

Figure 3-1: SEM images of Indian bauxite ores heated at 100°C and 300°C at 2K, 4K, and 8K magnification
Figure 3-2: Schematic representation of the flow of mined bauxite ore to central processing plants and water treatment plants
Figure 3-3: Map of districts in India with fluorosis, fluoride contamination, and relative locations of bauxite mines, CPP, and WTP
Figure 3-4: Schematic representation of treatment processes at a village-scale community water treatment plant
Figure 3-5: Characterization of thermally activated Indian bauxite mass loss, mineralogy, particle size, and specific surface area measurements
Figure 3-6: Fluoride concentration as a function of contact time for thermally activated Indian Bauxite in alkaline synthetic Sri Lankan groundwater
Figure 3-7: Effect of various groundwater acidification methods on fluoride removal (HCl or CO_2)
Figure 3-8: Comparison of minimum required doses for various combinatorial treatment scenarios

---

Figure 4-1: Derivation of Stokes Law to calculate terminal settling velocity of a spherical particle
Figure 4-2: Effect of particle size of Indian bauxite on fluoride removal
Figure 4-3: Effect particle size of Indian bauxite on settling
Figure 4-4: Photos of Indian bauxite in beakers and turbidity vials during settling experiments
Figure 4-5: Settling velocity of bauxite particles calculated using Stokes Law
Figure 4-6: Mass fraction of suspended particles remaining in solution

Figure 4-7: Fluoride concentration during a 1-hour settling period of acidified synthetic groundwater
Figure 4-8: XRD spectra of bauxite samples taken pre- and post- fluoride adsorption in desorption experiments of Figure 4-7

List of Abbreviations

AA	Activated Alumina
ALCOA	Aluminum Company of America
BET	Brauner-Emmett-Teller
BGS	British Geologic Survey
CA	Component Additivity
CFSTR	Continuous Flow Stirred Tank Reactor
CO_2	Carbon Dioxide
CPP	Central processing plant
CSIR-IICT	Council of Scientific and Industrial Research-Indian Institute of Chemical Technology
DOC	Dissolved organic carbon
DI	Deionized
DIC	Dissolved Inorganic Carbon
DLS	Dynamic Light Scattering
EAWAG	Swiss Federal Institute of Aquatic Science and Technology
EDF	Electrolytic defluoridation
EDX	Energy Dispersive X-ray
EPA	Environmental Protection Agency
EXAFS	Extended X-ray absorption fine structure
GC	Generalized Composite
HATR-FTIR	Horizontal Attenuated Total Reflectance- Fourier Transform Infrared Spectroscopy
HCl	Hydrochloric Acid
IC	Ion Chromatography
ICP-MS	Inductively coupled plasma mass spectroscopy
ICP-OES	Inductively coupled plasma optical emission spectroscopy
IR	Infrared
MCL	Maximum Contaminant Level
MES	2-(*N*-morpholino)ethanesulfonic acid

NEERI	National Environmental Engineering Research Institute
NF	Nanofiltration
NOM	Natural Organic Matter
NPOC	Non-Purgeable Organic Carbon
NMR	Nuclear Magnetic Resonance
O & M	Operation and Maintenance
PACL	Poly-aluminum Chloride
PFR	Plug Flow Reactor
PZC	Point of Zero Charge
RO	Reverse Osmosis
SAFR	Scalable and Affordable Fluoride Removal
SCM	Surface Complexation Modeling
SEM	Scanning Electron Microscopy
SMCL	Secondary Maximum Contaminant Level
SSA	Specific Surface Area
TC	Total Carbon
TDS	Total Dissolved Solids
TSS	Total Suspended Solids
TGA-MS	Thermogravimetric Analysis and Mass Spectrometry
TISAB	Total Ionic Strength Adjustment Buffer
UC	University of California
USGS	United States Geologic Survey
WHO	World Health Organization
WTP	Water treatment plant
XAS	X-ray Absorption Spectroscopy
XPS	X-ray Photoelectron Spectroscopy
XRD	X-ray Diffraction
XRF	X-ray Fluorescence

Acknowledgements

I want to start by thanking my parents, Durga and Gandhi Cherukumilli, for bringing me into this world and sacrificing some of their dreams and aspirations in hopes of giving me and my sister more opportunities and freedom to create our own future. Without their patient and unending support, I would not have had the privilege to receive an incredible education over the past two decades and I would not be where I am today.

I feel lucky and blessed that I had such a strong support system of friends and family to rely on during the most challenging and testing times of the PhD experience. I want to express deep gratitude to my loving and understanding husband for providing me a constant source of existential stability, an open heart and mind to listen to various qualms and proposals, and a strong sense of logic to offer counterarguments when I needed someone to disagree with my stance. In addition, my exuberant and inspiring group of best friends should be awarded for their kindness, compassion, and fortitude for spending countless hours with me, talking on the phone, sharing potlucks, playing board games and sports, going on random adventures, celebrating my successes, and providing consolation, distractions, and valuable advice exactly when I needed them most. My sister, cousins, aunts, uncles, and extended family throughout the U.S., Europe, and India all deserve credit for always being willing to spend time me, nurturing me in their homes with warm food, and supporting me through my numerous moves, trips, and wedding, without expecting anything in return other than love.

I am grateful to my PhD advisor, Ashok Gadgil, for being an inspirational figure in my life, mentoring me personally and professionally, encouraging me to pick a challenging and rewarding research topic, and sharing the lessons he learned about implementing sustainable technologies in the developing world. I feel indebted to Professors David Sedlak and Laura Lammers for spending countless hours with me in their office hours to give me useful advice about my ongoing research and for having deep scientific conversations with me that helped me get back on track whenever I veered off course. I want to express gratitude to Professors John Harte, Kara Nelson, and Bill Nazaroff for inspiring me to go to graduate school and for mentoring me on interesting research projects and teaching experiences that have prepared me for a lifelong career in academia.

The work presented in this dissertation would not have been possible without the valuable assistance given by those who helped with the collection of bauxite samples from India, Guinea, Ghana, and the USA (e.g., Durga and Gandhi Cherukumilli, Shannon Parks, Laura Craig, and Bill Price of Bledsoe Mining Company), my undergraduate research assistants (Catinca Negru, Subiksh Chandrasekhar, and Yash Mehta), many others who helped with experimental design, data collection, data analysis, or manuscript editing (Tessa Maurer, Tim Teague, Siva Bandaru, Tom Owens, Tracy Mattox, Nate Hohman, Daniel Wilson, David Dzombak, Rachel Scholes, Will Tarpeh, James Barazesh, Casey Finnerty, Jessica Ray, Katherine Boden, and Dana Hernandez), and the Gadgil Water lab for moral support and constant feedback on my research updates. I want to especially thank my lab mate and wonderful friend (Caroline Delaire), postdoc and constant source of support (Chinmayee Subban), and senior scientist and lab manager (Susan Amrose) for refining my experimental design skills, improving my scientific and proposal writing, teaching me to be a critical thinker and effective communicator, and helping me countless times throughout my graduate career.

Finally, I want to acknowledge all my funding sources and partners that enabled my doctoral research. This work was supported by the Andrew and Virginia Rudd Foundation Endowed Chair in Safe Water and Sanitation to A. Gadgil and the Big Ideas@Berkeley Award to K. Cherukumilli, both administered by the Blum Center for Developing Economies; an Explore Travel Grant from the Development Impact Lab (USAID Cooperative Agreement AID-OAA-A-13-00002), part of the USAID Higher Education Solutions Network; the Maharaj Kaul Memorial Fund Grant for Travel; and an NSF Graduate Research Fellowship to K. Cherukumilli. Work at the Molecular Foundry was supported by the Office of Basic Energy Sciences of the U.S. Department of Energy under Contract No. DE-AC02-05CH11231. Additional funding sources included gift funds by A. Gadgil to LBNL, the SMART mentorship program award, the DOW SISCA award, and the Graduate Division Conference travel grant. Institutional (and personal) support from the following organizations was also invaluable: the Blum Center for Developing Economies @ Berkeley, the Development Impact Lab, Development Engineering program, Molecular Foundry, Indian National Environmental Engineering Research institute (Dr. Pawan Labhasetwar and Dr. Katherine Alfredo), Berkeley Water center, EPS department, and EAWAG (Dr. Annette Johnson).

CHAPTER 1. Introduction

1.1. GROUNDWATER FLUORIDE CONTAMINATION: AN OVERVIEW

1.1.1. Global Distribution of Geogenic Fluoride

More than 200 million people worldwide drink groundwater containing naturally occurring[1] fluoride concentrations[2] surpassing the World Health Organization's recommended maximum contaminant level (WHO-MCL) of 1.5 ppm F^-.[3] The fluoride-affected areas shown in Figure 1-1 include arid regions of India, China, the East African Rift Valley, the Middle East, northern Mexico, and central Argentina.[4,5]

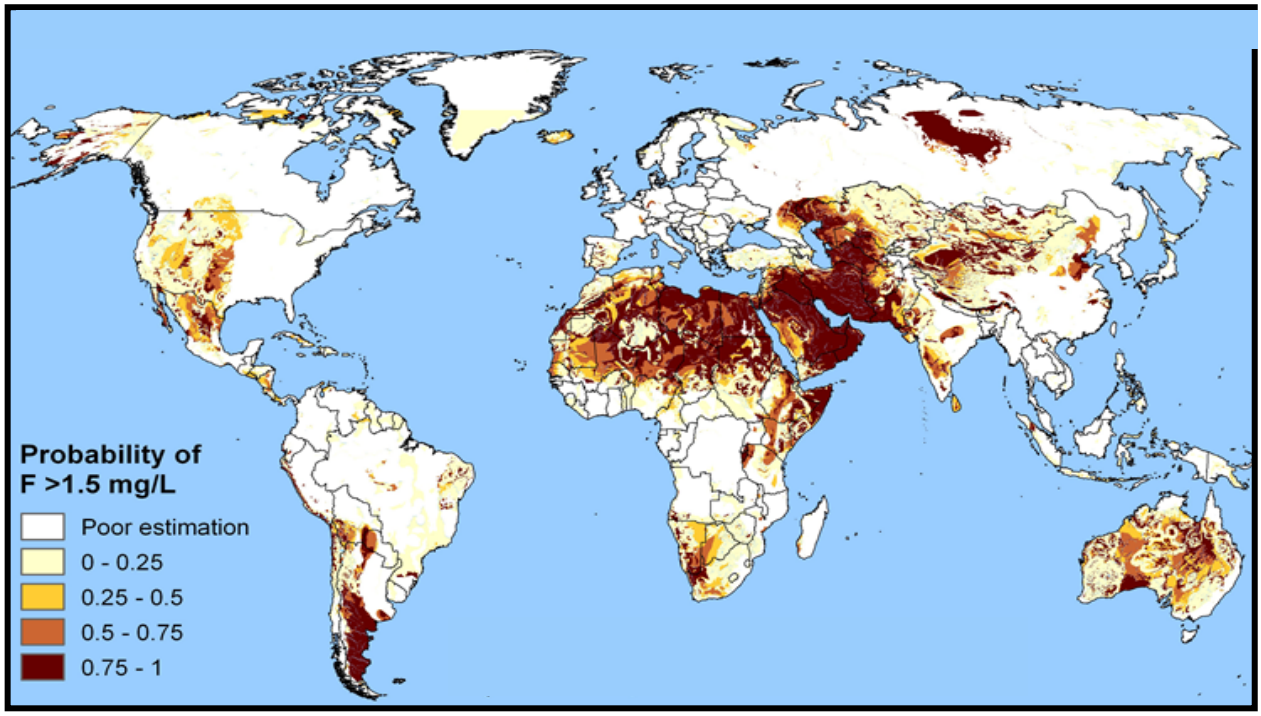

Figure 1-1: Probability of groundwater fluoride concentrations exceeding the WHO-MCL (1.5 mg F^-/L) according to EAWAG's predictive models from Amini et al., 2008[117].

Although fluoride can enter the environment through effluent from anthropogenic sources such as industries (e.g., aluminum smelters) and use of phosphate fertilizers, its high concentration in groundwater is *primarily* due to the dissolution of fluoride-rich minerals in sedimentary (e.g., limestone) and igneous (e.g., granite) rocks (Table 1-1).[1,2] The concentration of fluoride in groundwater is controlled by the solubility of these fluoride-bearing minerals and is dependent on several factors including the aquifers' geochemical composition, alkalinity, pH, total dissolved solids, hardness, temperature, residence times, and climatic conditions.[6] Surface waters and shallow hand-dug wells do not contain high fluoride concentrations due to high rainwater infiltration/dilution and short contact times between water and fluoride-bearing minerals in rocks.[5] In contrast, deep borewells in contact with older aquifer zones contain higher

fluoride concentrations due to lower groundwater flow rates and longer contact time available for equilibration. Fluoride concentrations in rainfall and surface waters are typically 1-2 orders of magnitude lower (less than 0.03 and 0.3 ppb F^-, respectively)[2] than in groundwater but shallower aquifers can also be contaminated with fluoride in certain volcanic areas with hydrothermal activity due to the increased solubility of fluoride-rich minerals at higher temperatures.[7] In general, geochemists have demonstrated that deeper/older groundwater aquifers in arid climates characterized by low calcium ("soft water"), high temperatures, high bicarbonate alkalinity (high pH), high silica content, and high salinity/ionic strength, are more likely to have higher concentrations of fluoride due to increased solubility of the fluoride bearing minerals.[5–8]

Table 1-1. Mineral sources of fluoride found in sedimentary and igneous rocks. From Madhukar et al., 2014[7].

Category	Mineral Source	Formula
Sedimentary	Sellaite	MgF_2
	Fluorite/Fluorospar	CaF_2
	Villiaumite	NaF
Igneous	Cryolite	Na_3AlF_6
	Fluorapatite	$Ca_5(PO_4)_3F$
	Topaz	$Al_2SiO_4(F,OH)_2$
	Bastnaesite	$(Ce, La)CO_3F$
	Lepidolite	$K(Li, Al)_3(Al, Si, Rb)_4O_{10}(F, OH)_2$
	Phlogopite	$KMg_3(AlSi_3O_{10})(F, OH)_2$
	Biotite	$K(Mg, Fe)_3(AlSi_3O_{10})(F,OH)_2$
	Muscovite	$KAl_2(AlSi_3O_{10})(F, OH)_2$

1.1.2. Impacts of Excess Fluoride Intake on Health

Fluoride at low concentrations (0.5-1.5 mg F^-/L) is often intentionally added to drinking water supplies to prevent dental caries by strengthening enamel through the formation of an acid resistant fluorapatite layer.[9] However, prolonged exposure to excessive fluoride concentrations can cause lower IQ,[10] mottling of tooth enamel (dental fluorosis), irreversible bone deformities in children (skeletal fluorosis), and anemia attributed to poor nutrient absorption (Table 1-2).[4]

The occurrence and intensity of fluorosis is dependent on the fluoride concentration in drinking water and additional factors including dietary habits/nutritional intake and overall physical activity. High fluoride content has been reported in major agricultural crops and edible products including cereals (e.g., wheat, rice), maize (e.g., legumes, lentils soy beans), vegetables (e.g., lettuce, spinach, cabbage, tomato, cucumber, potato, okra, carrot, etc.), fruits (e.g., mango,

apple, guava), nuts (e.g., almond, peanuts, etc.), spices (e.g., coriander, garlic, turmeric, rock salt), meat (e.g., mutton, beef, pork, fish), and beverages (e.g., black tea).[8] Furthermore, a reduced intake of dietary calcium and vitamin C has been linked to an intensification of the impacts of fluoride consumption through drinking water. An initial exploratory field visit to endemic fluorosis villages in Nalgonda District, Telangana, India, showed the drastic effects of excess fluoride intake on children and adults (Figure 1-2).

Table 1-2. Health effects of fluoride consumption. From Mohapatra et al., 2009[19].

Fluoride Concentration (mg/L)	Health Outcome
< 0.5	Dental Caries
0.5-1.5	Optimal Dental Health
1.5-4.0	Dental Fluorosis
4.0-10.0	Dental/Skeletal Fluorosis
> 10.0	Crippling Fluorosis

Figure 1-2: Photographs of dental and skeletal fluorosis patients in Nalgonda District, Telangana, India taken during a field visit (October 2013).

High levels of fluoride in groundwater are clearly correlated with the incidence of endemic skeletal fluorosis around the world, as shown in Figure 1-3. Nearly half of the total population in countries suffering from fluoride contamination live in rural areas, which increases the likelihood of communities being disconnected from the municipal water piped water supply and having to rely heavily on contaminated groundwater (Figure 1-4).

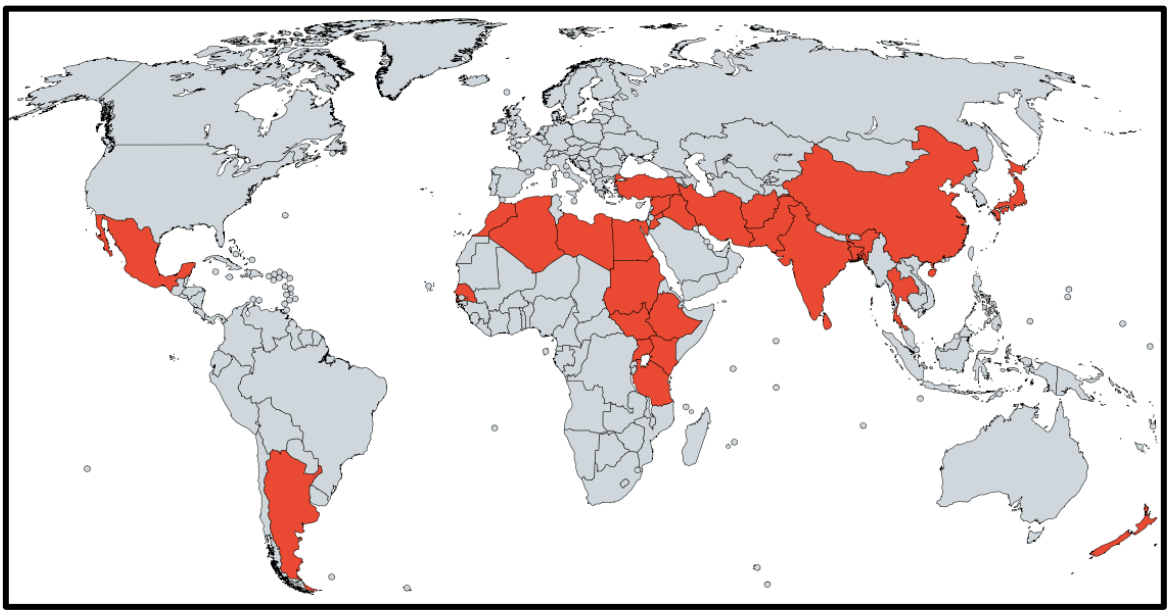

Figure 1-3: Map of countries with reported endemic fluorosis resulting from reliance on fluoride contaminated groundwater as a primary source of drinking water. Map created using www.mapchart.net based on data provided by UNICEF (1999)[11].

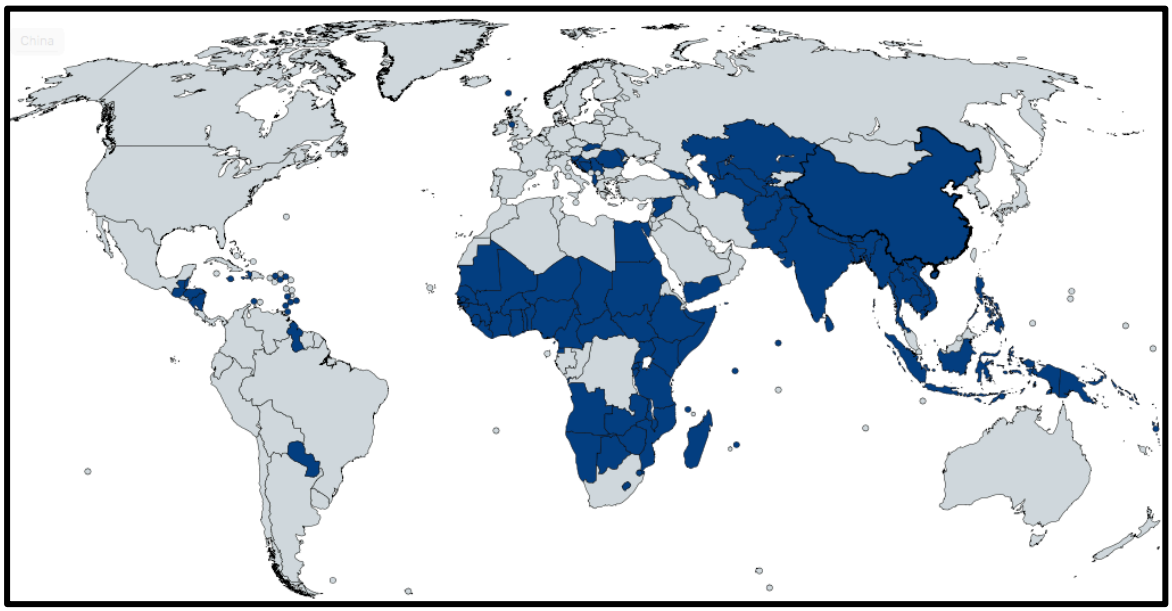

Figure 1-4: Map of countries with over 40% of the total population living in rural areas. Map created using www.mapchart.net based on data provided by World Bank (2015)[118].

1.1.3. Indian Context: Nalgonda District, Telangana

In India alone, over 66 million people[11] are at risk of developing fluorosis and resulting significant adverse social, economic, and health impacts. In rural India, a majority of the drinking and irrigation water requirements (80% and 50%, respectively) are met with

groundwater[5]. Nalgonda District, Telangana, offers an appropriate site to study this global development challenge because the problem there is severe, long standing, and still largely unresolved. Due to widespread illiteracy and unemployment in the region, Nalgonda is classified as one of India's 250 poorest districts (out of 640 total) by the Backward Region[a] Grant Fund program[12]. Nalgonda District is semi-arid with 1,135 rural villages and a total population of 3.5 million people, with approximately 81% of the population living in rural areas and working as agricultural laborers and cultivators[13].

The aquifers in Nalgonda District contain granitic rocks with average fluoride content much higher than the world average concentration, resulting in groundwater concentrations reaching up to 20 mg F^-/L, approximately thirteen times the WHO-MCL[14]. According to the 2011 Indian Census, 65% of households in rural Nalgonda used untreated water sources and groundwater (e.g., wells, tubewells/boreholes, and handpumps) as their primary supply of drinking water[13]. Due to the high fluoride content in local aquifers and the population's heavy reliance on groundwater, an estimated 10% of the district population has been affected adversely by fluoride contamination and about 10,000 residents in Nalgonda District are irreversibly crippled due to skeletal fluorosis[15]. These grave statistics indicate an urgent need for the development of a lasting solution. Despite awareness of the problem for over 6 decades, fluoride contaminated water continues to be consumed due to the lack of affordable groundwater treatment technologies and piped surface water alternatives.

1.2. EXISTING DEFLUORIDATION TECHNOLOGIES

1.2.1. Overview

Many defluoridation technologies have proven to be effective in the lab, but most are neither sustainable nor effective in remote rural regions of developing countries because they are cost-prohibitive and dependent on intensive skilled labor for maintenance (e.g., Nalgonda technique,[5] reverse osmosis, activated alumina, and aluminum electrocoagulation),[16] difficult to source and culturally inappropriate in India (e.g., bone char),[16] or unreliable and challenging to scale up in arid rural communities (e.g., rainwater harvesting).[17] To assess whether or not the following existing defluoridation methods are appropriate and effective for rural settings, we should consider many factors that play a role in determining a technology's success when implemented in the field, including technical factors (e.g., fluoride removal effectiveness, added contaminants in treated water), operational factors (e.g., material sourcing, disposal of spent waste, need for skilled labor in maintenance/operation, monitoring), and social factors (e.g., treatment cost, user acceptance, community participation).[2]

[a] This program by the Indian government aims to rectify regional inequalities by allocating funds to districts identified as "backward". The Ministry of Panchayati Raj is responsible for planning and implementing the grants, but it is still unclear if funds have been sent to each district, how often they are distributed, and whether the program has improved the residents' access to public services such as clean drinking water.

1.2.2. Membrane-Based Solutions

Reverse osmosis (RO) is a water treatment technology developed in the latter half of the 20th century to desalinate ocean water[18]. Since then, RO has been widely used in advanced water treatment plans to remove other impurities in wastewater, surface water, and groundwater, including minerals, pathogens (e.g., protozoa, bacteria, viruses), organic pollutants (e.g., pesticides), total dissolved solids (TDS), and inorganic contaminants (e.g., Pb, As, and F). Membrane processes such as RO are advantageous because they remove many contaminants and particles (larger than 0.1 nm) in one step without extra chemical addition, work in a wide pH range, do not have problems with ion interference, and can be automated to minimize the manpower requirement.[8] However, because RO removes all the ions present in the water including some thought to be beneficial to human health, remineralization for drinking water purposes may be necessary and creates added recurring operational costs. Furthermore, water treated using RO operated at the community scale in India as shown in Figure 1-5 is inaccessible to most rural residents because the RO filtered water is bottled, marketed, distributed, and sold at a high retail cost of approximately Rs.38/L ($0.6/L = $1642.5/yr/person[b])!

Figure 1-5: Photograph of Reverse Osmosis (RO) plant at the Council of Scientific and Industrial Research's Indian Institute of Chemical Technology (CSIR-IICT) in Hyderabad, Telangana, India taken during a field visit (October 2013).

Another related technology, nanofiltration membranes, can more selectively filter out fluoride (in comparison to other monovalent ions chloride or nitrate) because of the fluoride ions' steric effect (i.e., F^- ions are more strongly hydrated due to its high charge density).[19] In comparison to RO, nanofiltration membranes also have larger pores, lower resistance, and require lower pressures to remove solutes. However, due to their reliance on the application of high external pressure to overcome the osmotic pressure across a semi-permeable membrane, both RO and nanofiltration membrane processes have large capital and operational costs and

[b] Value calculated using WHO requirement of 7.5 L drinking water/day/person and cost of RO water given in http://www.sevea-asso.org/wa_files/Case_20study_20Sarvajal_vcomp.pdf

require highly skilled labor for operation and maintenance. Moreover, low water recovery rates and the generation of a concentrated salty brine waste stream create waste disposal problems and make RO and nanofiltration unacceptable for use in remote water-scarce regions.[16]

In contrast to RO and nanofiltration, dialysis and electrodialysis are atmospheric pressure membrane processes that do not require application of an external pressure. Dialysis membrane pores are typically larger and allow solutes to pass through the membrane (via the Donnan effect) rather than been retained like in RO and nanofiltration.[19] However, because electrodialysis requires an electric potential and uses direct current to control the selective flow of charged ions to separate them from water, it remains to be an energy intensive defluoridation technique.[5,7] In general, all of these membrane processes have certain challenges that must be overcome before being applied in a rural settling: the requirement for literate and skilled operators, their prohibitively high capital cost, and the need for regular replacement (or regeneration) of membranes after frequent fouling and degradation.[2,20]

1.2.3. Precipitation Methods

Precipitation methods are another class of defluoridation technologies that remove fluoride ions through the formation of solids such as fluorapatite ($Ca_5(PO_4)_3F$), fluorite (CaF_2), and sellaite (MgF_2) after the addition of aluminum, calcium, or magnesium salts.[21]

In 1961, the Indian National Environmental Engineering Research Institute (NEERI) developed a now well-known defluoridation method called the Nalgonda Technique (named after Nalgonda District, Telangana). This technique requires the addition and rapid mixing of lime ($Ca(OH)_2$), a coagulant (alum ($Al_2(SO_4)_3$) or poly-aluminum chloride (PACL)), and bleaching powder into a tank followed by flocculation, sedimentation, and filtration of the precipitated solids.[21] In this two-step process, the addition of lime causes precipitation of fluoride as fluorite (CaF_2) and the addition of alum or PACL is a dual purpose: to enhance floc formation and settling of the precipitates and to generate another adsorbent, aluminum hydroxide ($Al(OH)_3$), that further removes fluoride.[8]

The Nalgonda technique has been implemented in India, Kenya, Senegal, and Tanzania.[20] Despite its apparent simplicity in design and operation, numerous barriers have prevented the Nalgonda technique from scaling up: 1) the presence of phosphate ions in groundwater complex calcium and reduce the precipitation of fluorite,[20] 2) the high alum dosage requirement (700-1200 ppm) causes high residual concentrations of sulfate and aluminum in the product water[8], sometimes exceeding the 400 ppm and 0.2 ppm permissible limits for SO_4^{2-} and Al, and 3) a low defluoridation efficiency (70%) due to the solubility limit of fluorite and formation of aqueous aluminofluoro complexes restricts this process to only treating groundwater with less than 5ppm F^-.[5,8,16]

Although the Nalgonda Technique has been implemented at the community level in resource constrained regions, users have complained about numerous issues including the salty taste of the treated drinking water, high maintenance cost of the community plants, the need for a large sludge drying bed area, and the lack of automation of the process (an attendant is needed for processing steps and dose calculation for different groundwater compositions).[8] In particular, this requirement for skilled manpower has made the Nalgonda Technique unsuitable for widespread application at the household level in remote, rural, regions.[5]

Other salts of calcium and magnesium (e.g., $CaCl_2$, $CaSO_4$ (gypsum), and $CaMg(CO_3)_2$ (dolomite), MgO (magnesia), $Mg(OH)_2$ (brucite)) have also been tested for fluoride removal, but these methods often require additional chemicals to soften or neutralize the treated water and they also face similar solubility limit problems like the Nalgonda Technique.[2,21]

Figure 1-6 demonstrates the difficulties of implementing any of these precipitation methods in the form of household-scale filters in rural India. The photo was taken during a two-week field visit to NEERI, the research institute that distributed hundreds of sand filters and adsorbent chemical sachets to enable individual households to defluoridate 30 L of groundwater daily. The household owners are responsible for adding the required dose of chemicals (calcium salts) to the contaminated water, mixing them for approximately 20 minutes with a stick, and allowing the water to flow through the sand filter. Over 1-2 months of operation, a thick layer of sludge (e.g., precipitates and bacterial growth) develops and clogs the sand filter, which must be scraped off and cleaned[22]. The capital cost of this household unit in 2012 was Rs. 2000 (~$36) and the treatment cost incurred by the households was about 20 paise/L (0.36 cents/L).

(A) **(B)** **(C)**

Figure 1-6: Photograph of the National Environmental Engineering Research Institute's (NEERI) household filters in Chichkavtha village, Nagpur District, Maharashtra, India taken during a field visit (October 2013). Panels **A-C** from left to right) show an intact filter, an emptied disassembled filter, and a NEERI official conducting regular household surveys with village filter users.

Informal interviews at over 30 households in two fluoride-affected villages in Maharashtra (comparable in size and poverty level to villages in our target study area of Nalgonda District, Telangana) revealed the following difficulties associated with expecting end users to maintain their own drinking water treatment systems: a) families complained that the containers holding the filtration unit were leaking, b) many used the tanks as storage space for grains rather than as filters, c) people went against the prescribed cleaning instructions and emptied the sand out completely rather than scraping the top layer, and d) some people were not

receiving chemical sachets containing the adsorbent due to personal issues with the community distributor. Many previous studies support the consensus that household filters most commonly fail in poor areas because users are unable to maintain them due to a lack of time or because they are misused and abandoned.[16,23] Combined, these shortcomings observed with the use of household filters in Maharashtra provide motivation for community-scale defluoridation systems in rural remote regions of resource constrained parts of the world.

One such example of a community-scale defluoridation system is the bone char plant installed in Nakuru, Kenya, shown in Figure 1-7. Bone char is prepared by heating animal bones (e.g., birds, pigs, and cows) in a furnace at T=300-800 °C for 1-3 hours to increase surface area and remove the organic content in the bones.[7,21] The major components of bone char include the primary active calcium phosphate component, hydroxyapatite, (57-80%), calcium carbonate (6-10%), and carbon (7-10%), with trace amounts of Fe, Al, Mg, and N (< 1%).[7] To increase fluoride removal efficiency (> 90%), water treated with bone char is put into contact with calcium phosphate pellets to catalyze the formation of fluorite and fluorapatite precipitates on bone char, which acts as the substrate material. This process is commonly known as contact precipitation.[7,21] The primary issues limiting the widespread use of bone char as a defluoridation technology globally include lack of religious/cultural acceptance, problems routinely sourcing the raw material at the required scale, and users' dislike of the taste and odor of the treated water.[2]

Figure 1-7: Photographs of the Nakuru Defluoridation Company's bone char plant in Nakuru, Kenya taken during a field visit (July 2013). Panel **A** shows raw bones stored for charring, panel **B** shows crushed/sieved bone char, and panels **C** and **D** show community water kiosks selling treated water.

1.2.4. Adsorbents

Adsorbents are widely used because of their relative ease of operation and cost effectiveness in comparison to membrane/pressure driven systems and precipitation techniques. In the adsorption process, the active agent (i.e., "adsorbent") has surface sites that can retain the contaminant of concern (i.e., "adsorbate") through physical (e.g., electrostatic) or chemical (e.g., specific complexation) mechanisms. Whether the adsorbent is used as a filter bed media or a dispersive batch media, over time the active material reaches saturation and must be either discarded or regenerated.[21] Adsorbents can be further classified as low-cost materials, inorganics, and ion exchange resins.[5,24] Hydroxides of Ca, Al, Mg, and Ba are often used because of the similar charge and size of OH^- and F^-. Various naturally found materials have also been tested for use as defluoridation adsorbents including biosorbents (e.g., drumstick seeds, Vetiver grass roots, tamarind seeds, carboxylated chitosan beads, chitin, citrus peels, alginate beads, tea ash, and egg shell powder), fly ash, clays (e.g., zeolites, bentonite, kaolinite, smectites, montmorillonite, and layered double hydroxides), and metal oxides (e.g., Fe, Al, Ti, etc.).[2,21,25]

Of these various tested adsorbents, Activated Alumina (AA) defluoridation filters are most widely used due to their effectiveness and relative affordability for the upper middle class.[26] In addition to removing fluoride through a ligand exchange surface reaction[21], AA is also generally used to remove Si, Se, As, and natural organic matter (NOM).[7] AA is produced by first extracting aluminum oxides from bauxite, a composite ore that also contains oxides of iron, silicon, and titanium as well as other trace minerals. Industrial refining methods such as the Bayer process utilize pressurized sodium hydroxide and temperatures exceeding 1000°C to eliminate impurities, concentrate the Al fraction of bauxite, and generate AA (Al_2O_3) through further calcination. As a result of these industrial processing methods, the generation of AA is extremely resource-intensive in terms of capital and operating costs, energy, and greenhouse gas emissions.[27]

Additional disadvantages of AA include the required use of caustic chemicals for regeneration (high TDS can cause fouling of the AA filter bed media)[8,19], and the need for trained operators and chemicals that are not always locally available.[2] In an attempt to increase AA's defluoridation kinetics and capacity, some researchers have coated its surface with cationic compounds such as oxides and hydroxides of Mn[28–30], Cu[31], La, and Y.[32] Studies on fluoride removal with AA in the presence of co-occurring groundwater ions (e.g., sulfate, carbonate, nitrate, silicate, and phosphate) have demonstrated that the presence of bicarbonate, sulfate, and phosphate negatively impacted fluoride removal, either due to the ions' effect on solution pH or due to direct competition with active surface sites.[20]

Through a collaboration between UNICEF and IIT Kanpur in India, AA has been marketed and implemented in two configurations to lower treatment costs by reducing the volume of water treated (for only drinking/cooking): domestic household filters and hand pump attachments.[21] Based on experiences during our initial field visit to India in Fall 2013, it is clear at AA filters sold in Indian markets target the middle income households rather than the rural residents because of their high market price ($30-50 depending on capacity) and recurring maintenance costs ($5/yr) to replace filter media.

Aluminum electrocoagulation, also termed electrolytic defluoridation (EDF), is another technology that has been implemented in multiple villages and schools across India through the combined efforts of UNICEF, private vendors, the Ministry of Drinking Water and Sanitation, and local offices of state's Public Health Engineering Departments. Developed over a decade ago by NEERI, EDF is a technique used to generate in-situ aluminum hydroxides that serve as efficient fluoride sorbents and are removed by settling. An external voltage is applied to an electrochemical cell to oxidize an Al anode to Al^{3+}, which then hydrolyzes to form $Al(OH)_3$, the primary adsorbent. At the cathode, hydrogen ions are reduced to hydrogen gas, causing high local pH, which sometimes induces cathodic dissolution and creates a super Faradaic efficiency (i.e., more Al is generated than predicted by Faraday's law for a given voltage). The $Al(OH)_3$ precipitates generated in-situ have a strong affinity for fluoride ions, which they adsorb, and a coagulant can be added to settle out and remove the solids.[7]

Currently, at least 20 plants of varying capacity (250L- 4000L per day) are operating in communities throughout India and many dozens more are being constructed by private vendors (Figure 1-8). Field visits to existing EDF plants in Maharashtra, Madhya Pradesh, Chhattisgarh and discussions with scientists at NEERI shed light on the operation, maintenance, and efficiency of the technology. The overall management plan of EDF follows a structure where NEERI develops the technology and receives proposals to build EDF plants from various state or local entities, such as the Ministry of Drinking Water and Sanitation, Municipal Corporations (in cities), Public Health Engineering Departments (in rural areas), NGOs, or multilateral agencies (e.g., UNICEF). Next, private firms are hired to manufacture electrodes and construct EDF plants based on blueprints developed by NEERI for knowledge transfer, and municipal corporations or private firms are contracted to operate and maintain EDF plants for a set number of years.

Figure 1-8: Photograph of the National Environmental Engineering Research Institute's (NEERI) Electrolytic Defluoridation (EDF) plant in Dongargaon, Chhattisgarh, India taken during a field visit (October 2013). Panels **A-C** (from left to right) show a full scale EDF plant, the electrodes submerged in the tank, and a local miner fetching fluoride-free water at the EDF plant.

Based on the aforementioned criteria for an "appropriate" technology in rural settings (Section 1.2.1), EDF appears to be more promising than membrane technologies, precipitation methods, and most adsorbents because it can reliably and effectively treat raw water with typical initial fluoride concentrations found in India (5-10ppm), it requires minimal maintenance (operator cleans cathode weekly), produces minimal sludge, has a low estimated operating cost (Rs 20/1000L), is based on a modular system that is easy to fabricate/scale up, and the main material (Al) can be found ubiquitously in India.[33] Despite these advantages however, NEERI's long-term experience with this technology has unearthed the following challenges with EDF including lack of proper maintenance of plants not operated by private vendors, difficulty changing user behavior and encouraging users to purchase treated groundwater, limited technological reach to other fluoride-affected states (except in cases where local governments took initiative), and a potentially prohibitive capital cost for plant construction.

Table 1-3 outlines a summary of challenges associated with various defluoridation methods currently used in the developing world. Based on lessons learned from countries where these technologies have been implemented in rural settlings (e.g., India, Kenya, and Ethiopia), a majority of these methods were not suitable due to issues including unaffordability and maintenance difficulties (e.g., for RO and AA), chemical and mechanical equipment supply chain challenges (e.g., for Nalgonda Technique), bad taste of product water (e.g., for Nalgonda Technique and bone char), and cultural/religious prohibitions (e.g., for bone char).[16]

Table 1-3. Limitations of existing defluoridation technologies. From Mohapatra et al., 2009[19] and Jagtap et al., 2012.[5]

Category	Technology or Method	Limitations/Disadvantages
Membrane Process	Reverse Osmosis (RO) Nanofiltration (NF) Dialysis Electrodialysis	Requires pretreatment High capital and O&M costs Low efficiency, water wastage Disposal issue with toxic salty brine Completely demineralizes water: RO Skilled labor required
Precipitaion Methods	Nalgonda Technique (NT) Magnesium Oxide Bone Char/$Ca_3(PO_4)_2$ (BC)	Requires pH adjustment of product water Requires frequent addtion of chemicals Labor intensive processs Water reported to have bad taste Large quantity of sludge (with Al & SO_4): NT Cannot treat high F^- concentrations: NT Culturally inappropriate for India: BC
Adsorption	Activated Alumina (AA) Clays, biosorbents Aluminum Electrocoagulation (EDF)	High manufacturing cost Process is pH dependent/ sensitive Slow rate of adsorption Requires regeneration of filter media or electrodes Difficult to scale up and source locally Need periodic monitoring of residual Al
Non-technical methods	Piped water supply Dilution via recharge	High capital cost Time intensive construction projects Inaccessible infrastructure in rural areas Unreliable, intermittent rainfall (dilution)

1.3. OUTLINE OF REMAINING CHAPTERS

The remainder of this dissertation is organized in four chapters.

Chapter 2 establishes proof of concept that mildly processed bauxite can effectively remediate field-relevant fluoride concentrations to below the WHO-MCL in synthetic and real groundwater matrices at comparable rates and significantly lower cost than AA. In this chapter we also characterize intrinsic features of globally diverse bauxite ores (from Guinea, Ghana, USA, and India) using analytical techniques (X-ray fluorescence, X-ray diffraction, gas-sorption analysis) and batch adsorption experiments to identify factors predicting bauxite's performance. We demonstrate that chemical composition, and therefore the geographical origin of the bauxite ore, could substantially impact its fluoride removal performance through the presence of trace minerals that modify the solution pH.

Chapter 3 utilizes insights on underlying molecular mechanisms from Chapter 2 to propose thermal activation and groundwater pH adjustment as two processing methods to optimize the fluoride removal performance of Indian bauxite. We also conduct an in-depth cost analysis to compare the various combinatorial treatment scenarios and find that using bauxite heated at 300°C with acid treatment of groundwater is the cheapest option, although using heated bauxite *without* acid treatment of groundwater may be the most feasible and appropriate treatment option for a rural setting.

Chapter 4 highlights and addresses some remaining practical challenges and unknowns for implementing the complete defluoridation process in the field. This chapter demonstrates that a bauxite-based defluoridation process has potential for success in future field implementation trials because more coarsely milled bauxite powders (large particle sizes reflective of industrial mills used in the field versus the smaller ball mills used in the lab) produced similar fluoride removal results and desorption of fluoride after 1 hour of settling was negligible.

Chapter 5 concludes this dissertation by discussing the implications of the research findings and by suggesting additional future studies needed prior to field implementation of the proposed groundwater defluoridation technology.

CHAPTER 2. Factors Governing the Performance of Bauxite for Fluoride Remediation of Groundwater

Adapted with permission from Cherukumilli, K.; Delaire, C.; Amrose, S.; Gadgil, A., Factors Governing the Performance of Bauxite for Fluoride Remediation of Groundwater. *Environmental Science & Technology* **2017**, 51 (4), 2321-2328. DOI: 10.1021/acs.est.6b04601

2.1. BACKGROUND

Activated alumina is a widely used and highly efficient adsorbent[34,35] because of the strong affinity between aluminum and fluoride. Per tonne, alumina ($300/tonne) costs approximately ten times more than its parent ore bauxite ($30/tonne), due to expenses associated with processing and purifying the bauxite.[36] Alumina (Al_2O_3) is then thermally activated to make the commonly used AA filter media ($1500/tonne)[37] with a final material cost fifty times higher than raw bauxite ore. AA's parent ore, raw bauxite, is comprised of a primary aluminum oxide mineral known as gibbsite ($Al(OH)_3$),[35,38,39] which also has a strong adsorption affinity for fluoride.

Although several studies have reported fluoride adsorption on bauxite,[40–48] the existing literature does not rigorously demonstrate that mildly processed bauxite can produce the level of fluoride removal required to meet the WHO-MCL, nor does it investigate the fluoride removal performance of bauxites of diverse origins with significantly different chemical compositions. The adsorption of numerous cationic (e.g., Cu^{2+}, Pb^{2+}, Co^{2+}, Cd^{2+}, Mn^{2+}, Fe^{2+}, Ca^{2+}, Zn^{2+}, $Hg(OH)_2$, UO_2^{2+}, Th^{4+}) and anionic (e.g., PO_4^{3-}, AsO_4^{3-}, SO_4^{2-}, MoO_4^{2-}, SeO_4^{2-}, CrO_4^{2-}, H_3BO_3, $H_2SiO_4^{2-}$) species on gibbsite has been reported,[49] but very few studies have focused on the adsorption of fluoride (F^-) on pure gibbsite[38] or on its composite bauxite ore.[43,47] More generally, the adsorption behavior of composite mineral assemblages such as bauxite is not well understood because published surface complexation and spectroscopic studies have primarily focused on surface interactions with pure mineral phases. Specifically, the effect on fluoride removal of non-Al minerals present in bauxite (e.g., hematite, goethite, kaolinite, calcite, etc.), which could impact adsorption through modifications in the adsorbent's elemental composition, surface area, and affinity for fluoride, has not been investigated in prior literature. Thus, characterizing and elucidating the performance of diversely sourced bauxite ores with different compositions may allow for the design of an effective and low-cost solution to remediate fluoride-contaminated groundwater.

Bauxite deposits are present worldwide, including in countries with fluoride-contaminated regions (e.g., India, Ghana, and China). India has over 66 million people facing risk of developing fluorosis[11] and it is also home to the 5th largest bauxite deposit (3037 million tonnes).[50] Hence, replacing AA with mildly processed (e.g., dried/milled) bauxite ore has the potential to create a fluoride removal method that is more (a) effective at remediating contaminated groundwater in $/volume of water treated, (b) affordable to low-income households, and (c) widely available in affected regions (Figure 2-1).

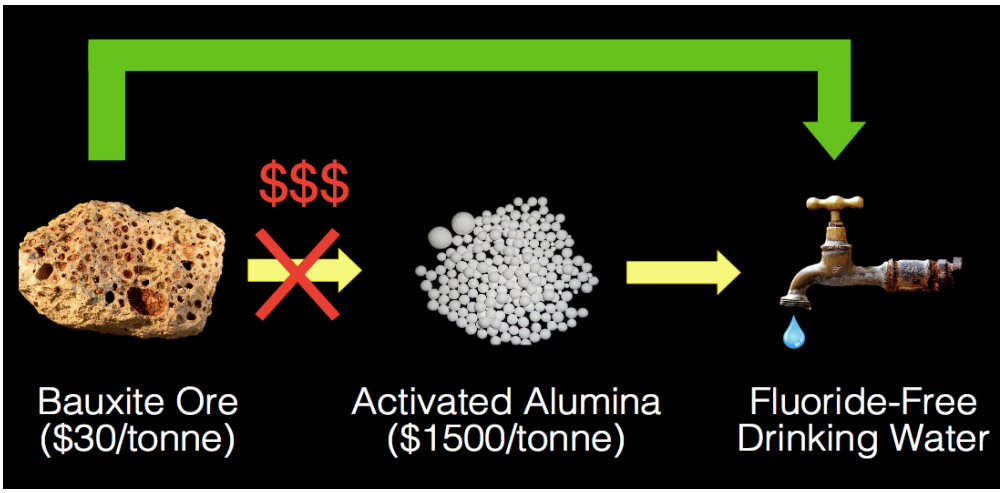

Figure 2-1: Flow diagram demonstrating cost savings associated with using raw bauxite as opposed to activated alumina as an adsorbent material for remediating fluoride contaminated groundwater.

The objectives of this Chapter are 1) to demonstrate and compare the fluoride removal performance of diversely sourced bauxite ores used as dispersive batch media, 2) to elucidate factors governing fluoride removal with mildly processed bauxite ores, and 3) to conduct a rigorous cost comparison of treating fluoride-contaminated groundwater with AA and bauxite. To meet these objectives, batch fluoride adsorption experiments were conducted with four bauxite ores originating from India, Guinea, Ghana, and USA. Except for USA bauxite, these source regions were selected because of the severity of their fluoride contamination problem and their large share in global bauxite production.[50–52] Molecular-level and macroscopic experimental techniques were used to characterize the ores in terms of elemental and mineral composition, adsorption affinity and capacity, surface area, and equilibrium suspension pH. Results elucidating factors influencing fluoride removal efficiency strongly suggest that mildly processed bauxite ore is a cost-competitive alternative to AA and consequently has the potential to substantially improve access to safe water in fluoride-affected low-income communities.

2.2. METHODS

2.2.1. Adsorbents Preparation and Characterization

Bauxite ores were collected or received from mines in India (Visakhapatnam, Telangana), Guinea (Boke), Ghana (Western Region), and USA (Eufaula, Alabama) (Figure 2-2). After oven-drying raw bauxite at 100°C for 24 hours to remove moisture, 5 g of each sample was milled for 60 minutes in an agate milling jar of a shaker ball mill (SPEX8000) to generate submicron-sized powders, as confirmed by scanning electron microscopy (SEM) and dynamic light scattering (Malvern Zetasizer Nano ZSP). In a number of experiments, Activated Alumina (AA) powder (0.58 ± 0.56 μm, Sigma Aldrich, MO) was used as-received and was measured to have a comparable particle size to that of milled bauxite ores from India, Guinea, Ghana, and USA (respectively 0.71 ± 0.10, 0.76 ± 0.08, 0.55 ± 0.27, and 0.91 ± 0.84 μm). Images of each bauxite ore after milling and with SEM are shown in Figure 2-3. Zeta potentials of all adsorbent materials were measured using a Malvern Zetasizer Nano ZSP, with a matrix containing

deionized (DI) water and an adsorbent solid:volume ratio of 0.05 mg/L to maintain a stable suspension of particles. The pH of the test solutions was adjusted approximately to pH 2, 4, 6, 8, and 12 using 1M HCl and 1M NaOH stock solutions.

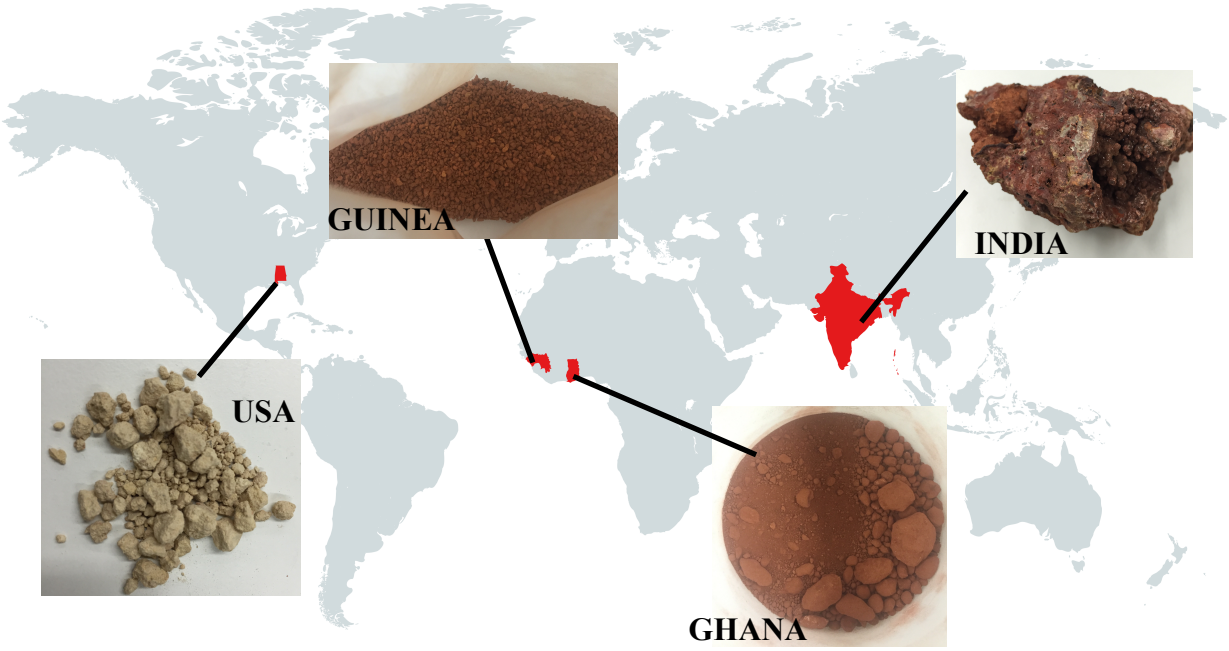

Figure 2-2: Geographical origin of bauxite samples used in this study. Photos show raw bauxite ores as received, before milling.

Figure 2-3: Images of raw bauxite ores shown **(A)** after ball milling and **(B)** at 8K magnification using a Scanning Electron Microscope (SEM). Sources of bauxite ores as presented from left to right in both panels: USA, Guinea, Ghana, and India.

Bulk elemental composition was measured by energy dispersive X-Ray fluorescence spectroscopy using the parameter-free Turboquant method (Spectro Xepos ED-XRF), which does not account for light elements such as C and N in the total mass. Bulk crystalline mineral

composition was determined from X-ray diffraction (XRD) patterns obtained using a Bruker D8-Discover diffractometer with a Co source (Co Kα = 1.79Å) and a Vantec-500 area detector. XRD patterns were collected using a coupled scan with 4 frames at 300 seconds/frame (θ1 and θ2 ranging from 10,10 to 40,40). XRD peaks for each bauxite sample (processed as 0.1-0.5g of dry powder) were integrated and merged using Diffrac Eva and the peaks were identified using the Jade software program.

Multipoint Brunauer-Emmett-Teller (BET) measurements were made using a Micromeritics Tristar II 3020 to determine the specific surface area (SSA) of the milled bauxite ores. For BET surface area analysis, approximately 0.5-0.7 g of bauxite powder was added to glass tubes, dried overnight in a vacuum at 100°C, and analyzed using nitrogen gas sorption.

Suspensions of each milled bauxite ore (dose: 1 g/L) were mixed in open glass beakers containing 35 mM NaCl for 24 hours and the final pH, henceforth referred to as "equilibrium pH", was measured. To understand the reported differences in equilibrium pH between the four bauxite ores, separate experiments were conducted with higher doses (4 g/L) of bauxite, and dissolved calcium and inorganic carbon (DIC) concentrations in the filtrate (0.2 μm nominal filter poresize, VWR) were measured after overnight mixing. Calcium was measured using ion chromatography (IC, Metrohm Chromatograph, IonPac CS12 column) and dissolved inorganic carbon was determined with a total carbon analyzer (Shimadzu TOC-V_{CSH}) as the difference between Total Carbon (TC, representing inorganic and organic carbon) and Non-Purgeable Organic Carbon (NPOC, representing non-volatile organic carbon).

2.2.2. Preparation of Synthetic Groundwater

Recipes for synthetic Ghana, Sri Lanka, and Tanzania groundwater matrices are shown in Table 2-1. These groundwater matrices were developed based on British Geologic Survey (BGS)[2] measurements and prepared using stock solutions of 100 mM $CaCl_2$, 100 mM $MgCl_2$, 200 mM $NaHCO_3$, 100 mM Na_2SO_4, 10 mM SiO_2 (Na_2SiO_3-$5H_2O$), and 10 mM $NaNO_3$. Intial fluoride concentrations of all lab-synthesized groundwaters were set to 10 mg F^-/L using a stock solution of 100 mg/L NaF. Real groundwater samples from Telangana (Nalgonda District) and West Bengal (South Dinjapur District), India, were collected after flushing the tubewells for several minutes and stored in sealed plastic bottles until later characterization. Initial pH of all tested waters was set to 6 (± 0.1), near the pH of minimum solubility of gibbsite, by addition of drops of 1M HCl or 1M NaOH, as necessary. Concentrations of ions (e.g., Fe, Ca, Mg, Si, and P) were characterized in real groundwater samples using Inductively Coupled Plasma Optical Emission Spectroscopy (ICP-OES, Perkin Elmer 5300) following US-EPA Method 200.7.[2] Reported error for ICP-OES is ±10%.

The real and synthetic groundwater matrices described in Table 2-1 were used in the following batch experiments designed to be representative of real treatment conditions (including ionic strength, which is mostly unaffected by fluoride adsorption). Binary-solute buffered electrolytes (e.g., NaCl + $NaHCO_3$) were used mainly in bauxite characterization experiments and were not designed to be representative of drinking water.

Table 2-1. Chemical composition of synthetic and real groundwater matrices used in this study. Values reported are gravimetric target concentrations or measured concentrations with errors (errors represent the larger of the standard deviation from repeated tests and ICP-OES measurement errors). Dashes indicate that the ions were not expected or measured.

Component	Synthethic Groundwater				Real Groundwater	
(mg/L)	Binary Solute	Ghana	Sri Lanka	Tanzania	West Bengal	Telangana
F	10.0	10.0	10.0	10.0	6.2 ± .62	8.4 ± 0.8
Ca	0.0	27.6	173.0	17.6	8.0 ± 0.8	19.7 ± 2.0
Mg	0.0	13.7	179.0	1.4	1.0 ± 0.1	35.1 ± 3.5
HCO_3^-	305.1	146.0	516.0	845.0	-	-
SO_4^{2-}	0.0	1.7	15.5	20.8	-	-
Si	0.0	34.4	45.0	54.2	11.0 ± 1.1	35.1 ± 3.5
NO_3^- as N	0.0	4.9	9.0	7.8	-	-
NaCl	2021.3	0.0	0.0	0.0	-	-
Fe	0.0	0.0	0.0	0.0	0.0 ± 0.01	0.0 ± 0.01
P	0.0	0.0	0.0	0.0	0.1 ± 0.01	0.0 ± 0.01

2.2.3. Batch Adsorption Experiments

Standard batch adsorption experiments were designed to determine the respective effects of the solid:liquid ratio (referred to as 'dose' henceforth), initial fluoride concentration, pH, ionic strength, and reaction time on fluoride removal with the 4 bauxite ores. Table 2-2 provides a detailed summary of experimental conditions. Adsorbents were added to select electrolytes in 15 mL polypropylene centrifuge tubes at doses differing for each experiment. An Analog Rotisserie Tube Rotator (Scilogex, MX-RL-E) allowed maintenance of well-mixed suspensions during the full duration of the batch adsorption experiments, which were conducted for 24 hours for consistency with other studies.[6,35] The kinetics of fluoride removal were investigated in synthetic Sri Lankan groundwater with AA and milled Guinea bauxite (doses of 4 g/L (40 ± 0.1 mg/10 mL) and 10 g/L (100 ± 0.1 mg/10 mL), respectively) by monitoring fluoride concentrations after 1, 3, 5, 8, and 24 hours (Table 2-1).

Table 2-2. Detailed summary of experimental conditions in Chapter 2

Goal of Experiments	Electrolyte Composition	Initial pH; pH held Constant?	Adsorbent Used; Dose (g/L)	# of Replicates	Corresponding Figure
Minimum Dose	Sri Lankan groundwater (Table 2-1)	6, No	All bauxite ores; 2-11 g/L	2	2-5, 2-10a
Dissolved Al/Fe Measurements	NaF (10 mg/L) NaCl (35 mM) HCO_3^- (5 mM) DI Water (Binary-Solute matrix, Table 2-1)	6, No	All bauxite ores; 10 g/L	2	-
Adsorption Isotherms	NaF (10-100 mg/L) NaCl (1-6 mM) MES (50 mM) HCO_3^- (5 mM) DI water	6, Yes	All bauxite ores; 4/L	2	2-7a
Adsorption Envelopes	NaF (10 mg/L) NaCl (6-16.5 mM) Varying Buffers HCO_3^- (5 mM) DI water	4-8, Yes	All bauxite ores; 6/L	2	2-7b
Equilibrium pH	NaCl (35 mM) DI water	-	All bauxite ores; 1 g/L	2	Table 2-3
Calcium and Carbonate Measurements	DI water	No	All bauxite ores; 4 g/L	2	Table 2-3
FTIR	NaF (100 & 500 mg/L) DI water	-	Guinea bauxite 2 g/L	2	2-8a
Effect of Ionic Strength	NaF (10 mg/L) NaCl (1-100 mM) HCO_3^- (5 mM) DI water	6, No	Guinea bauxite 10 g/L	3	2-8b
Cost Calculations	Synthetic and real groundwater (Table 2-1)	6, No	Guinea bauxite & AA; 2-11 g/L	2	2-10b
Kinetics	Sri Lankan groundwater (Table 2-1)	6, No	Guinea bauxite & AA; 10 & 4 g/L	2	2-11

Upon completion of each adsorption experiment, a 5 mL aliquot of the slurry was collected in a syringe and filtered using 0.2 μm filters before analysis. Filtered aliquots were then mixed with equal volumes of Total Ionic Strength Adjustment Buffer (TISABII) to complex aluminum and iron, and free-fluoride (F^-) was measured using a fluoride ion-selective electrode (Mettler Toledo SevenMulti, perfectION). A Consort meter (R3620) was used to measure pH.

2.2.4. Calculating Minimum Required Dose

Experiments to determine the minimum bauxite dose (g/L) to mitigate an initial fluoride concentration of 10 mg F^-/L to below the WHO-MCL (1.5 mg F^-/L) were conducted in a synthetic Sri Lankan groundwater matrix (4.3 mM Ca^{2+}, 7.5 mM Mg^{2+}, 8.5 mM HCO_3^-, 0.2 mM SO_4^{2-}, 1.6 mM Si, and 0.6 mM NO_3^- as N) derived from British Geologic Survey (BGS)[2] measurements to represent the average composition of groundwater in fluoride-contaminated regions in South Asia (Table 2-1). The pH was initially set to 6.0 ± 0.1 and was not kept constant during experiments (final pH values ranged between 6.3 and 7.5). Batch tests using incremental adsorbent doses allowed us to narrow down the range of the minimum required dose, which was determined by linear interpolation of three separate doses yielding an equilibrium fluoride concentration that tightly bracketed the target of 1.5 mg F^-/L. Figure 2-4 shows an example of the method used to calculate minimum doses of adsorbents required to reach the WHO-MCL. Dissolved aluminum (Al) and iron (Fe) concentrations were measured using inductively coupled plasma optical emission spectroscopy (ICP-OES, Varian 720 Series) upon bauxite's equilibration with a binary-solute matrix (5 mM HCO_3^- + 35 mM NaCl + 10 mg F^-/L) for 3 hours (Table 2-1).

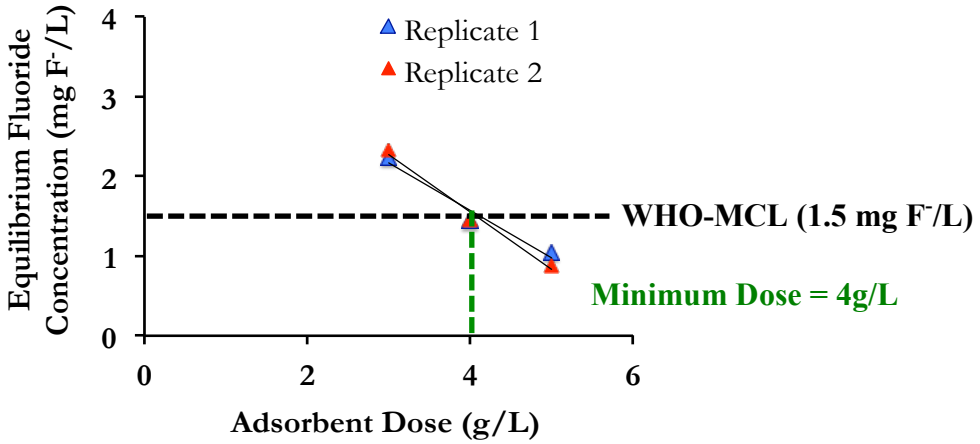

Figure 2-4: Determination of minimum required adsorbent dose using linear regression. Replicate data on the fluoride removal performance of three different adsorbent doses are plotted and the approach to find the x value for y = 1.5 (WHO-MCL) is shown.

2.2.5. Adsorption Isotherms and Adsorption Envelopes

Experiments to determine the adsorption isotherm of each ore were conducted in DI water with 50 mM 2-(*N*-morpholino)ethanesulfonic acid (MES, to maintain the pH at 6.0 ± 0.2) and 5 mM HCO_3^- (to introduce a natural source of buffering/alkalinity) amended with 5, 10, 20, 40, 60, 80, and 100 mg/L of NaF. Ionic strength was kept constant at 61 mM by adding NaCl as necessary and a constant bauxite dose of 4 g/L (40 ± 0.1 mg/10 mL) was used in these experiments. Adsorption isotherms were fitted against the Langmuir and Freundlich models using ISOFIT (non-linear regression). The intrinsic fluoride adsorption capacity and affinity of each ore were then determined using the best-fit model.

Experiments to determine the adsorption envelope of each bauxite ore were conducted in 5 mM HCO_3^- amended with the following buffers: 50 mM $NaCH_3COO/CH_3COOH$ (pH 4 and 5), 50 mM MES (pH 6), 14 mM Na_2HPO_4/NaH_2PO_4 (pH 7), and 10 mM $Na_2B_4O_7/H_3BO_3$ (pH 8). Ionic strength was kept constant at 61 mM across experiments by adding NaCl as necessary. A constant initial fluoride concentration of 10 mg F^-/L and a bauxite dose of 6 g/L (60 ± 0.1 mg/10 mL) were used in these experiments.

Additional studies described in the following Sections 2.2.6 and 2.2.7 (e.g., ionic strength, FTIR, and treatment costs) were conducted using Guinea bauxite ore due to its high performance in fluoride removal.

2.2.6. Investigation of Removal Mechanisms

Experiments to determine the effect of ionic strength on fluoride removal were conducted with Guinea bauxite (dose: 10 g/L (100 ± 0.1 mg/10 mL)) in 5 mM HCO_3^- and 10 mg F^-/L amended with increasing concentrations of NaCl (1, 10, 100 mM). All experiments were conducted in duplicate or more.

To detect potential changes in hydroxyl (-OH) peaks before and after batch adsorption experiments, Guinea Bauxite was analyzed by horizontal attenuated total reflection Fourier transform infrared spectroscopy (HATR-FTIR, Perkin Elmer Spectrum One). Samples were prepared by exposing 2 g/L of milled bauxite ore either to a solution of 500 mg F^-/L or to a solution of 100 mg F^-/L replaced every hour for 4 hours. All samples were allowed to equilibrate for 24 hours and dried overnight at 100°C before analysis. ATR-FTIR analysis was conducted by setting a force gauge to 60N to press 0.1 g of each dry powdered bauxite sample completely flat on a glass slide (covered area was approximately 0.2 mm^2, the size of a ballpoint pen tip).

2.2.7. Estimating Treatment Costs

Per capita annual material costs of remediating fluoride-contaminated groundwater with Guinea bauxite and with AA were compared in the various synthetic and real groundwater matrices listed in Table 2-1. For these calculations, adsorption tests were conducted using each adsorbent a single time in a batch process where the adsorbent was dispersed in the water and kept well mixed for 24 hours. For AA, additional calculations were made based on conservative assumptions that AA could be used in a column filter (breakthrough at 75% capacity), regenerated (through NaOH treatment) to 70% of its previous capacity, and re-used for 4 cycles, consistent with data from a 2014 EPA report.[37] These estimates did not include potential material losses during treatment or the cost of treatment chemicals (e.g., acids and bases). The following assumptions were also made: volume of drinking water per capita per day = 7.5 L[53] and material costs of AA and bauxite = \$1.5/kg[37] and \$0.03/kg[36], respectively, according to current market prices.

2.3. RESULTS AND DISCUSSION

2.3.1. Differences in Bauxite Ore Performance

Figure 2-5 shows the minimum dose of each bauxite ore required to reduce fluoride from an initial concentration of 10 mg F^-/L in synthetic Sri Lankan groundwater to below the WHO-MCL of 1.5 mg F^-/L. Guinea, Ghana, and USA bauxites performed similarly, with minimum required doses of 9.5-10.6 ± 1.0 g/L, while India bauxite had a significantly lower performance, with a minimum required dose of 22.8 ± 1.0 g/L. This result shows that the geographical source of bauxite ore can greatly impact its fluoride removal performance, and suggests that the chemical composition of the ore may affect fluoride removal. Compared to previous studies, which used different bauxite ores (e.g., from Malawi, Texas, Tanzania, etc.), levels of processing, solution matrices, and initial fluoride concentrations, the measured minimum required doses in Figure 2-5 are lower, possibly due to a finer particle size.[40–48]

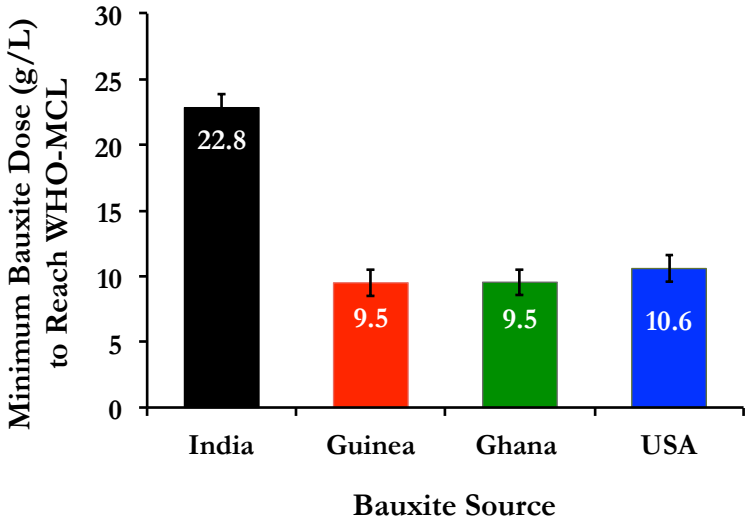

Figure 2-5: Minimum bauxite doses required to remediate 10 mg F^-/L to below the WHO-MCL (1.5 mg F^-/L) in synthetic Sri Lankan groundwater (initial pH of 6.0). We present averages from duplicate experiments and error bars are the larger of (1) the range from duplicate tests and (2) measurement errors associated with the fluoride probe.

2.3.2. Chemical Characterization of Bauxite Ores

Figure 2-6a reports zeta potentials of bauxite ores measured between pH 2 and 12 in deionized (DI) water along with points of zero charge (PZC). The measured PZC of India and Ghana bauxites (6.8 and 7.2) are higher than the PZC of Guinea and USA bauxites (5.0 and 5.3), indicating that bauxites from India and Ghana may have higher surface charge in some electrolytes, which should have a positive (if any) effect on fluoride adsorption, not a detrimental effect. In comparison, the reported PZC of the pure minerals gibbsite and hematite respectively range from 8-9[49,54] and 5.5-7.5.[55] Differences in PZC cannot account for the lower performance of India bauxite in comparison to Ghana, Guinea, and USA bauxites (Figure 2-5).

Figure 2-6b shows the chemical composition of the 4 bauxite ores as determined by XRF. All bauxites contained approximately 22-29% Al and < 2% Ti (LOD_{Al}= 0.1%, LOD_{Ti} = 0.01%). Ghana, India, and Guinea bauxites had significant and comparable fractions of Fe (~11-14%) (LOD_{Fe}= 0.005%). Si was found in all bauxite ores, and its content ranged from 0.5% in Ghana bauxite to approximately 9% in USA bauxite (LOD_{Si}= 0.1%). The Ca content in most bauxite ores was below the detection limit (LOD_{Ca}=0.02%) except in India bauxite, which contained 1.8% Ca. Figure 2-6c shows the XRD patterns of the 4 bauxite ores. The main crystalline Al phase in all bauxites was gibbsite, and an additional crystalline Fe phase, hematite, was detected in Ghana, India, and Guinea bauxites. Consistent with XRF results, kaolinite was found only in USA bauxite and calcium carbonate ($CaCO_3$) was found only in India bauxite.

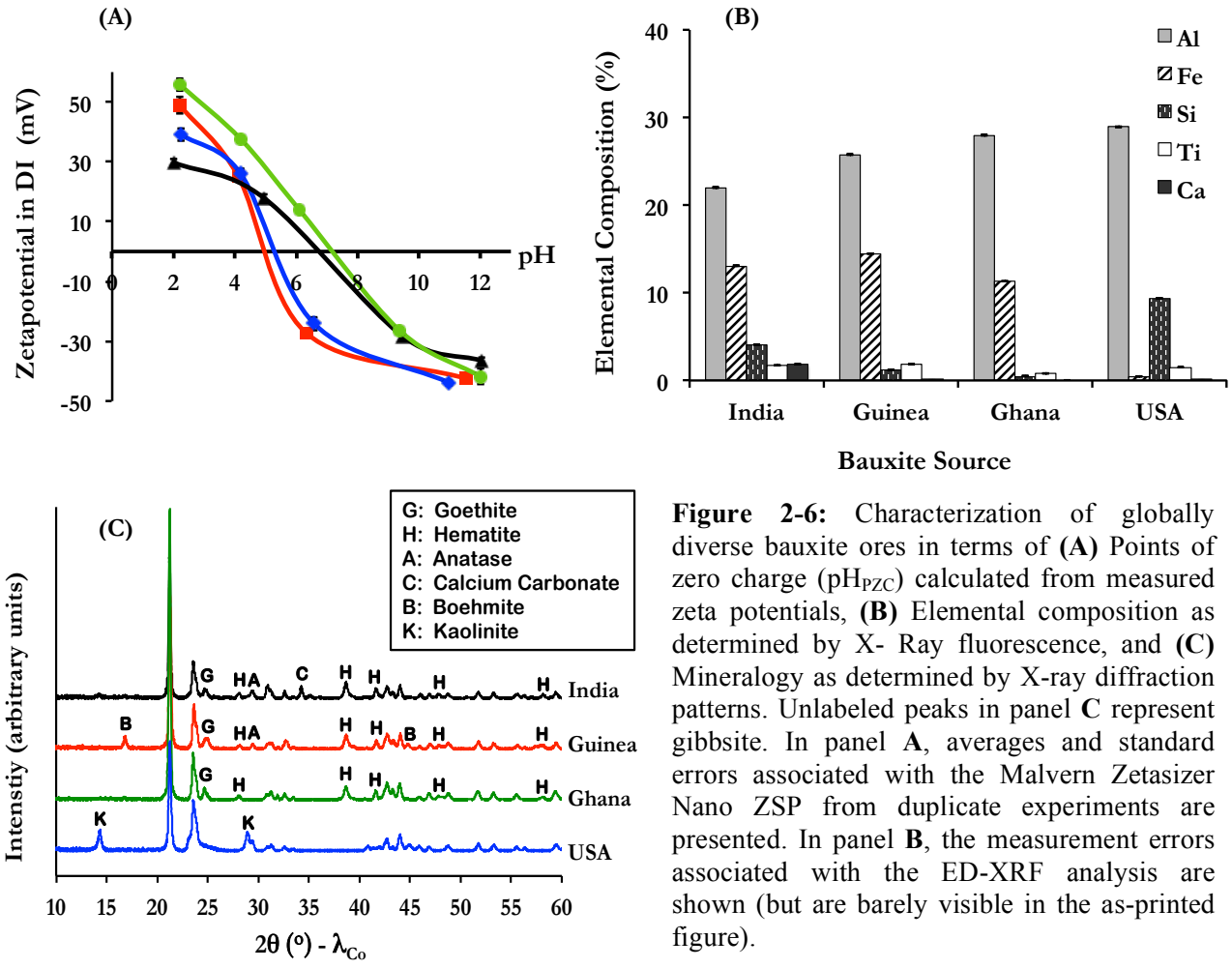

Figure 2-6: Characterization of globally diverse bauxite ores in terms of **(A)** Points of zero charge (pH_{PZC}) calculated from measured zeta potentials, **(B)** Elemental composition as determined by X- Ray fluorescence, and **(C)** Mineralogy as determined by X-ray diffraction patterns. Unlabeled peaks in panel **C** represent gibbsite. In panel **A**, averages and standard errors associated with the Malvern Zetasizer Nano ZSP from duplicate experiments are presented. In panel **B**, the measurement errors associated with the ED-XRF analysis are shown (but are barely visible in the as-printed figure).

Taken together, the results in Figures 2-6 show that India bauxite's point of zero charge, Al content, and dominant mineral phases cannot explain its lower fluoride removal performance. In particular, the small difference in Al content between India bauxite and the 3 other ores (3.8-6.9%) would not likely result in a greater than two-fold difference in the minimum required dose (as suggested by the similar fluoride removal performance of Guinea and USA bauxites despite their 3.2% difference in Al content) (Figure 2-5 and 2-6b). Similarly, the observed differences in fluoride removal performance do not appear to be correlated with the Fe, Si, and Ti contents and

phases. In contrast, the presence of $CaCO_3$ in India bauxite might be correlated with its poorer fluoride removal performance. Regardless of the bauxite ore used, ICP-OES results demonstrated minimal leaching of Al and Fe ions (final concentrations were below the detection limit; < 0.01 ppm), resulting in treated water in conformity with WHO standards for Al and Fe (< 0.2 and < 0.3 ppm respectively).

2.3.3. Effect of Initial Fluoride Concentration and Solution pH on Fluoride Removal

Figure 2-7a shows the relationship between adsorption density and equilibrium solute concentration for each bauxite ore. The experimental isotherms were best fitted to the Freundlich model described by: $q=KC_e^{1/n}$ where q (mg/g) is the adsorption density, C_e (mg/L) is the equilibrium adsorbate (fluoride) concentration, and K (adsorption capacity) and n (adsorption strength) are constants. The shape of the Freundlich isotherm indicates potential multi-site complexation, especially given the first dip, which indicates saturation of a high-affinity site. The fitted Freundlich parameters (K and 1/n) of the 4 ores, specified in Figure 2-7a, showed no statistically significant difference (overlapping 95% confidence intervals), which indicates that all four bauxites have a similar intrinsic capacity and affinity for fluoride. This finding suggests that differences in fluoride removal efficiencies seen between the 4 bauxite ores in Figure 2-5 are not caused by differences in intrinsic adsorption capacity or affinity (e.g., a lower K value for USA bauxite compared to Guinea and Ghana bauxites did not result in significantly lower fluoride removal). Consistent with the virtually identical adsorption isotherms, the BET surface areas of the 4 milled bauxite ores were not significantly different, ranging from 14.1 ± 4.0 to 17.2 ± 2.5 m^2/g, indicating comparable adsorption capacities (Figure 2-7a).

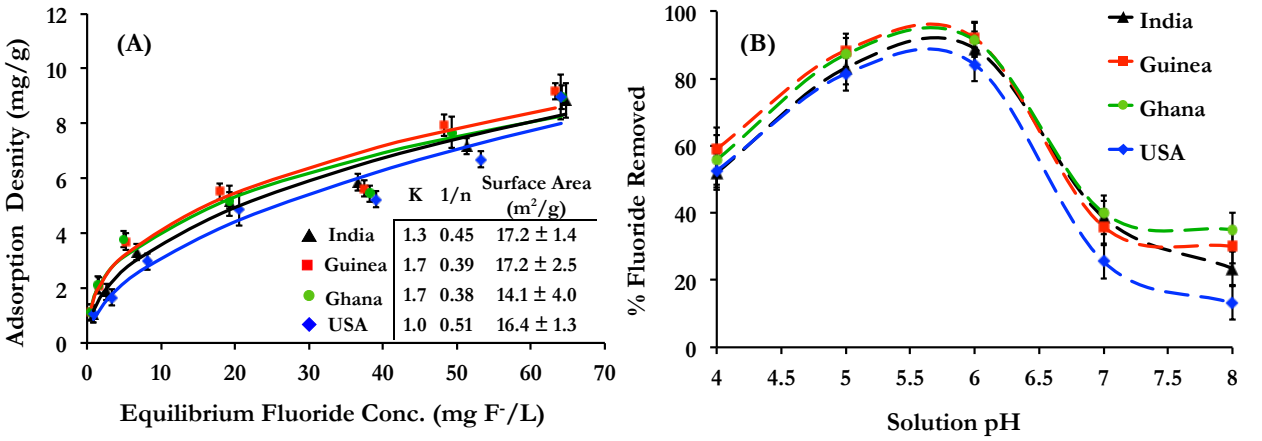

Figure 2-7: Adsorption **(A)** Isotherms and **(B)** Envelopes of the 4 bauxite ores showing the respective effects of equilibrium fluoride concentration and pH on fluoride removal. Adsorption isotherms were characterized in 50 mM MES + 5 mM HCO3, at a constant pH of 6.0, with solid lines indicating the Freundlich model fit generated by ISOFIT (fitted model constants and BET surface area are also indicated). Adsorption envelopes were characterized in 5 mM HCO3 + buffers, at constant ionic strength, with dashed lines drawn to guide the eye and not to represent a model fit. Averages from duplicate experiments are presented and error bars are the larger of the range from duplicate tests and measurement errors associated with the analytical equipment used (e.g., fluoride probe, Tristar II 3020).

Figure 2-7b shows that the adsorption envelopes of the 4 bauxite ores were close to identical, indicating a similar adsorption behavior throughout a wide pH range (4-8). In addition, all ores had an optimal adsorption pH of 5.0-6.0. The adsorption envelopes demonstrate that pH has a substantial influence on fluoride removal, with a unit pH increase above the optimum pH leading to a 50-59% decrease in fluoride adsorption. These adsorption envelopes are characteristic of anion sorption, with a decrease in removal both at lower and higher pH, due to competing reactions of surface protonation and OH^- complexation, respectively. At acidic pH, the ligand-promoted dissolution of gibbsite and the formation of aqueous fluoride complexes (e.g., HF, AlF^{2+} AlF_2^+, AlF_3, AlF_4^-, AlF_5^{2-}, or AlF_6^{3-}) might also contribute to the decrease in fluoride removal.[35]

2.3.4. Influence of Equilibrium pH on Fluoride Removal

In batch adsorption experiments in Sri Lankan groundwater with an initial pH of 6.0 ± 0.1 (Figure 2-6), it was observed that the final solution pH after 24 hours was significantly higher for India bauxite (average final pH 7.5 ± 0.1) compared to the 3 other ores (average final pH 6.4 ± 0.1, 6.3 ± 0.1, and 6.5 ± 0.1 for USA, Guinea, and Ghana bauxites, respectively). Although a minor pH increase is expected upon fluoride adsorption due to the replacement of OH^- groups on the surface of gibbsite,[35,49,56] this ion exchange process cannot account for the observed differences in final pH between India bauxite and the other 3 ores.

To further understand the effect of bauxite addition on solution pH, experiments were conducted in a simpler electrolyte (35 mM NaCl) in the absence of fluoride and characterized the equilibrium pH and composition of the suspension after 24 hours. As summarized in Table 2-3, India bauxite had a significantly higher equilibrium pH (pH 8.1 ± 0.1), compared to Guinea, Ghana, and USA bauxites (pH 6.6 ± 0.1, 6.5 ± 0.1, and 6.2 ± 0.4 respectively), which coincided with substantially higher concentrations of Ca and inorganic carbon (334 ± 2 μM Ca and 398 ± 9 μM C, respectively, for India bauxite, compared to ≤ 3 μM Ca and ≤ 35 μM C, respectively, for the other bauxites).

Table 2-3. Characterization of a suspension (initially 35 mM NaCl) in equilibrium with each bauxite ore in terms of pH, dissolved calcium, and dissolved inorganic carbon (DIC). We present averages from duplicate experiments and reported errors are the larger of the range from duplicate tests and measurement errors associated with the analytical equipment used (e.g., pH probe, Ion Chromatograph, and Total Carbon Analyzer).

Bauxite Source	Equilibrium pH	Equilibrium [Ca^{2+}] (μM)	Equilibrium [DIC] (μM)
India	8.1 ± .1	334 ± 2	398 ± 9
Guinea	6.6 ± .1	1.0 ± .4	21 ± 12
Ghana	6.5 ± .1	0.2 ± .1	30 ± 6
USA	6.2 ± .4	3 ± 1	35 ± 10

These results are indicative of the dissolution of $CaCO_3$ (only present in India bauxite, Figure 2-6b and 2-6c), and the following theoretical calculation supports the idea that observed increase in pH corresponds to the increase expected from the dissolution of ~3mM $CaCO_3$. The increase in pH resulting from the dissolution of calcium carbonate when India bauxite is mixed into a solution with 35mM NaCl can be estimated assuming an open system with zero initial alkalinity (see calculation in Table 2-4). The calculations demonstrate that under these conditions, the dissolution of 334 μM of $CaCO_3$ is theoretically expected to increase the solution pH to approximately 8.1, which is equal to the measured value reported in Table 2-3.

Table 2-4. Calculation of equilibrium solution pH in open system with dissolution of calcium carbonate.

$$2\,[Ca^{2+}] + [H^+] = [OH^-] + [HCO_3^-] + 2\,[CO_3^{2-}]$$

$$[Ca^{2+}] = 0.000334\ \text{M (measured value from Table } 2-3)$$

$$[OH^-] = \frac{10^{-14}}{[H^+]}$$

$$[HCO_3^-] = \frac{10^{-11.23}}{[H^+]}$$

$$[CO_3^{2-}] = \frac{10^{-21.56}}{[H^+]^2}$$

Substitution yields a cubic function, which can be used to solve for x = $[H^+]$

$$[H^+]^3 + 2 * (0.000334)[H^+]^2 - (10^{-14} + 10^{-11.23})\,[H^+] - 2 * 10^{-21.56} = 0$$

$$[H^+] = 8.92 * 10^{-9}$$

$$pH = -\log[H^+] = -\log[8.92 * 10^{-9}] = \mathbf{8.05}$$

It can thus be concluded that the substantially higher equilibrium pH of India bauxite compared to the other ores is likely due to the presence and partial dissolution of $CaCO_3$. Because an alkaline pH (i.e., solution pH >> $PZC_{bauxite}$) is unfavorable for fluoride adsorption (Figure 2-7b), the dissolution of $CaCO_3$ is likely responsible for the lower performance of India bauxite (Figure 2-5, Figure 2-6a). This finding is also consistent with the adsorption isotherms of the globally diverse bauxite ores being similar under constant pH conditions (Figure 2-7a). Taken together, the results suggest that when surface capacities and affinities are comparable, fluoride removal is primarily influenced by the presence of trace alkaline minerals such as $CaCO_3$, which alter the equilibrium solution pH.

2.3.5. Fluoride Adsorption Mechanism

HATR-FTIR measurements showed a decrease in transmittance in –OH peaks (3650-3350 cm^{-1}) upon fluoride adsorption, independent of the loading method (Figure 8a). Previous FTIR studies have shown that the peak at ~3400 cm^{-1} is characteristic of the stretching vibration of hydroxyl groups on the surface of gibbsite. [51,57] Therefore, these results suggest that similar to pure gibbsite, bauxite also forms a specific, inner-sphere complex with fluoride through ion exchange with –OH groups. Figure 2-8b shows that varying ionic strength over 2 orders of magnitude (1-100 mM) did not affect fluoride removal with Guinea bauxite, despite increased charge screening of the adsorbent surface. This finding (along with the PZC data presented in Figure 2-6a) indicates that weak, outer-sphere electrostatic interactions do not play a major role in fluoride adsorption on bauxite in the pH range of interest, consistent with the primary role of inner-sphere complexation previously reported for pure gibbsite.[35,49,56] A visual representation of the inner-sphere complexation mechanism is shown in Figure 2-9.

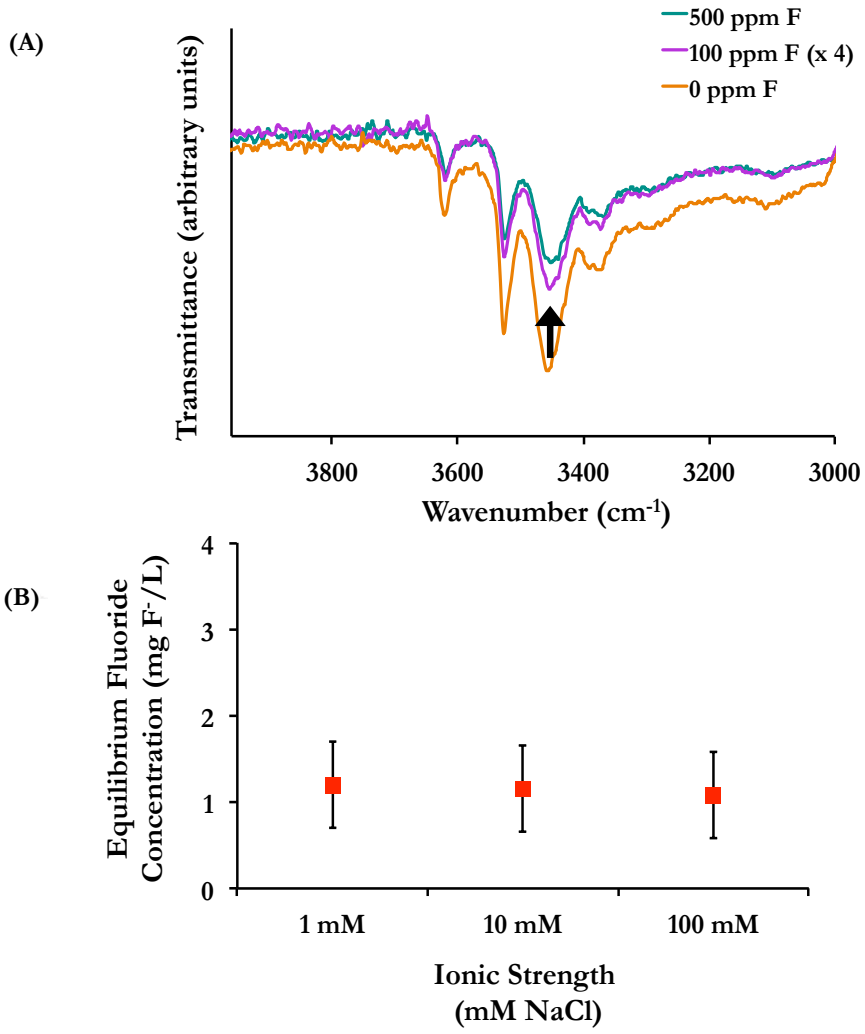

Figure 2-8: Investigation of fluoride removal mechanisms through **(A)** HATR-FTIR absorbance spectra for Guinea bauxite (2 g/L dose) with an initial fluoride loading of 0, 100 x 4 (replaced every hour for 4 hours), and 500 ppm F^-, respectively, and **(B)** Study on effect of ionic strength on fluoride removal using Guinea bauxite. Initial [F^-]: 10 mg F^-/L; Dose: 10g/L.

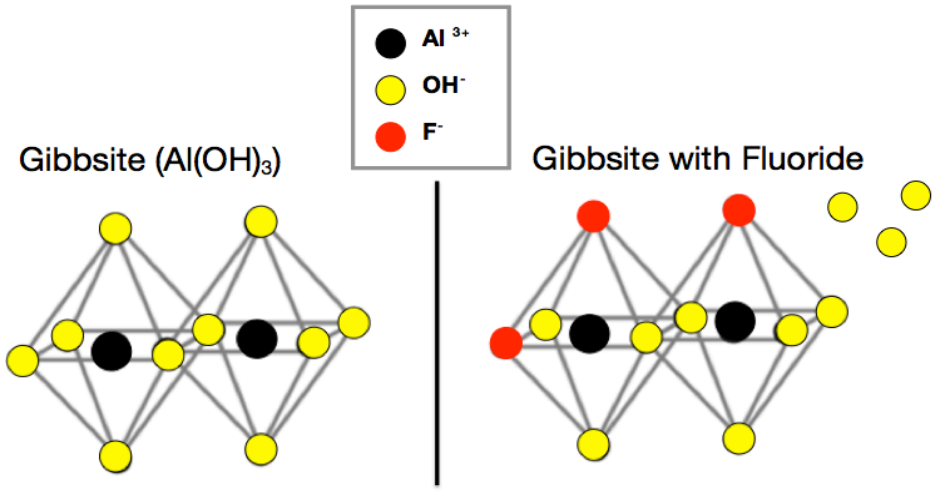

Figure 2-9: Diagram demonstrating the removal mechanism of fluoride on gibbsite as through ion exchange between fluoride (F-) and hydroxyl groups (OH-) on the surface of gibbsite. Image adapted from Dr. Katherine Alfredo's dissertation.[119]

2.3.6. Comparison between Activated Alumina and Guinea Bauxite

Figure 2-10a compares the minimum required doses and materials costs for remediating a simple binary-solute electrolyte and several synthetic and real groundwater matrices (Table 2-1) with AA and Guinea bauxite (the best performing bauxite ore, Figure 2-5). The cost estimates are based on experimentally determined minimum required doses, which demonstrate that on average, Guinea bauxite requires 1.5-2.3 times the dose of AA (depending on groundwater composition) to remediate an initial fluoride concentration of 10 mg F^-/L to the WHO-MCL (Figure 2-10a). Larger doses required for bauxite are consistent with its lower specific surface area and thus lower adsorption capacity (Figure 2-8a). For both AA and bauxite, the minimum dose required to reach the WHO-MCL is higher in synthetic and real groundwater than in the simple binary-solute electrolyte (NaCl + $NaHCO_3$). This trend is likely due to the presence of potentially competitive species such as oxyanions (e.g., $Si(OH)_4$, HCO_3^-, SO_4^{2-}, NO_3^-),[6,47,58] as well as NOM (likely to be present in real groundwater).[6,59]

Figure 2-10b shows that the material cost of fluoride remediation with Guinea bauxite is consistently and substantially lower than with AA across all tested groundwater matrices: ~23-33 times lower if AA is assumed to be used in a single-use batch process and ~ 11-18 times lower if AA is assumed to be used in a column process with media regeneration. Even when using regenerated AA (which is ~50% cheaper than single-use AA), treatment with AA is still significantly more expensive than with Guinea bauxite as single-use batch media. When considering the worst performing ore (India bauxite, which requires 2.4 times the minimum dose of Guinea bauxite to remediate Sri Lankan groundwater, as shown in Figure 2-5), the material cost of using bauxite remains 4.7-8.8 times lower than AA.

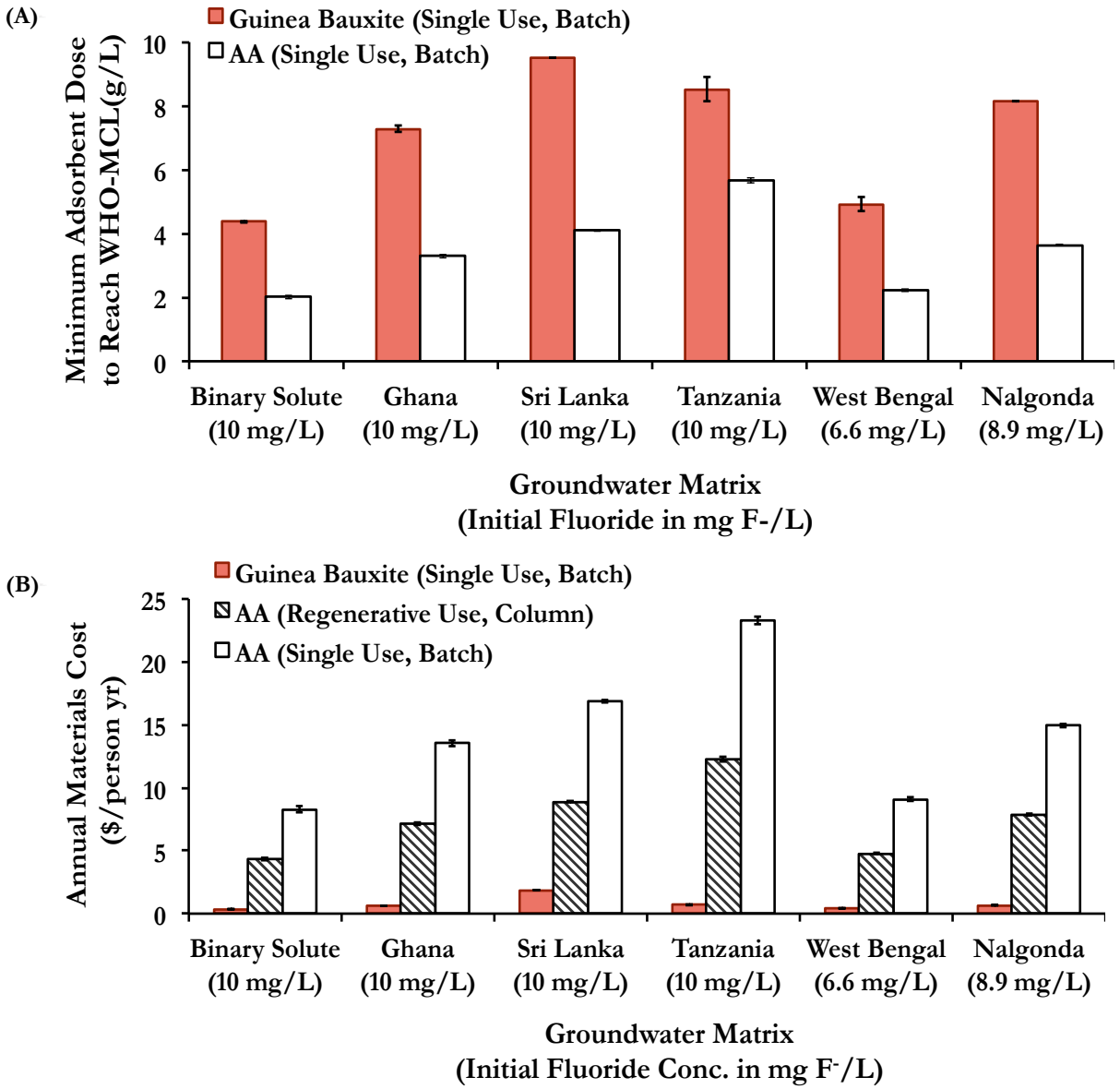

Figure 2-10: Comparison of **(A)** Minimum required doses and **(B)** Annual per capita material costs for remediating several synthetic groundwater matrices containing 10 mg F^-/L and two real groundwater matrices (West Bengal and Nalgonda) to the WHO-MCL (1.5 mg F^-/L) using milled Guinea bauxite (single-use batch process) and unmodified AA (both in single-use batch process and in column process with media regeneration). Averages are presented and error bars represent the larger of the range from duplicate tests and measurement errors associated with the fluoride probe. Cost calculations are described in Section 2.2.7 and recipes for the groundwater matrices are given in Table 2-1.

In addition to the cost advantage, another benefit of using mildly processed bauxite as single-use batch media is that in contrast to AA, the preparation of the bauxite adsorbent does not involve any activation or regeneration with hazardous chemicals that can increase the leaching of metals in the product water. Finally, it should be noted that Guinea bauxite has fluoride removal kinetics comparable to AA, with approximately 80% of total fluoride removal occurring in the first hour in synthetic Sri Lankan groundwater, confirming that bauxite can realistically be used in field applications (Figure 2-11).

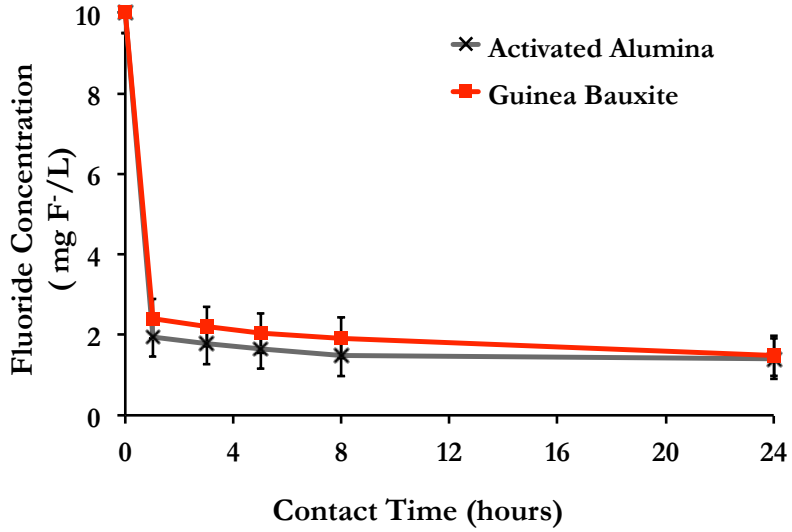

Figure 2-11: Fluoride concentration as a function of contact time for Activated Alumina and Guinea Bauxite (respective doses: 4 and 10 g/L) in synthetic Sri Lankan groundwater (Table 2-1). Doses used correspond to the minimum required doses to reduce initial fluoride concentrations of 10 mg/L to the WHO-MCL (1.5 mg/L) after 24 hours of contact time. Averages and ranges from duplicate experiments are presented.

2.3.7. Implications for Groundwater Treatment

Overall, the findings of Chapter 2 demonstrate that mildly processed bauxite ore is an effective fluoride removal adsorbent capable of remediating high fluoride levels (up to 10 mg F^-/L) to below the WHO-MCL in groundwater characteristic of affected regions, and is a cost-competitive alternative to AA. When considering fluoride removal on a per unit surface area basis, the shown results suggest that bauxite has a stronger affinity for fluoride adsorption than AA (i.e., bauxite requires only approximately twice the dose despite having seven times lower SSA than AA).

The key results showed that the chemical composition, and therefore the geographical origin of the bauxite ore, could substantially impact its fluoride removal performance. Specifically, it was found that the presence of trace minerals such as $CaCO_3$ could reduce the affinity of bauxite ore for fluoride by modifying the equilibrium suspension pH. Similarly, other alkaline (e.g., $MgCO_3$, $CaMg(CO_3)_2$, etc.) or acidic (e.g., humic materials, silicates) minerals often present in bauxite ores[52] may affect their fluoride removal performance. It was also shown that fluoride adsorbs to bauxite through an ion-exchange process; therefore future work should focus on the effect of potential competitors commonly found in groundwater (e.g., Cl^-, NO_3^-, SO_4^{2-}, PO_4^{3-}, NOM), which may significantly impact the efficiency of fluoride removal by bauxite in the field. Of the four tested ores, India bauxite was the least efficient, but it is geographically closest to 1/3 of the fluoride-affected population,[11] which highlights the need to analyze the tradeoffs between transportation costs and adsorption efficiency. In the following chapter, we investigate non-hazardous and locally appropriate activation methods to potentially enhance India bauxite's performance and cost-competitiveness.

CHAPTER 3. Effective Groundwater Fluoride Remediation Using Inexpensively Processed Indian Bauxite

Submitted to *Journal of Hazardous Materials* on June 30th, 2017. Adapted with permission from Cherukumilli, K.; Maurer, T.; Hohman, N. J.; Mehta, Y.; and Gadgil, A., Effective Groundwater Fluoride Remediation Using Inexpensively Processed Indian Bauxite.

3.1. BACKGROUND

In Chapter 2, we proposed the use of mildly processed bauxite, a globally abundant ore of aluminum, as a potentially viable, effective, and ultra low-cost fluoride adsorbent alternative to activated alumina. We established that globally diverse bauxite ores vary dramatically in terms of fluoride removal performance.[60] When controlling for adsorbent surface area and intrinsic fluoride affinity and capacity, fluoride removal efficiency was primarily governed by solution pH and adsorption was highest at a pH range of 5.0 - 6.0, consistent with prior studies.[47,61] In comparison to bauxites ores from sites in Ghana, Guinea, and the USA, an Indian-sourced bauxite had the worst fluoride removal performance because it contained the trace mineral calcite ($CaCO_3$), which upon dissolution increased solution pH well above the optimal pH for fluoride removal.

India represents one-third of the global fluorosis burden.[11,62] Excess fluoride contamination of groundwater occurs in approximately 70% of the states in the country.[63] However, India is also the fifth major global producer and exporter of bauxite[50], so there exists a promising opportunity to better utilize the abundant bauxite ore available throughout India rather than importing more efficient raw ores from other countries for affordable fluoride remediation. If the performance of Indian bauxite could be modified through a mild, low-cost processing method, the use of locally sourced bauxite might be a practical and inexpensive route towards alleviation of a significant source of chronic human suffering. To understand and overcome the challenges with using Indian bauxite as presented in the previous study[60], here we report a straightforward route to enhance its fluoride removal performance via thermal treatment of the ore at 300°C. We also investigate the feasibility and impact of acidification of the fluoride-contaminated groundwater using readily available mineral acids or carbon dioxide gas (CO_2).

The primary objectives of Chapter 3 are 1) to report the impact of heating and chemical transformation of bauxite on fluoride removal, 2) to discuss the effects of groundwater acidification on fluoride removal, and 3) to evaluate cost tradeoffs of the various combinatorial treatment scenarios to determine the feasibility of using Indian bauxite as an effective groundwater defluoridation method in low-income regions.

3.2. METHODS

3.2.1. Indian Bauxite Preparation and Characterization

The bauxite used in this study was collected from the same mine in Visakhapatnam, Andhra Pradesh, India as in Chapter 2. For brevity, we hereafter refer to this bauxite as "Indian Bauxite" while recognizing that India is a very large country and diverse sources (of differing physical and chemical compositions) of bauxite exist within India. This bauxite was dried overnight (T=100°C) to remove moisture prior to milling 15 g for 15 minutes in an agate milling jar of a shaker ball mill (SPEX8000) to generate micron-sized powders, as confirmed by dynamic light scattering (Malvern Zetasizer Nano ZSP). The powdered Indian bauxite was then heated in a muffle furnace (Fisher Scientific, Isotemp) for 4h at the desired temperatures (100°C, 200°C, 300°C, and 400°C) for heat activation studies, based on previously documented methods.[61,64,65] Scanning electron microscopy (SEM) images of some of the thermally activated bauxite samples are shown below in Figure 3-1.

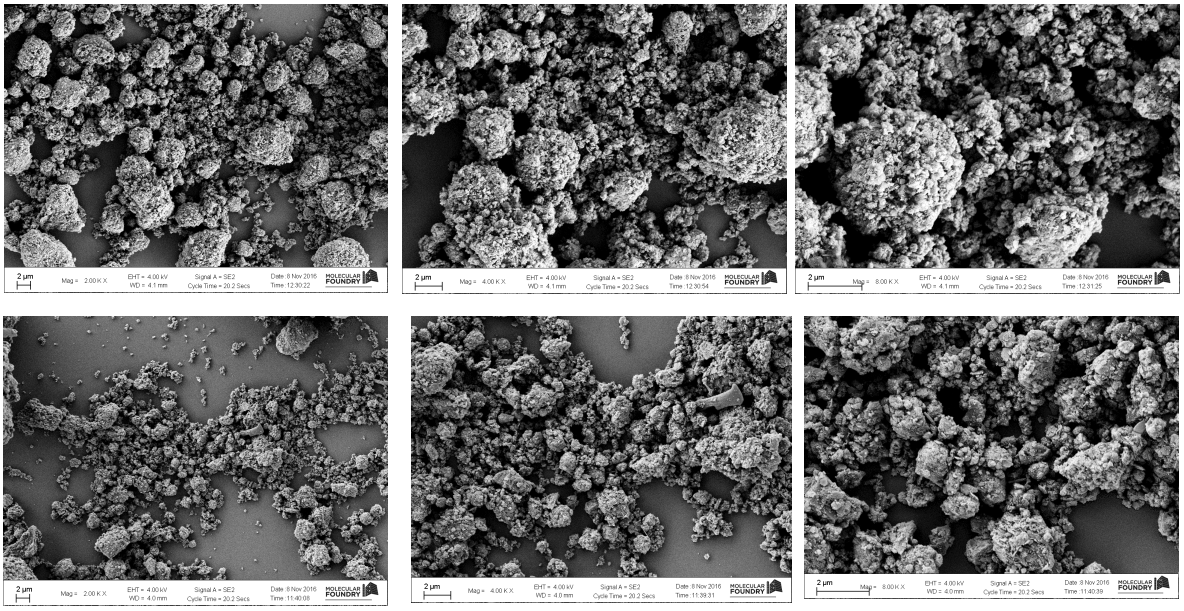

Figure 3-1. Images of milled Indian bauxite ores heated at 100°C (top row) and 300°C (bottom row) at 2K, 4K, and 8K magnification (left to right) using a Scanning Electron Microscope (SEM).

Percent mass loss and chemical composition of the effluent gases resulting from heating of the bauxite samples were measured using Thermogravimetric Analysis and Mass Spectrometry (TGA-MS, TA Instruments Q5000IR TGA, with attached Pfeiffer Vacuum Thermostar Mass Spec). Procedures to determine bulk crystalline mineral composition from X-ray diffraction (XRD) patterns and specific surface area (SSA) using multipoint Brunauer-Emmett-Teller (BET) measurements have been described in our previous publication[60] and are detailed in Section 2.2.1.

3.2.2. Batch Adsorption Experiments

Standard batch adsorption experiments were designed to determine the respective effects of reaction time, bauxite activation temperature, groundwater acidification method, and bauxite dose (g/L) on fluoride removal in a synthetic Sri Lankan groundwater matrix. The recipe for this matrix shown in Table 3-1 was based on data from the British Geological Survey and selected to overlap with our previous work[60] in Chapter 2 (Section 2.2.2). The initial fluoride concentration for all lab-synthesized groundwater for the batch adsorption experiments in this study was set to 10 mg F^-/L using a stock solution of 100 mg/L NaF. Measurement of fluoride concentration and preparation of stock solutions for the Sri Lankan synthetic groundwater were as outlined in Section 2.2.3.

Table 3-1. Chemical composition of synthetic groundwater matrix used in this study. This recipe is based on British Geologic Survey (BGS)[120] measurements and values are reported as gravimetric target concentrations in ppm (mg/L). This synthetic groundwater was prepared using stock solutions of 100 mM $CaCl_2$, 100 mM $MgCl_2$, 200 mM $NaHCO_3$, 100 mM Na_2SO_4, 10 mM SiO_2 ($Na_2SiO_3 \bullet 5H_2O$), and 10 mM $NaNO_3$.

Component	Sri Lankan Groundwater (mg/L)
F	10.0
Ca	173.0
Mg	179.0
HCO_3^-	516.0
SO_4^{2-}	15.5
Si	45.0
NO_3^- as N	9.0

To determine the effects of reaction time on fluoride removal, kinetics experiments were conducted for 2 h and samples were taken at 5,10, 20, 40, 60, 90, and 120 min. All subsequent batch adsorption studies were conducted for a shorter reaction time (20 min) because fluoride adsorption after 20 min was marginal and shorter reaction times lower field operational costs, making the overall process more attractive for real-world application.

In each acidification experiment, 20 mL of synthetic Sri Lankan groundwater was acidified using either 1.1M Hydrochloric acid (HCl) or pressurized CO_2. The desired solution pH for these experiments was selected based on previous studies[47,60] which experimentally verified pH 6.0 ± 0.1 as an optimal pH for fluoride adsorption with bauxite ore. To determine differences in fluoride removal based on timing of groundwater acidification, we experimentally examined the following two cases where (1) the source of acidification (HCl or CO_2) was gradually added

in small quantities over the duration of the study to control solution pH at 6.0 ± 0.1, and (2) the measured total volumes of HCl and CO_2 required to maintain the pH at 6.0 ± 0.1 in case (1) were initially added at once in bulk, so that the desired pH was reached by the end of the experiment. In total, approximately 5-10 mL of 1.1M HCl and 0.02-0.04 kg CO_2 were added per liter of water to maintain the solution pH at 6.0. To determine the influence of drastic solution pH changes in case (2) on the potential leaching of harmful trace contaminants from the dispersive bauxite adsorbent, we used an Inductively Coupled Plasma Mass Spectrometer (ICP-MS, Agilent Technologies 7000 series) to measure drinking water contaminants regulated by the US Environmental Protection Agency's enforceable Maximum Contaminant Limits (EPA-MCL) for primary contaminants (e.g., Ag, As, Cd, Cr, Pb, Se) and non-mandatory Secondary Maximum Contaminant Limits (SMCL) for secondary contaminants (e.g., Al, Cu, Fe, Mn, Zn) in the product water.[66]

Six combinatorial treatment scenarios (i.e., 100°C and 300°C with and without groundwater acidification using HCl or CO_2) were compared in terms of fluoride removal performance by calculating the optimal solid: liquid ratio (referred to as henceforth 'minimum required dose') to remediate 10 mg F^-/L down to the WHO-MCL (1.5 mg F^-/L) using a method described previously in Section 2.2.4.[60]

3.2.3. Estimation of Combinatorial Treatment Costs

For each combinatorial treatment scenario described above, we estimated annual per-capita costs of remediating fluoride-contaminated groundwater using conservative assumptions about material and electricity costs, supply chain logistics, and bauxite processing and water treatment plant design.

As demonstrated in Figure 3-2, our model assumes that raw bauxite ore is first transported from a mine to a central processing plant (CPP) located 500 km away, the average distance between bauxite-producing mines and Indian districts with endemic skeletal fluorosis.[67] The CPP in our analysis was designed to have appropriate infrastructure to process (e.g., crush, mill, and heat) enough raw bauxite for 500 villages of 1,000 people each. We assumed each village would have a separate water treatment plant (WTP) and that the villages were located at an average of 25 km from the CPP. The average village population was chosen based on a previous publication[68] and the population density for the circular area covered by the CPP was calculated (~300 people/km^2) using Indian Census data[69] for the three most heavily affected states with endemic fluorosis (i.e., Gujarat, Rajasthan, and Madhya Pradesh).

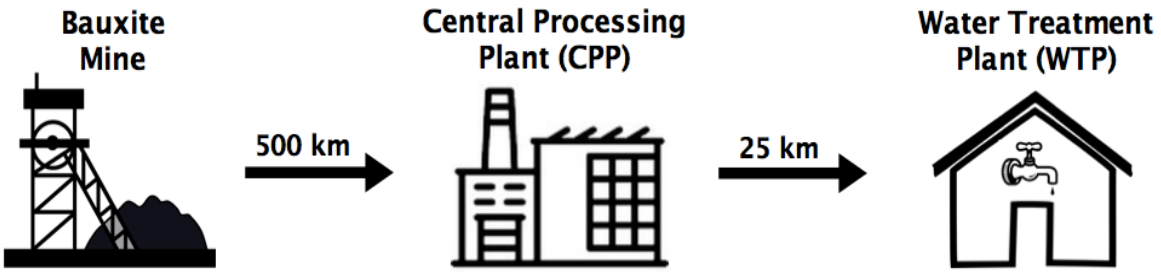

Figure 3-2: Schematic representation of the flow of mined bauxite ore to central processing plants and water treatment plants.

Figure 3-3a shows a map of districts in India with reported endemic fluorosis, excess groundwater fluoride contamination, and locations of bauxite mines. To generate this map, we used data outlined and sourced in the following spreadsheet: https://tinyurl.com/fluoride-bauxite-locations. Polygon shape files were sourced from the GADM database of Global Administrative Areas (http://gadm.org) and the map data was visualized using R libraries (raster, sp, maptools, and ggplot2). Details regarding distances between locations and population densities are also provided in the spreadsheet above. The example in Figure 3-3b demonstrates the feasibility of the assumptions used in our cost model by showing that the bauxite used in this study (from Visakhapatnam) could realistically be transported to a CPP in Nalgonda District (a fluorosis affected region located approximately 500km away).

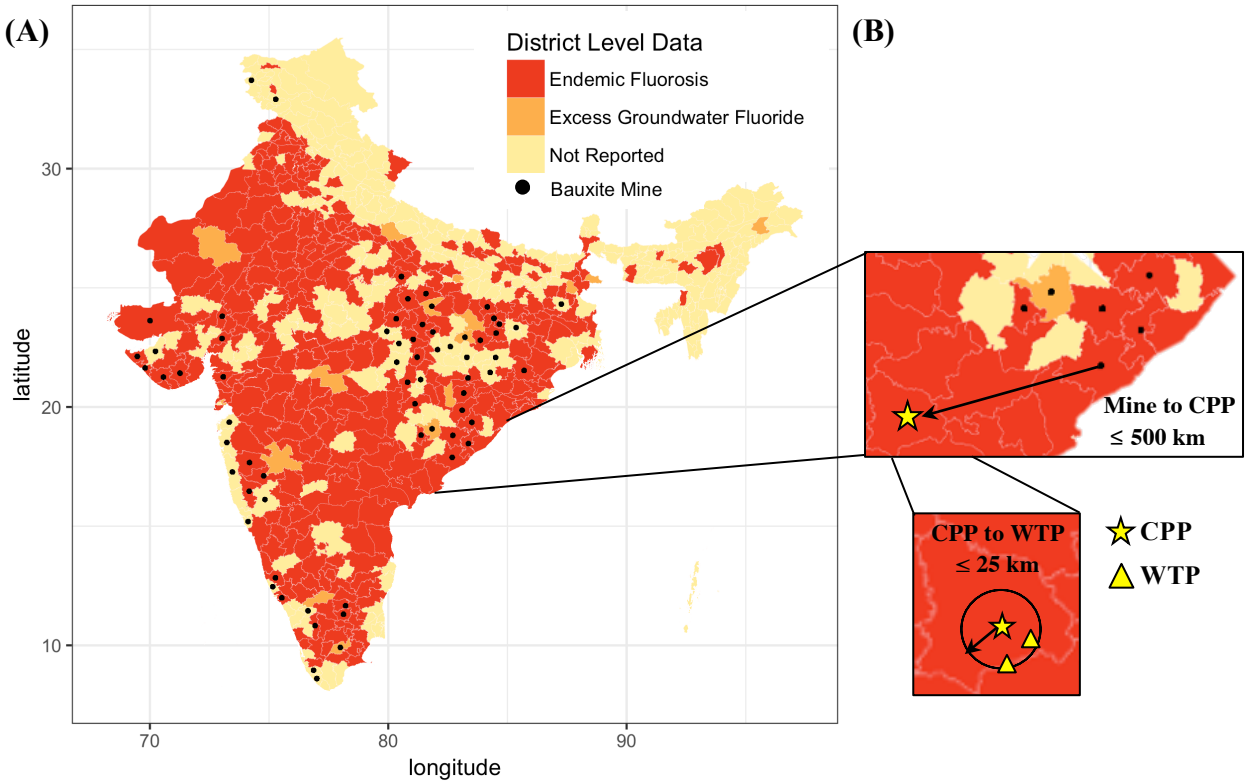

Figure 3-3: Maps of **A)** districts in India with endemic fluorosis (red), excess groundwater fluoride (orange), and bauxite mines locations (black dots), and **B)** A realistic example of the relative locations of a bauxite mine in Visakhapatnam, a central processing plant (CPP, shown as a yellow star) in Nalgonda District, and water treatment plants (WTP, shown as yellow triangles). This figure was generated using R visualization packages.

The WTP shown in Figure 3-4 was designed to operate at a minimum capacity of 5000 L water/day to meet the daily need for the village, assuming a per capita use of 5 L/person. We selected this value as a field-relevant compromise between the anecdotal reports of daily per capita water purchase value in rural regions (2 L/person) from small commercial water providers in India (e.g., WaterLife, and WaterHealth (India)) and the WHO's recommendation for daily per capita drinking and cooking water needs (7.5 L/person).[53] We assumed that a realistic field pilot WTP relying on bauxite-based defluoridation would require a mixing tank (for addition of

bauxite and acid/CO_2 to fluoride-contaminated groundwater), a settling tank (as an initial clarification step through alum coagulation and sedimentation), a tube settler and micron filter (to reduce the turbidity of the water to < 1 NTU), and a holding tank (for storing treated water) (Figure 3-4).

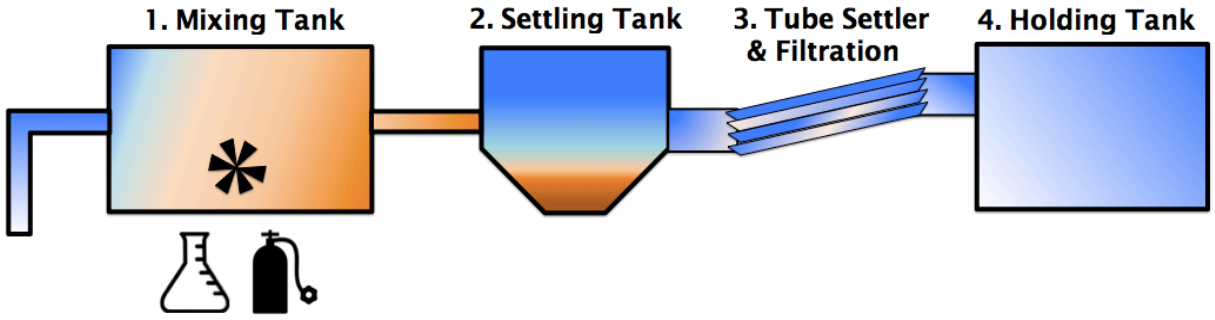

Figure 3-4: Schematic representation of treatment processes at a village-scale community water treatment plant. Bauxite is injected and mixed into pumped groundwater for 20 minutes after which it enters a settling tank. The supernatant water is dosed with 30 mg/L alum and run through tube settler for additional particle removal to ensure WHO turbidity standards are met (< 1 NTU). Treated water is stored in a holding tank, which can be connected to automated dispensing machines or kiosks for sale of water.

Machinery was assumed to have a lifetime of 10 years, a conservative estimate that also accounts for the possibility of premature obsolescence due to up-scaling and growth. For each piece of equipment, cost estimates were solicited for products currently available on the market. Additionally, we made the conservative assumption that physical assets had no resale value at the end of their lifetimes. The costs of specific portions of the WTP, namely the pumps, tube settler, and power supply, were obtained from actual fabrication cost estimates of a 10,000 L/day field implementation of an electrochemical arsenic remediation technology in operation since April 2016 in West Bengal, India.[70] This large pilot demonstration plant is a scaled up implementation of a 600L prototype, whose cost estimates are reported by our group in an earlier publication.[71] Since that field trial involved daily processing twice the amount of water as ours (10,000L versus 5,000L), we are comfortable with these estimates being especially conservative.

For cost estimation, we chose current market prices of tanks (3), pumps (5), and consumables (e.g., bauxite ore, alum, acid, and CO_2), and reasonable values for shipping costs, which are all outlined in a spreadsheet found at https://tinyurl.com/cpp-wtp-cost-analysis. This spreadsheet contains references and information relating to the capital costs and electricity consumption of each piece of equipment, including specific companies and model numbers used to get a range of quotes. In addition, lifetime and duration of use assumptions are listed. The spreadsheet is divided into four primary sections reflecting the stages of processing: mining (raw bauxite costs); transportation; central processing plant; and water treatment plant costs.

We estimated electricity costs based on the power rating of the machinery; the number of hours of use based on laboratory tests; and an assumed electricity cost of $0.07/kWh. The plant was assumed to be able to operate up to 16 hours per day. Additional details regarding the cost estimation data (e.g., equipment model numbers, companies, lifetime and usage assumptions, etc.) are also in the spreadsheet (link provided above). Since the primary purpose of the cost

estimate is to compare processing options, the analysis ignores the time value of money and uncertainties around the exchange rate between dollars and rupees. All estimates are given in current (2017) USD assuming an exchange rate of 67 rupees to the dollar. Our estimates include core technology costs and exclude costs of land, operator salaries, buildings, storage sheds, public education, marketing, and outreach to target populations. We have excluded these latter costs since they contain greater uncertainty and since they are common to all treatment options, they do not contribute to differentiating between the different treatment options.

3.3. RESULTS AND DISCUSSION

3.3.1. Characterization of Thermally Activated Bauxite

Figure 3-5a shows the percent mass loss from the Indian bauxite ore during heating, as determined by Thermogravimetric Analysis (TGA). Approximately 15% of the mass loss occurred at temperatures between 250°C and 300°C, and the compound given off was identified via Mass Spectrometry (MS) to be water. Figure 3-5b shows the XRD patterns of Indian bauxite heated at four temperatures (100°C, 200°C, 300°C, and 400°C). The main crystalline Al phase was gibbsite, and additional crystalline Fe oxide phases (goethite and hematite) and Ti oxide phase (anatase) were detected. The diffraction patterns for crystalline gibbsite in bauxite samples heated at 100°C and 200°C were indistinguishable (100°C peaks have been truncated in Figure 3-5b for convenient display) and these same major peaks were absent when the bauxite was heated at 300°C or 400°C. The iron and titanium oxide phases present in bauxite did not show the same structural deformations or changes in crystallinity at 300°C or 400°C. Figure 3-5c presents surface area and particle size measurements of the heated Indian bauxite. The particle size remained constant across samples heated between 100°C and 400°C but the surface area increased dramatically (> 15X) from approximately 11 m^2/g at 100°C to 170 m^2/g at 300°C.

Taken together, the results in Figure 3-5 show that the major impacts of heating Indian bauxite occur between 200°C and 300°C, indicated by the decrease in crystallinity and increase in surface area due to loss of structural waters of hydration. Other studies have reported a similar structural deformation of crystalline gibbsite minerals present in bauxite when heated between 200°C and 300°C, as it transforms to the more amorphous boehmite phase through partial dehydroxylation (e.g., loss of two waters of hydration).[49,61,72,73]

(A)

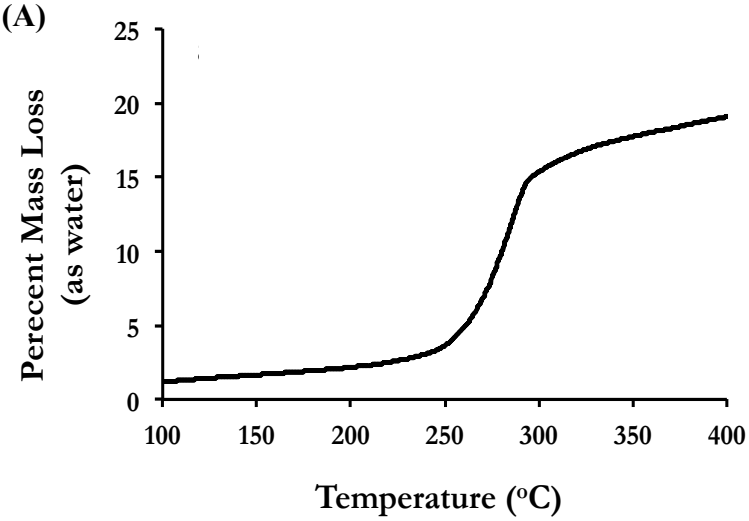

(B)

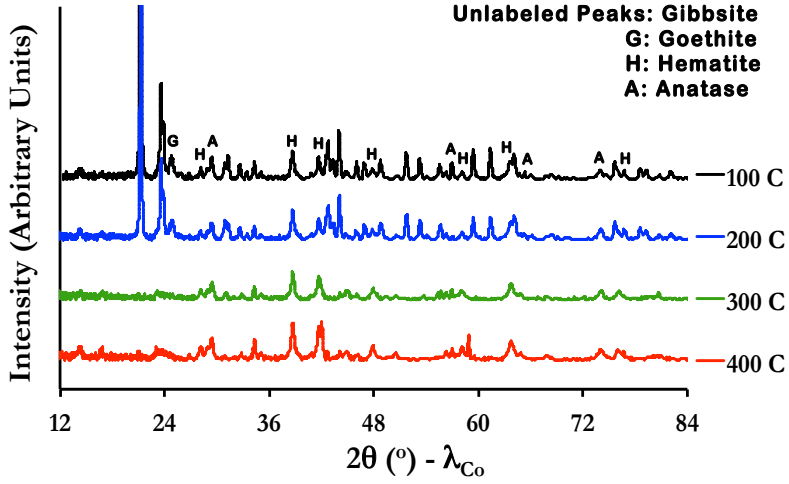

(C)

Heating Temperature (°C)	Particle Size (μ)	Specific Surface Area (m^2/g)
100	1.16 ± 0.56	11.0 ± 3.0
200	1.13 ± 0.42	11.6 ± 2.4
300	1.08 ± 0.45	169.2 ± 13.2
400	1.17 ± 0.4 4	173.4 ± 25.3

Figure 3-5: Characterization of thermally-activated Indian bauxite in terms of **A)** Mass loss measured using Thermogravimetric Analysis and Mass Spectrometry (TGA-MS), **B)** Mineralogy as determined by X-ray diffraction patterns, and **C)** Particle size and specific surface area measurements. In panel **C**, we present averages from duplicate experiments and errors are the largest of the range from duplicate tests and measurement errors associated with the analytical equipment used (e.g., DLS, Tristar II 3020).

3.3.2. Effect of Thermal Activation of Bauxite on Fluoride Removal

Bauxite samples heated at temperatures greater than 200°C showed substantial improvement in fluoride removal performance in batch adsorption studies using bauxite as a one-time-use dispersive media (Figure 3-6). Consistent with the similar XRD peaks and surface area measurements presented in Figure 3-5b and 3-5c, fluoride removal performance of bauxite samples heated at $T \leq 200°C$ or $T \geq 300°C$ were comparable. Figure 3-6 also demonstrates that fluoride adsorption using bauxite was rapid; within 20 minutes the system was close to reaching equilibrium (fluoride concentrations did not vary greatly between 20 min. and 2 hr.), a finding confirmed in our prior study.[60] This initial rapid uptake is likely due to surface adsorption and the flattening of the curve after 20 minutes represents a kinetically slower process of long-range diffusion into interior pores of our bauxite media. Researchers studying other aluminum-based adsorbents used for fluoride removal have reported similar kinetic trends.[28,29,74]

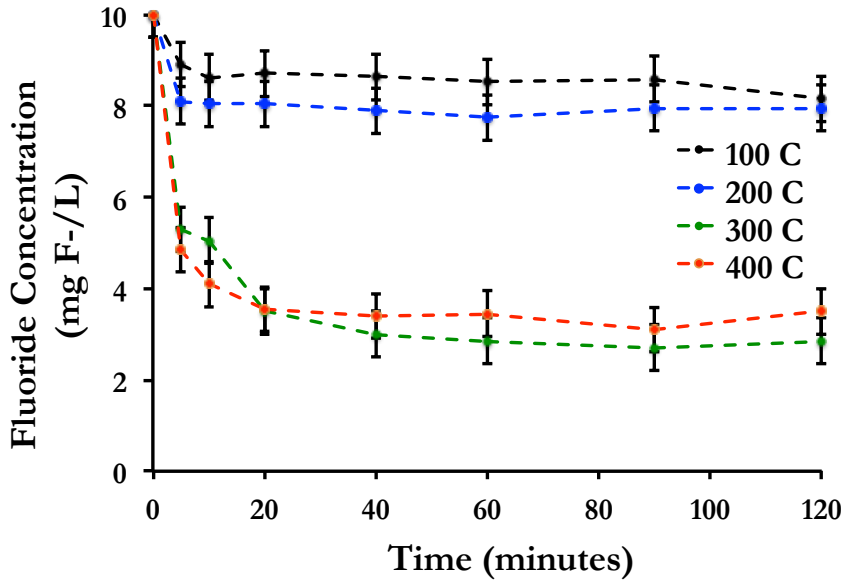

Figure 3-6: Fluoride concentration as a function of contact time for thermally activated Indian Bauxite (raw dose 10 g/L) in alkaline synthetic Sri Lankan groundwater (initial pH 8.7). We present averages and error bars as the larger of the range from duplicate batch adsorption tests and measurement errors associated with the analytical equipment used (e.g., fluoride probe).

3.3.3. Effect of Groundwater Acidification on Defluoridation and Leaching of Metals

Figure 3-7 shows the improvement in fluoride removal performance a result of lowering the alkaline initial pH of Sri Lankan groundwater (pH ~ 8.7) down to 6.0 ± 0.1 through addition of HCl or bubbling of CO_2 gas. In all the experiments summarized in Fig 3-7, a dose of 10 g/L (= 0.169 g/20 mL) of raw bauxite (with or without heating) was added to synthetic Sri Lankan groundwater containing an initial fluoride concentration of 10 mg F^-/L. Regardless of the source of acidification, the improvement in fluoride removal due to groundwater acidification appears to be consistent. Furthermore, regardless of whether the acid source was added continually over the duration of the 20 min experiment or whether it was added in bulk initially did not make a difference in the overall percent of fluoride removal. At a dose of 10 g/L, bauxite heated to

300°C and added to acidified water is close to reaching the WHO-MCl for fluoride, but we require a much larger dose of 100°C bauxite to remediate an initial concentration of 10 mg F^-/L. Our ICP-MS data indicates the product water for all the treatment scenarios in Figure 3-7 is compliant with EPA guidelines for drinking water for a majority of the primary and secondary contaminants (e.g., aqueous concentrations of Ag, As, Cd, Cu, Fe, Pb, Se, and Zn were below 25% of the EPA-MCL or SMCL). Additional research must be conducted to measure the concentration of total dissolved solids (TDS) in solution after groundwater acidification with HCl because this could affect the taste of the product water.

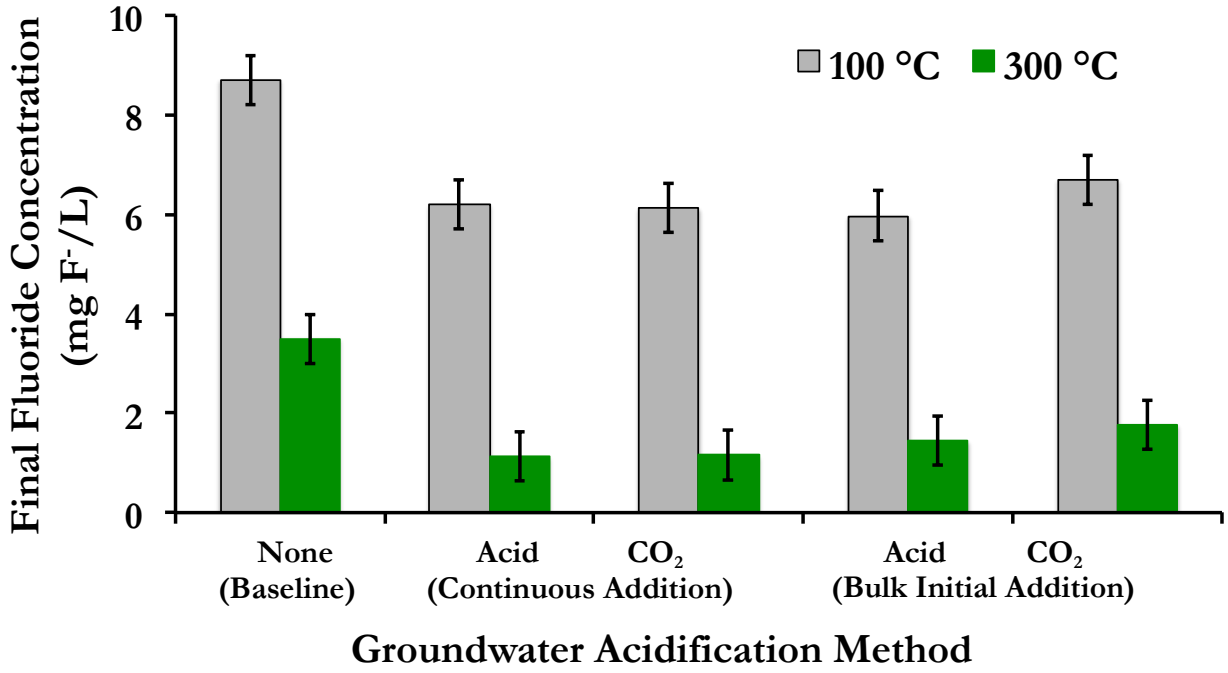

Figure 3-7: Effect of various groundwater acidification methods on fluoride removal (initial concentration 10 mg F^-/L). Batch adsorption experiments were conducted for 20 minutes in synthetic Sri Lankan groundwater using Indian bauxite (raw dose 10 g/L) heated at 100 °C or 300 °C. Solution pH was maintained at 6.0 ± 0.5 through either continuous or bulk initial addition of acid (1.1 M HCl) or CO_2 (rate 0.25 L/min). We present averages and error bars as the larger of the range from duplicate batch adsorption tests and measurement errors associated with the analytical equipment used (e.g., fluoride probe).

Table 3-2 highlights elements of concern (e.g., Cr, Mn, and Al) that approached or exceeded the EPA limit in the product water of our batch experiments outlined in Figure 3-7. Our data indicate that Cr dissolution was more prominent in treatment scenarios using 300°C bauxite although the Cr concentrations in product water were still below 75% of EPA-MCL (100 ppb Cr). This trend may be due to an increase in the reaction rate at higher temperatures for oxidation of insoluble Cr (III) to its more soluble Cr (VI) form. In scenarios where 300°C bauxite was added to acidified groundwater, Mn concentrations tended to be higher and the concentration of Mn exceeded the EPA-MCL (50 ppb Mn) for one particular treatment scenario where 300°C bauxite was used in groundwater acidified through bulk acid addition. It was also observed that for all treatment scenarios where 100°C bauxite was added to acidified groundwater, the concentration of Al in the product water exceeded the EPA-MCL (200 ppb Al).

One explanation for why Al dissolution is less prominent in 300°C bauxite is that bauxite dehydroxylates to boehmite in that temperature range and boehmite is generally less soluble than gibbsite, as reported by other theoretical studies.[75,76]

Table 3-2. Concentrations (in ppb) of metals of concern in product water from batch experiments outlined in Figure 3-7 measured using ICP-MS. We present averages and the range from duplicate batch adsorption tests.

EPA Standards (MCL in ppb)		100° C					300° C				
		No pH Adjustment	Continuous Addition		Bulk Addition		No pH Adjustment	Continuous Addition		Bulk Addition	
			Acid	CO_2	Acid	CO_2		Acid	CO_2	Acid	CO_2
Cr	**100**	0.7 ± 0.2	0.9 ± 0.2	0.8 ± 0.0	1.3 ± 0.2	1.0 ± 0.3	64 ± 3.4	54 ± 0.5	64 ± 1.5	49 ± 0.4	60 ± 1.4
Mn	**50**	1.6 ± 0.5	21 ± 1.5	25 ± 1.4	37 ± 8.7	23 ± 3.9	2.4 ± 0.8	46 ± 1.2	41 ± 1.7	57 ± 2.4	45 ± 3.3
Al	**200**	49 ± 4.2	253 ± 6.5	261 ± 38.6	619 ± 37.0	373 ± 18.6	65 ± 3.0	46 ± 2.1	101 ± 1.3	59 ± 11.2	103 ± 10.6

Ratio of Measured Concentration to MCL			
< 25%	25-74%	75-99%	≥ 100%

3.3.4. Comparing Combinatorial Treatment Scenarios

Figure 3-8 presents the minimum bauxite doses required to remediate 10 mg F^-/L down to the WHO-MCL in synthetic Sri Lankan groundwater. For the baseline (no acidification) scenario, the minimum required dose for 100°C bauxite (~287 g/L) is approximately 13.5 times larger than that for 300°C bauxite (~21 g/L). Irrespective of additional groundwater acidification by acid or CO_2, the minimum required dose for 100°C bauxite (~76 g/L) is approximately 7.4 times larger than that for 300°C bauxite (~11 g/L). Acidification reduces the required minimum dose for bauxite heated to 100°C and 300°C by approximately 3.7 times and 2.7 times respectively. Looking at magnitude of doses alone, it appears that a dose approaching or exceeding ~20 g/L is impractical, and that the most effective choice for defluoridation (requiring least material) would be heat-activated bauxite (at T= 300°C) in groundwater acidified with a mineral acid (e.g., HCl).

In addition, Table 3-3 presents the total cost for treating water for each of the possible processing methods. This analysis takes into account the capital and operational costs of the entire bauxite processing and water treatment process. Numbers are reported in USD per person per year; where multiple cost estimates were obtained, the median value is reported plus/minus the low-end range. The results indicate that the total cost of the unheated bauxite is up to an order of magnitude higher than it is for the heated bauxite. This implies that the additional cost of purchasing and operating an oven is offset by the substantially higher material and transportation costs associated with using the much larger required doses of raw unheated bauxite. The general trends were as expected: the raw material and transportation costs were significantly higher for the processes that required additional bauxite. On the other hand, the cost of the CPP step was lower for the unheated bauxite since no oven would be required. The costs at the WTP were highly dependent on the costs of hydrochloric acid and CO_2 for the cases where they are used.

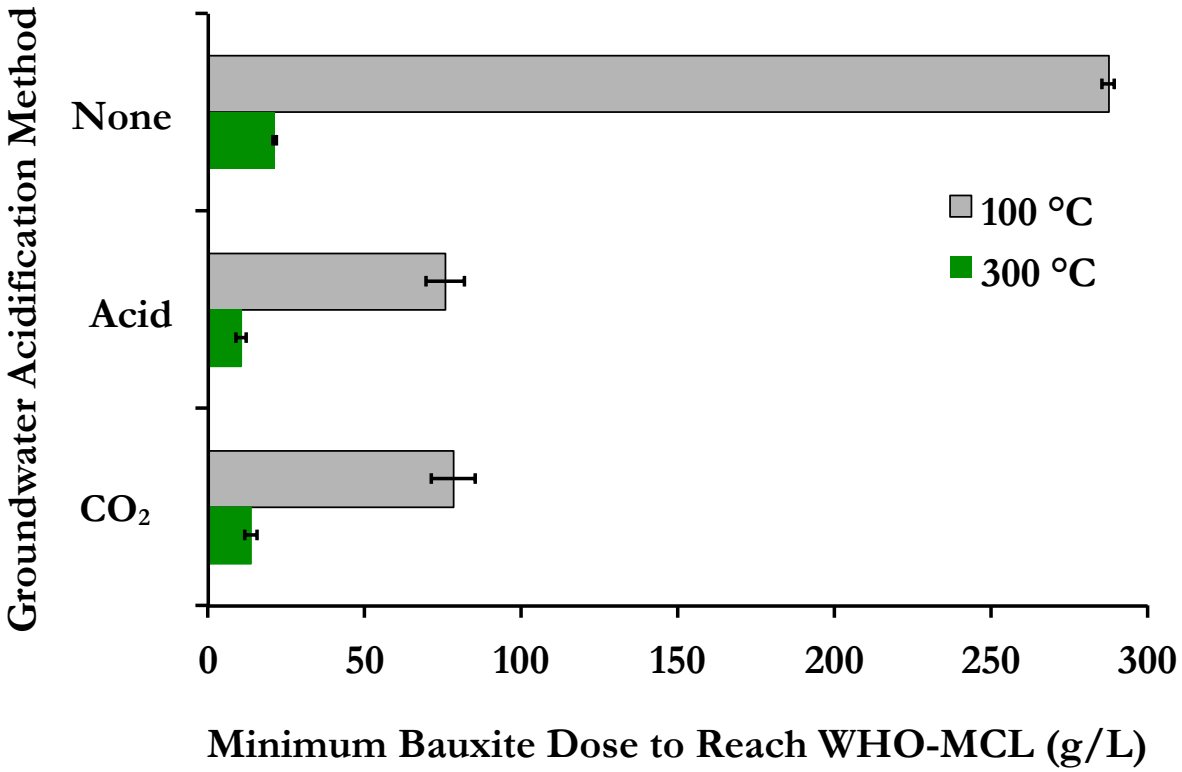

Figure 3-8: Comparison of minimum required doses for various combinatorial treatment scenarios. Batch experiments run for 20 minutes in Sri Lanka groundwater. We present averages and error bars as the larger of the range from duplicate batch adsorption tests and measurement errors associated with the analytical equipment used (e.g., fluoride probe).

Table 3-3. Treatment costs (in $ per person per year) of combinatorial treatment scenarios including heating Indian bauxite and acidifying groundwater using acid or CO_2. Costs for the baseline treatment scenario (no heating or groundwater acidification) are not reported because the minimum required dose (Figure 3-8) is unrealistically high for field operation. The values and errors presented in this table reflect the median cost estimate ± the low-end range based on three cost estimates obtained from quotes given by the manufacturing companies of the machinery and items (exceptions were instances where machinery was custom designed and estimated for this process). This reporting method avoids presenting potentially unrealistic extreme low and high cost estimates. Additional details can be found in Section 3.2.3.

Groundwater Acidification Method	Heating Temperature (°C)	Mining & Transport Costs	CPP Costs	WTP Costs	Total Costs
None	100	-	-	-	-
	300	7.22	0.059 ± 1.6E-04	1.60 ± 1.12E-04	8.88 ± 1.04E-02
Acid	100	25.8	0.018 ± 3.6E-04	4.72 ± 2.24E-05	30.6 ± 1.06E-02
	300	3.56	0.059 ± 1.6E-04	3.24 ± 1.02E-02	6.86 ± 1.04E-02
CO_2	100	26.7	0.022 ± 3.6E-04	35.5 ± 1.71E-01	62.3 ± 2.09E+01
	300	4.61	0.059 ± 1.6E-04	19.9 ± 2.49E-02	24.6 ± 9.08E+00

We found that using (300°C) heated bauxite in groundwater acidified with hydrochloric acid ("300-acid") was the cheapest option at $6.86 per person per year. This option benefits from significantly reduced raw material and transportation costs relative to the other options, though it makes the WTP process more expensive due to the cost of the acid. The second cheapest option was using heated bauxite without the additional groundwater acidification step ("300-only"); the total cost of this process was $8.88 per person per year, or about 23% higher than the cheapest option (300-acid). The other three options (300-CO_2, 100-acid, and 100-CO_2) were significantly more expensive (3.6, 4.5, and 9.1 times respectively) than the cheapest option.

The most significant sources of error in this analysis are likely the simplification of the material processing and water treatment steps for the purposes of cost comparison, since we did not consider land acquisition costs or labor costs. These estimates mean that the most field-relevant and favorable processing option is likely to be to use heated bauxite without groundwater acidification (300-only) because this treatment scenario balances the benefits of lower bauxite doses (Figure 3-8) with increased logistical simplicity. Moreover, since pH control using mineral acids and the Cr/Mn/Al data reported in Table 3-2 present potential additional safety constraints that are not included in this cost analysis but would certainly increase labor and operational costs, heating without any acidification may also be the most optimal and practical treatment scenario to follow in field operation. It is worth noting that the low-end ranges reported in Table 3-3 are significantly lower than the median total cost estimates, and the overall conclusion of the analysis remains unchanged. We therefore believe that uncertainty in the costs that were included is not a major source of error.

3.3.5. Implications for Groundwater Treatment

In this Chapter, we increased the effectiveness of Indian bauxite to be used as a locally sourced fluoride adsorbent through various treatment scenarios, which we compared using batch adsorption tests, analytical techniques (e.g., XRD, BET, TGA-MS, ICP-MS), and an in-depth cost analysis. Heating Indian bauxite ore above 300°C dramatically increased its surface area (due to dehydroxylation of gibbsite to boehmite) and improved its adsorption performance. The kinetics of fluoride adsorption with micron-sized particles were rapid and field-relevant; within 20 minutes the majority of the adsorption reaction was complete. Acidification of groundwater to maintain solution pH at 6.0 enhanced fluoride removal, regardless of whether HCl or CO_2 was added continuously during the experiment or initially in bulk. ICP-MS results showed that for all of the combinatorial treatment scenarios, concentrations of Ag, As, Cd, Cr, Cu, Fe, Pb, Se, Zn in treated product water were in compliance with the EPA primary and secondary standards for potable drinking water. The SMCLs were not met for Al in scenarios using 100°C bauxite in acidified groundwater and for Mn in one scenario using 300°C bauxite in groundwater acidified through bulk acid addition (300-acid). Our cost analysis showed that when considering all options except 100°C bauxite without groundwater acidification (because the dose was impractically high), using 300°C bauxite with acid treatment of groundwater was the cheapest (and lowest required dose) option. Despite this option (300-acid) being 23% cheaper than the next more expensive option (300-only), it seems likely that using heated bauxite *without* acid treatment of groundwater (300-only) may be the most feasible and field-appropriate treatment option.

CHAPTER 4. Remaining Practical Challenges and Unknowns

4.1. BACKGROUND

Thus far in the presented research, I have identified the main levers controlling fluoride removal efficiency in our system (e.g., dose, contact time, and solution pH) and have shown that suspension pH is the dominant feature explaining differences in performance between diverse bauxites. I have proposed thermal activation of bauxite and groundwater acidification as two alternative treatment methods to improve the performance of previously inefficient Indian bauxite. The aim of this chapter is to put these theoretical and scientific findings from Chapters 1-3 into a more practical context to provide justification for continuing this research into future field trials.

Here, I investigate the field relevance and application of earlier scientific findings by testing the following assumptions: 1) Using coarser bauxite particles generated by industrial mills as opposed to lab-grade ball mills should not dramatically alter bauxite's performance as a fluoride adsorbent, 2) Gravitational settling can be used to remove a large fraction of suspended bauxite particles after the adsorption process is complete, and 3) Fluoride does not desorb into the treated groundwater during this settling period.

4.2. METHODS

4.2.1. Testing Fluoride Removal With Coarser Bauxite Powders

One primary challenge with field processing methods is to mill large quantities of bauxite into fine, micron-sized particles. Given the large differences between lab-grade mills and industrial mills in terms of input mass, milling time, and output rate, we expect that in practice the particle size of bauxite powder useful for large-scale field use will be significantly larger. The lab-grade shaker ball mill (e.g., SPEX8000) used throughout this dissertation generated fine particles (1-10 microns) when 5-15 g of dry material was milled for approximately 15-60 minutes. Based on online specification sheets, the smallest particle size generated when using a large-scale industrial mill with a typical input mass of 5000 kg ranges from approximately 40-400 microns.

To determine the effect of particle size on fluoride adsorption, we crushed Indian bauxite using a ring and puck mill (Spex Shatterbox) for only one minute with a larger input mass (25 g). This mill allowed us to generate a heterogeneous powder with larger particle sizes. We further fractionated this coarse powder into the following output mesh size ranges using sieves: 39-45, 45-75, 75-106, 106-150, 150-250, and > 250 microns. Each powder was then heated for four hours at 300°C in an oven (Lindberg-Blue-M). We mixed a dose of 10 g/L (equivalent to 8.47 g/L dry dose, or 0.119 g in 14 mL) of Indian bauxite from each particle size bin into synthetic Sri Lankan groundwater and measured the final fluoride concentration after 20, 60, and 120 minutes using the methods described in the earlier Sections 2.2.2 and 2.2.3 of Chapter 2.

4.2.2. Settling Experiments

To determine the settling rates of each of these different particle size ranges, we vigorously mixed Indian bauxite heated at 300°C at a dose of 10 g/L (equivalent to 8.47 g/L dry dose, or 1.694 g in 200 mL) to synthetic Sri Lankan groundwater. We took water samples at 3 cm below the water surface in the 250 mL beaker at 0, 5, 10, 20, 40, and 60 minutes and measured their turbidity using a Turbidimeter (Orion Aquafast, AQ4500). Photos at each time interval were taken using a DSLR camera (Canon Rebel).

4.2.3. Stokes Law Calculations

The settling velocity (v_s) of a spherical particle is described by Stokes Law, which can be derived by balancing the net gravitational force and drag force on a spherical particle of a given diameter (d_p) and bulk density (ρ_p) traveling through a fluid of a given kinematic viscosity (v) and density (ρ_f) (see Figure 4-1).

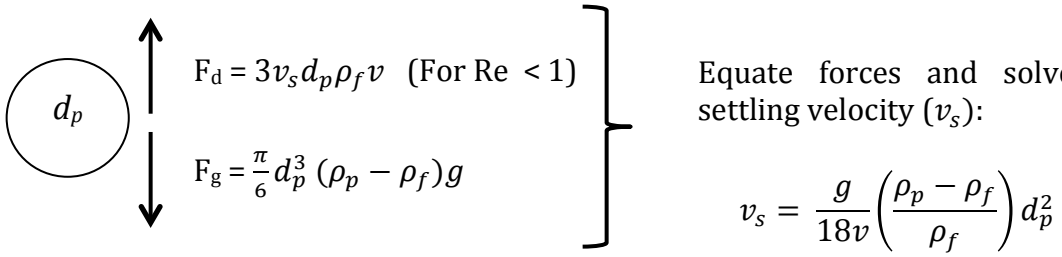

Figure 4-1: Derivation of Stokes Law[121] to calculate the terminal settling velocity of a spherical particle traveling through a fluid by balancing the gravitational and buoyant forces acting on it. Variables refer to settling velocity (v_s), particle diameter (d_p), fluid density (ρ_f), kinematic fluid viscosity (v), particle density (ρ_p), and the gravitational constant ($g = 980\ cm^2/s$).

We calculated Stokes settling velocities for the particles used in Section 4.2.2 based on the following assumptions: bauxite particles are spherical (average $d_p = 38 - 250$ µm and $\rho_p = 2.5\ g/cm^3$)[50] and moving through still water ($\rho_p = 1.0\ g/cm^3$, $v = 0.01\ cm^2/s$). The time required for a particle to settle (e.g., "detention time") was calculated by dividing the tank (or sampling) depth by the settling velocity of the particle.

Using our data on turbidity measurements over time (shown in Section 4.3.2), we can plot the mass fraction of total suspended solids (TSS) versus an apparent settling velocity, which is calculated by dividing the distance traveled by the particle (in our case, the sampling depth of 3 cm) by its time of travel (sampling times of 0, 5, 10, 20, 40, and 60 minutes). Because we did not measure TSS directly, we can use the fraction of initial turbidity ($x = T_i/T_o$) at each time point as a proxy for mass fraction of suspended particles remaining in solution (with settling velocities less than v=3 cm/time). Previous researchers have established strong linear correlations between measurements of turbidity and total suspended solids concentrations and have used turbidity, a faster and more easily measured parameter, as a proxy for monitoring fluxes of groundwater pollutants.[77–79]

4.2.4. Desorption Experiments

To measure the effects of groundwater acidification on fluoride desorption, we conducted batch adsorption experiments by vigorously stirring 10 g/L of the 15-min mill Indian bauxite samples (equivalent to 8.47 g/L dry dose, or 0.424 g in 50 mL) for 20 minutes in Sri Lankan groundwater. Solution pH was maintained at 6.0 using CO_2 and acid, as described in the earlier Section 3.2.2. After the completion of this 20-minute batch adsorption process (labeled "time 0"), we measured the fluoride concentration at regular intervals during the settling period for 60 minutes. The pH in the beaker suspension was also measured to correlate any changes in fluoride to changes in pH. Solid bauxite samples were taken before ("pre) and after ("post") the batch desorption experiments and dried overnight for XRD analysis to detect any changes in bauxite mineralogy due to fluoride adsorption or acidification.

4.3. RESULTS AND DISCUSSION

4.3.1. Effect of Particle Size on Fluoride Removal

Figure 4-2 shows the effect of using coarser particle sizes of Indian bauxite on fluoride removal. For particle sizes larger than 75 μm, the retardation of adsorption kinetics is clearly evident. Fluoride concentrations decrease with greater contact times from 20 minutes to 2 hours for the four particle size bins, 75-106, 106-150, 150-250, and > 250 microns. Across all particle sizes, the final fluoride concentration at 2 hours is approximately 2 ppm. The kinetics of fluoride adsorption are clearly slower for larger particle sizes, as shown by the fluoride concentration at 20 minutes for the >250 microns sample (4.3 ppm) being double that of the smallest 38-45 μm particles (2.0 ppm).

Previous studies evaluating a range of adsorbents (e.g., powdered activated carbon[80,81], activated alumina[28,82], gibbsite, bone char[83], iron and titanium nanoparticles[61,84]) to remediate a variety of contaminants (e.g., NOM, synthetic and organic chemicals, and inorganics like As, Pb, Cd, Cu, Zn, Ni, F, etc.) all demonstrate that finer particle sizes produce significantly higher adsorption capacities and removal efficiencies and faster adsorption kinetics. Our findings are also supported by mathematical models (e.g., the intraparticle diffusion model) for adsorption kinetics, which theoretically predict that the rate of adsorption tends to decrease as adsorbent particle size increases.[85]

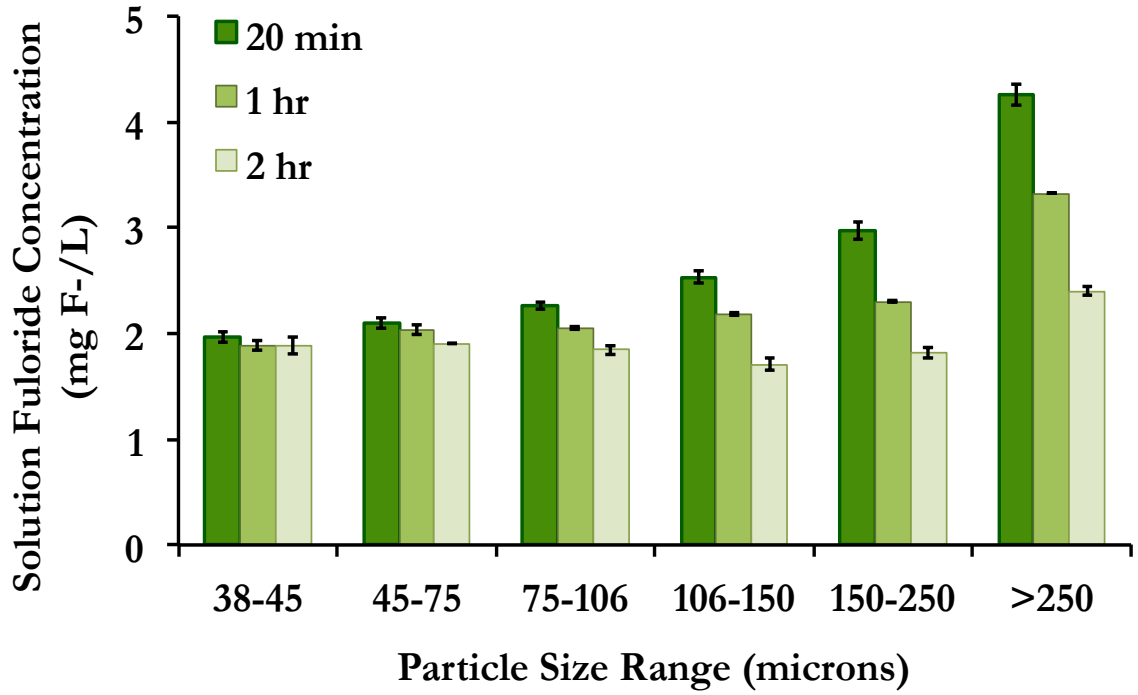

Figure 4-2: Effect of various particle sizes of coarsely milled Indian bauxite powder on fluoride removal. Batch experiments run for 20 minutes, 1 hour, and 2 hours in Sri Lanka groundwater. We present averages and error bars as the larger of the range from duplicate batch adsorption tests and measurement errors associated with the analytical equipment used (e.g., fluoride probe).

One empirical study[82] on activated alumina demonstrates that smaller particles have faster fluoride adsorption kinetics despite all particle sizes (ranging from 0.5-3 mm) having comparable total surface areas (300 m^2/g) due to AA's large intra-particle internal porosity. These researchers deduced that the faster adsorption rate of fluoride on smaller particles could be explained by their larger external surface area, which could provide easier access to active internal sites.[82] To determine if this same theory holds true for our bauxite samples, additional work has to be done to measure the BET surface areas of our various particle sizes.

Based on our specific surface area measurement for Indian bauxite milled for 15 minutes using a ball mill and heated at 300°C reported in Figure 3-5 (~170 m^2/g), we would expect that the coarser particles used in Figure 4-2 also have a similar or slightly lower specific surface area. Additional lab and field studies are necessary to determine the relationship between particle size and surface area, which are both influenced by milling and heating. The role of particle size and its impact on the chemical transformation of thermally activated gibbsite (the primary active mineral in bauxite) is described by some researchers[73,86] studying the thermal decomposition pathway of gibbsite to corundum (activated alumina). In particular, both groups[73,86] reported that in comparison to fine gibbsite particles, coarser particles underwent a more pronounced dehydroxylation and had a higher rate of conversion to gibbsite's intermediary amorphous product, boehmite.

4.3.2. Effect of Particle Size on Settling

Figure 4-3 shows the dependence of sedimentation rate on various particle sizes. Within the first ten minutes of the settling experiment, we observe an 85-88% reduction in turbidity for all particle sizes. By 60 minutes, 94-97% of initial turbidity is reduced through settling alone for all particle sizes. Figure 4-3a reveals an unexpected trend that the large particles (150-250 μm) remain suspended longer (i.e., their turbidities are higher at 40 and 60 minutes) than the smallest particles (38-45 μm). This counter-intuitive finding that larger bauxite particle sizes are settling slower could be explained by the following line of reasoning: bigger particles have bigger pores, which could create interstitial spaces with buoyant air trapped inside, which might be preventing these larger particles from settling. To test this hypothesis, future work can be done to use a surfactant (e.g., ethanol) to change wettability behavior of larger particles to see if they follow a similar settling trend.

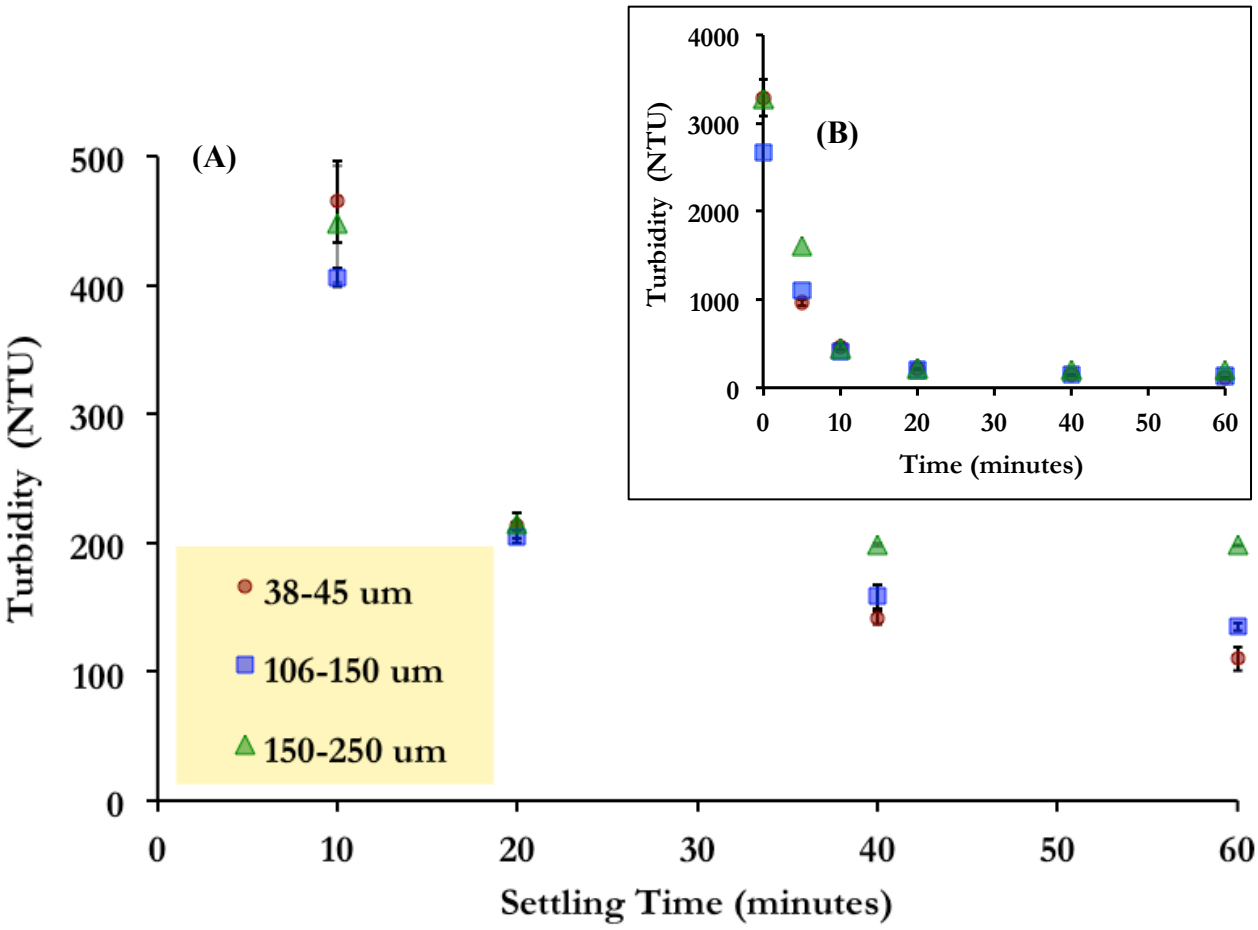

Figure 4-3: Effect of various particle sizes of coarsely milled Indian bauxite powder on settling, measuring using a Turbidimeter. Batch experiments run for 20 minutes were allowed to settle for 1 hour, with turbidity measurements taken every 10 minutes. Panel **(A)** shows a zoomed-in snapshot of panel **(B)** for the turbidity measurements taken between 10 and 60 minutes. We present averages and error bars as the larger of the range from duplicate turbidity tests and measurement errors associated with the analytical equipment used (e.g., Turbidimeter).

Despite the large initial clarification of the water as shown in the pictures in Figure 4-4, the turbidity is still 110-200 times above the acceptable limit (1 NTU). Even in the extreme case of 24 hours of settling, the final turbidity (7 NTU) is still above the recommended permissible limit despite the vial appearing to be clear (Figure 4-4b). Removing a large fraction of turbidity through settling basins (or quiescent sedimentation tanks) is generally accepted as a low energy, low cost, and easy (i.e., simple construction, installation and operation) pre-filtration step. Some disadvantages of sedimentation tanks include the large area (floor space) requirements and poor remove of colloidal suspensions formed by smaller particles. In some cases, filtration (using materials such as sand, ground coconut shells, rice husks, etc.) is often added as an extra step to remove any remaining suspended particles, organic matter, and bacteria[87] after settling to avoid clogging filter media. To determine the optimal solid separation method for our system in the field, we will have to test the cost-effectiveness of common methods used by other researchers including adding a coagulant (e.g., alum or poly aluminum chloride) and passing the supernatant through a tube settler, rapid sand filter, and micron filter.[71,83,87,88] Jar tests and additional experiments are necessary to determine optimal settling conditions (e.g., tank area, coagulant dose, mixing intensity/time, and settling time) for a given influent turbidity.

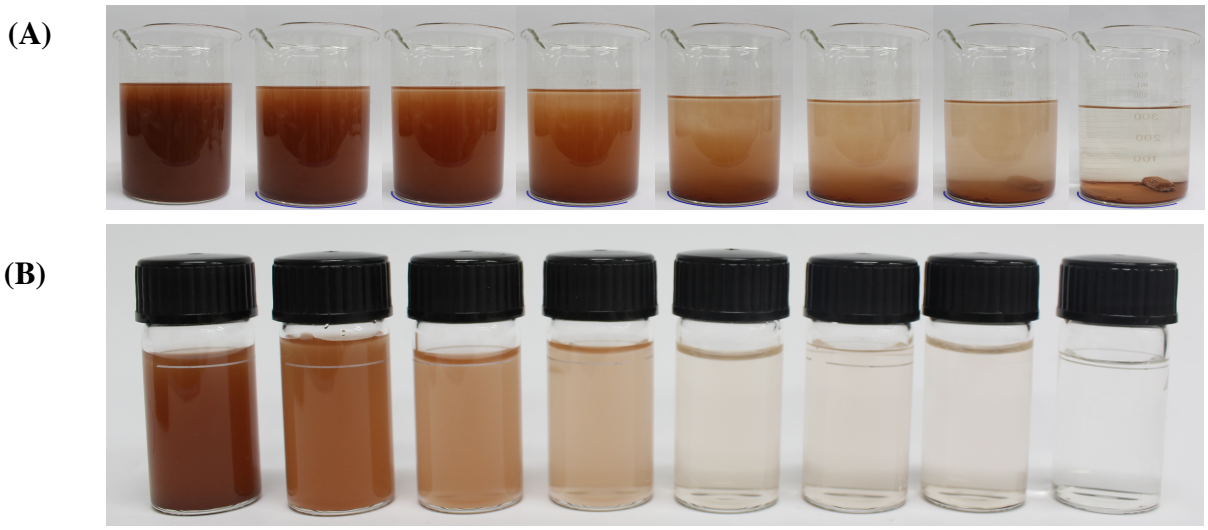

Figure 4-4: Photos of the settling experiment described in Figure 4-3 taken at times 0, 5, 10, 20, 40, 60,100, and 1440 minutes (from left to right). Panel **(A)** shows the 200mL experimental beaker at each time stamp and panel **(B)** shows the suspended particle concentration of measurement turbidity vials holding water samples taken from the top 3 cm of each beaker in panel **A**.

4.3.3. Application of Stokes Law

Figure 4-5 displays the quadratic relationship between bauxite particle diameter (in microns) and settling velocity (shown in cm/s, on a logarithmic scale) and indicates that bigger particles have higher settling velocities. Stokes law holds for particle sizes highlighted in the yellow region ($d_p < 100$ μm), where the Reynolds number ($R_e = v_s d_p/v$) is less than 1, allowing for a simplification of the coefficient of drag and drag force in the Stokes settling velocity calculation. For larger particles ($d_p > 100$ μm) the simplified Stokes law does not hold due to introduction of turbulence and the equation for settling velocity must be readjusted for a more complex drag coefficient expression.

Using our Stokes law calculations as a first order approximation of settling velocities, the detention time (time = depth/settling velocity) required for bauxite particles of diameters 38, 45, and 106 μm to be removed via settling in a sedimentation tank of 1 m depth is estimated to be 14.1, 10.1, and 1.8 minutes, which is reasonable for field conditions.

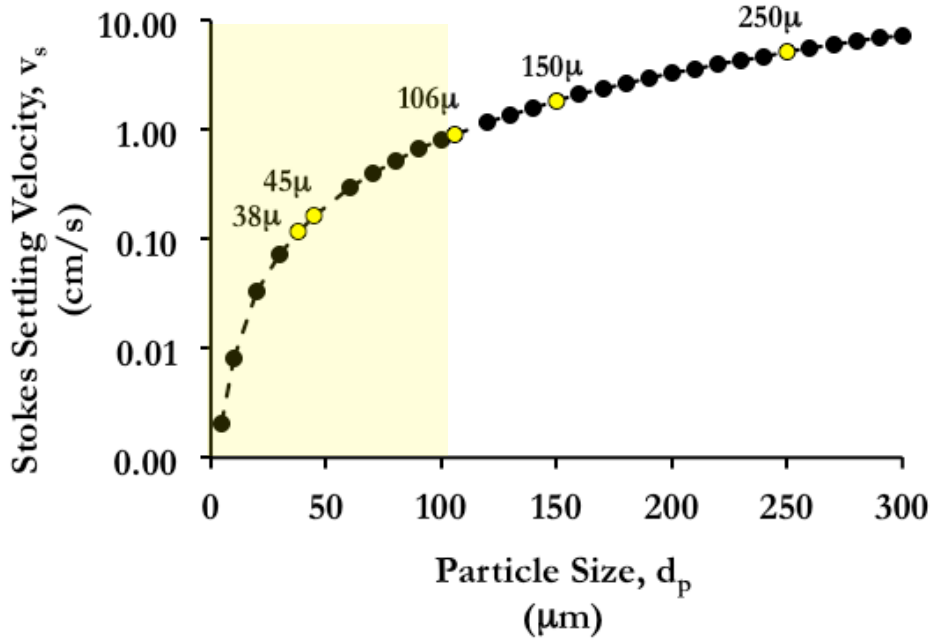

Figure 4-5: Terminal settling velocity of bauxite particles calculated using Stokes Law. The highlighted region shows where $R_e < 1$ and settling velocity can be calculated using a simplification of the drag coefficient in the Stokes law calculation. The yellow dots indicate the particle sizes of the bauxite samples used in the prior settling experiments.

Figure 4-6 transforms the settling experimental data presented in Figure 4-4. It shows the mass fraction of suspended particles (calculated using turbidity as a proxy for TSS) of sizes ranging from the 38-45 μm remaining in solution due to their settling velocities being less than the values shown on the x-axis (calculated by dividing the distance traveled, 3 cm, by the time of travel). Approximately 30% of the particles remaining suspended in solution have settling velocities lower than 0.01 cm/s, which according to Stokes Law corresponds to particles with diameters less than or equal to 10 μm. In other words, this finding implies that by 5 minutes (our first sampling time point), 70% of the particles removed had diameters larger than 10 μm.

In general, although mean particle sizes (based on sieving) can be used as a characterization technique to describe our samples, in reality the actual particle size distributions in our bauxite samples cover a much larger range. The smallest sub-micron particles (also known as colloidal particles) may remain in the supernatant regardless of settling time because their settling velocity is overcome by their random Brownian motions due to thermal collisions. Due to the large number of approximations used in Stoke's Law, experiments using a settling column can be conducted to obtain more accurate data on the distribution of settling velocities for a given suspension. Sources of error in our analysis include the following potential digressions

from our assumptions: bauxite particles are not spherical but more angular (like sand), discrete particles do not interact with neighboring particles during settling, particle size increases during settling due to agglomeration of similarly charged particles colliding, and the density of particles could change if water or air was trapped in their interstitial spaces.

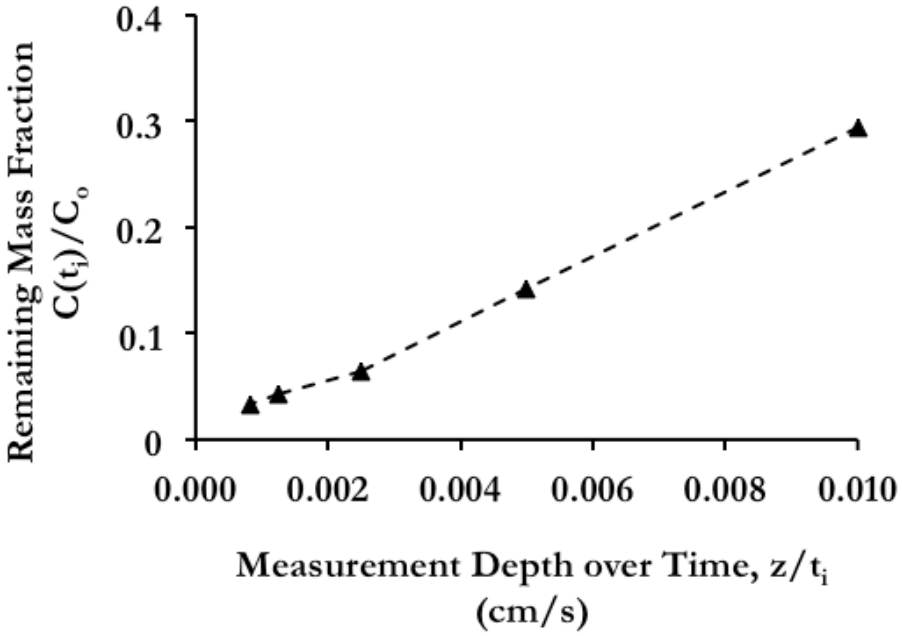

Figure 4-6: Mass fraction of suspended particles remaining in solution with settling velocities less than the fraction of distance traveled by the particle (sampling depth z = 3 cm) over the time of travel. Graph created using the turbidity vs. time data for the 38-45 μm particle size bin in Figure 4-4.

Taken together, our data from these figures show that assessing tradeoffs between settling velocity and fluoride adsorption kinetics will allow us to choose an appropriate particle size for field application. Although smaller particles generally take longer to settle, they take less time to reach equilibrium with regards to fluoride adsorption. Assuming the surface area of bauxite particles is dominated by internal porosity, larger particles have the same adsorption capacity but may take longer to reach equilibrium. Thus, one potential option to decrease settling times and improve fluoride removal efficiency could be to use smaller bauxite particles that are prewashed to remove finer colloidal particles that are more difficult to settle.

4.3.4. Fluoride Desorption During Settling

Figure 4-7 shows fluoride measurements taken at regular time intervals for 1 hour of settling after 20-minute batch adsorption experiments in groundwater acidified to pH 6.0 using HCl or CO_2. Regardless of the source of acid (mineral acid or carbonic acid), we did not observe fluoride desorption in this time period. Even in the case shown in Figure 4-4b, where groundwater was acidified with CO_2 and the solution pH rose slightly (to pH 6.2) during the settling period due to CO_2 evolution, adsorbed fluoride did not return to the groundwater matrix. This finding that fluoride remains adsorbed after 1 hour of post-adsorption settling is promising support for testing the performance of this defluoridation process in the field.

One explanation for why fluoride does not desorb could be the specific inner-sphere complexation mechanism uncovered in Chapter 2 (Figures 2-8 and 2-9). Fluoride is expected to form a specific and strong covalent bond with Al through exchange with –OH surface groups. Based on this same logic, we would also expect that bauxite could potentially be regenerated using a strong base (e.g., NaOH), but future tests are necessary to confirm this possibility.

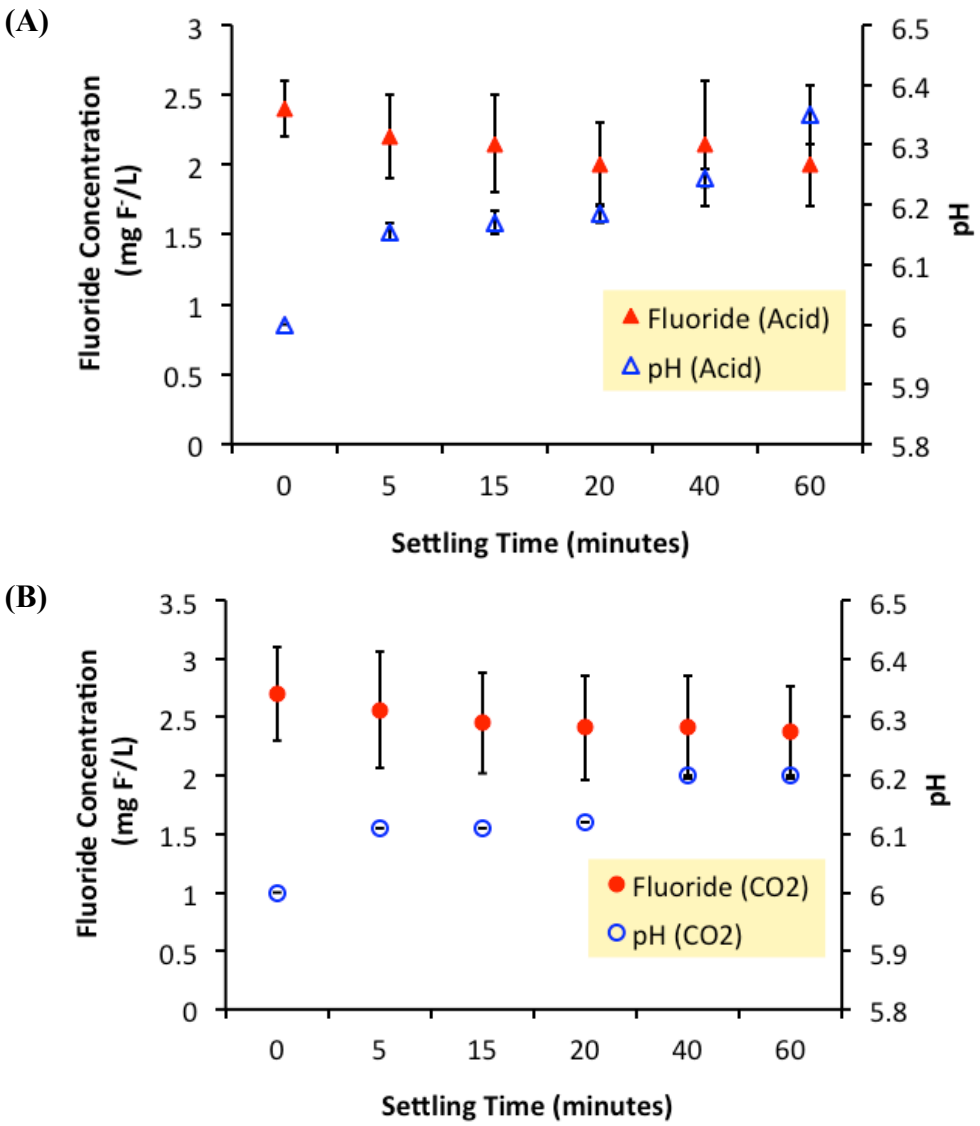

Figure 4-7: Tracking changes in fluoride concentration and solution pH during 60 min of settling time in batch experiments using **(A)** Acid (HCl) and **(B)** CO_2 for pH adjustment of Sri Lankan groundwater. Batch experiments run for 20 minutes, 1 hour, and 2 hours in Sri Lanka groundwater. We present averages and error bars as the largest of the range from duplicate batch adsorption tests and measurement errors associated with the analytical equipment used (e.g., fluoride probe).

Figure 4-8 compares the mineralogy of Indian bauxite samples taken before and after the batch desorption experiments described in Section 4.2.4. The XRD sepctra show that fluoride adsorption and acidification (using CO_2 and acid) do not have any effect on bulk mineralogy of

Indian bauxite. The spectra for all four scenarios (baseline without pH adjustment ("pre-none") and after fluoride adsorption with and without pH adjustment ("post-none", "post-acid", and "post-CO_2") look identical; there are no changes in the gibbsite peaks and no indication of new peaks. This finding implies that detection of these changes, which are most likely on the surface (and not in the bulk), requires more surface sensitive spectroscopic methods such as X-ray Photoelectron Spectroscopy (XPS) or SEM-EDX.

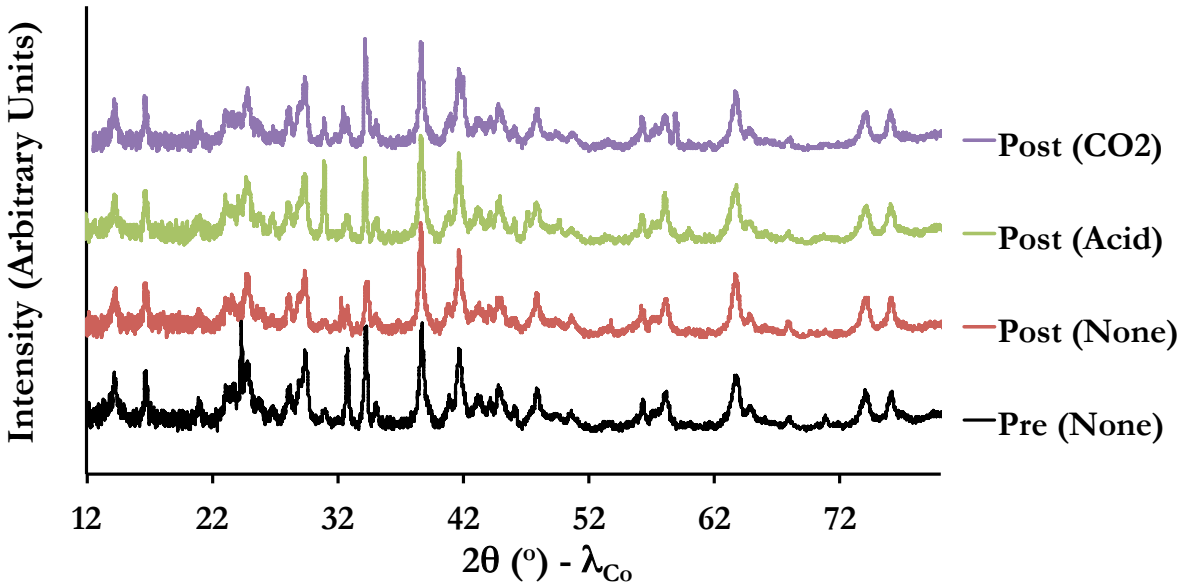

Figure 4-8: Mineralogy as determined by X-ray diffraction patterns of Indian bauxite (15 min mill) samples taken pre- and post- fluoride adsorption in desorption experiments shown in Figure 4-7. The mode of pH control to acidify the groundwater is shown in parentheses.

CHAPTER 5. Conclusion

The primary goal of my doctoral research was to design the foundation of a low cost technology to remediate excess groundwater fluoride contamination in rural, resource-constrained regions. My motivation for addressing this particular problem arose from a multitude of reasons; fluoride was the root cause of a widespread global health crisis that held geographical and cultural significance to me, children living in resource constrained regions were a disproportionately affected subpopulation, and there was a clear knowledge gap for the development of an affordable breakthrough technology that was affordable, culturally appropriate, easy to operate and maintain, locally sourced, and scalable. To achieve this broad objective, I conducted focused research to test the use of bauxite, an aluminum rich ore, as a potential dispersive batch adsorbent to remove fluoride. My initial consideration of existing technologies and proof of concept experiments comparing the performance of bauxite to activated alumina led me to ask the following questions, upon which I structured the remaining chapters of my dissertation: Ch. 2) What are the primary factors governing the performance of bauxite for fluoride remediation of groundwater? Ch. 3) What are mild and inexpensive processing methods to improve Indian bauxite's fluoride removal performance? and Ch. 4) What practical challenges should be addressed prior to field implementation of our proposed bauxite-based defluoridation method?

In this final chapter, I summarize the main findings and contributions of my doctoral research and outline the remaining scientific questions and unknown challenges related to field implementation of this technology.

5.1. Lab Studies: Fluoride Remediation Using Bauxite

5.1.1. Summary of Results

Despite almost a century of endemic fluorosis reported worldwide[89–92] due to chronic ingestion of fluoride-contaminated groundwater, an appropriate technology to address this global health crisis has not yet been implemented at scale in rural, resource-constrained regions. Although numerous materials (e.g., bio-sorbents, bone char, synthetic hydroxyapatite, activated alumina, clays, etc.) have been tested and proposed as adsorbents for fluoride removal[2,5,7,8,16,20,23,93], few are readily accessible to those most disproportionately affected by natural fluoride contamination of their primary drinking water source, groundwater. Such natural methods and lab-derived technologies have not been successfully scaled up in the field due to various barriers including sourcing and cost of materials, social acceptability, processing methods, and complexity and laboriousness of operation and maintenance.

Bauxite, a globally abundant ore of aluminum, is a viable, effective, and low-cost fluoride adsorbent alternative. Earlier researchers have reported bauxite's ability to adsorb fluoride[47,61,72] but many of them did not explore the specific dose of bauxite needed to remediate fluoride-contaminated groundwater to the WHO-MCL. Our findings suggest that bauxite ore is a cost-competitive alternative fluoride adsorbent to activated alumina (AA), despite bauxite's lower surface area and lower adsorption density. Across a range of synthetic and real

groundwater matrices, the material cost of remediating high fluoride levels to below the WHO-MCL with bauxite is consistently and substantially lower than with AA, whether AA is assumed to be used in a single-use dispersive batch process or in a column process with media regeneration. Geographical origin of bauxite ore substantially impacts its fluoride removal performance. In particular, bauxite ores from Guinea, Ghana, and USA required a similar minimum dose (~10 g/L) to reduce 10 ppm F^- to 1.5 ppm F^-, while Indian bauxite required twice the dose (~22 g/L) to achieve the same end result. The lower performance of Indian bauxite in comparison to bauxites from Ghana, Guinea, and USA cannot be explained by differences in their points of zero charge, dominant crystalline mineral phase (e.g., gibbsite), aluminum content, surface area, or intrinsic affinity and capacity for fluoride adsorption (as described by the Freundlich adsorption isotherm model). Indian bauxite's reduced affinity for fluoride uptake is due to the presence and dissolution of the trace mineral calcium carbonate, which increases the equilibrium suspension pH above the optimal pH (5-6) for fluoride adsorption. Ionic strength and spectroscopic studies confirm that like gibbsite, bauxite also primarily forms a specific, inner-sphere complex with fluoride through ion exchange with surface –OH groups and that weak, nonspecific outer-sphere electrostatic interactions do nor play a major role in fluoride adsorption.

Understanding the governing factors and removal mechanisms of raw globally diverse bauxite ores helped inform subsequent work on the enhancement of Indian bauxite's performance and cost-competitiveness through non-hazardous and locally appropriate activation methods. When heated at temperatures between 250°C-300°C, Indian bauxite undergoes partial dehydroxylation (loss of waters of hydration) as the crystalline gibbsite in bauxite transforms to a more amorphous boehmite phase. As a result of this loss of structural water and substantial increase in surface area due to heating, we see a large improvement in Indian bauxite's performance as dispersive batch media for fluoride adsorption. Additionally, lowering the alkaline initial pH of synthetic groundwater (pH ~ 8.7) down to pH 6.0 through addition of HCl or bubbling of CO_2 gas is an alternative method for improving fluoride removal. Considering the capital and operational costs for the entire water treatment process including bauxite processing and transport indicates that using heated bauxite in groundwater acidified with HCl is the cheapest option due to its relatively lower raw material and transportation costs. However, the use and handling of hydrochloric acid in rural areas presents potential additional safety constraints including the leaching of certain elements of concern (Mn, Al) from bauxite at low pH into the treated water. Thus, since groundwater acidification would increase labor, operational, and safety costs, we suggest that using heated bauxite without any groundwater acidification (the second cheapest option) is the most favorable, logistically simple, and practical treatment scenario for field operation.

Overall, the bauxite-based defluoridation process studied in this dissertation appears to meet the requirements of locally affordability, fluoride removal effectiveness, simplicity (i.e., low skilled labor required), and culturally appropriateness. Despite these apparent advantages, further research on other technical, operational, and social factors (described in the remaining sections) must be conducted to determine the feasibility of SAFR as an appropriate technology for fluoride remediation in rural impoverished settlings.

5.1.2. Future Work: Surface Complexation Modeling

Additional laboratory studies are necessary to systematically investigate the impact of potential competitive species found in groundwater such as commonly occurring anions (e.g., HCO_3^-, Cl^-, $Si(OH)_4$, SO_4^{2-}, NO_3^-, PO_4^{3-})[6,47,58], pathogens, and NOM.[6,59] It is likely that some of these components in real groundwater may significantly impact the efficiency of fluoride removal by bauxite in the field; we found larger doses were required to remediate complex synthetic and real groundwater matrices in comparison to a simpler binary-solute electrolyte ($NaCl + NaHCO_3$). In addition to altering the required material dose of bauxite, groundwater composition may also impact fluoride removal mechanisms and the potential for metals in bauxite (e.g., Al, Fe, Ti) to be solubilized at undesirable levels.

Our experimental adsorption data can be fit to a surface complexation model generated using PHREEQC, a tool developed by the US Geologic Survey (USGS) to better understand geochemical reactions between water and minerals such as bauxite. Advantages of using PHREEQC include predicting bauxite's adsorption behavior in various solution compositions, calculating equilibrium concentrations of aqueous fluoride complexes and other dissolved metals at various pH, and determining the selectivity of fluoride adsorption versus other ions that might interfere with the removal process. Useful applications include determining if alum addition would decrease fluoride removal due to presence of sulfate and calculating solubility of Al in different mineral phases found naturally or produced during thermal activation (e.g., boehmite).

PHREEQC's generalized two-layer mode developed by Dzombak and Morel[94] and based on Stumm's diffuse layer model[95,96] allows for adsorbed species to form specific inner-sphere complexes and ignores the possibility of weaker, outer-sphere complexes by considering the remaining counter ions in solution as being part of the diffuse layer. To simplify the simulation of fluoride adsorption onto bauxite, it can be assumed that surface binding sites are homogeneous (i.e., there are no weak or strong sites), surface precipitation does not occur, and gibbsite is the primary active component in bauxite that dominates adsorption and complexation reactions. The input parameters for a chosen quantitative model can be determined without requiring spectroscopic data if a simple Generalized Composite (GC) model is used. The GC model, a theoretical framework described in a study on the adsorption of zinc on aquifer sediment[97], requires fewer adjustable parameters (e.g., surface area, site density, and thermodynamic equilibrium logK constants) that can be derived from previous literature for generic surface sites on gibbsite. To produce an initial simulation, some experimental conditions can be held constant (e.g., solution composition, adsorbent dose, adsorbent surface area, solution pH, points of zero charge, etc.). The generated model can later be fit to empirical data by varying non-experimentally derived parameters (e.g., log K values, surface complexation/acidity reactions, site densities, etc.). In contrast to the GC model, the Component Additivity (CA) approach predicts adsorption based on the summing the contribution of each active component in the complex mineral assemblage. This latter CA approach requires detailed spectroscopic data (e.g., surface site densities, relative proportions of minerals, stability constants, etc.) for each mineral component of bauxite (e.g., hematite, goethite, anatase, etc.).

5.1.3. Future Work: Spectroscopic Studies

The nature of fluoride adsorption (e.g., specificity and strength of Al-F bond), formation of complexes at surface sites on bauxite, and interaction of bauxite's surface functional groups with fluoride in different conditions (e.g., pH, temperature, NOM, co-occurring ions, etc.) can be studied using spectroscopic methods. The aluminum fluoride bond and overall coordination environment can be studied at multiple scales using different techniques, including FTIR (to study other functional groups at different wavelengths in addition to the –OH peaks we focused on), X-ray photoelectron spectroscopy (XPS, to quantify elemental composition of the top 10nm of the surface and determine binding energies), and scanning electron microscopy with energy dispersive X-ray spectroscopy (SEM-EDX, to visualize surface topography and elemental mapping).

Extended X-ray absorption fine structure (EXAFS) and X-ray absorption near edge structure (XANES) spectra can also be used gather detailed localized structural information around the aluminum metal centers in bauxite. Researchers have investigated the electronic structures, molecular orbitals, and coordination numbers and states of crystalline and amorphous materials by comparing measured and calculated XANES at the F K-edges of aluminum fluoride solids polymorphs (AlF_3)[98] and at the Al K-edge of transitional poorly-crystalline aluminas (Al_2O_3)[99] and other aluminum oxide minerals (e.g., gibbsite, boehmite, diaspora, kaolinite, etc.).[100] Other groups have used Nuclear Magnetic Resonance (NMR, 27Al and 19F)[101] to study the coordination geometry of aqueous fluoroaluminate complexes (AlF_4^-) or have relied on combined spectroscopic studies (e.g., XAS and IR)[59] to characterize the geometric and electronic structural characteristics of aqueous aluminum-organic complexes (e.g., Al-EDTA, Al-oxalate, $AlCl_3$, etc.)[102] and determine the impact of varying pH and NOM on aluminum speciation in soils and streams.[59]

5.1.4. Future Work: Variations in Bauxite Composition

In addition to these spectroscopic studies, future work should explore the role of different co-occurring minerals in bauxite for fluoride uptake to better understand the nature of fluoride's affinity for aluminum. In our study, we primarily focused on gibbsite as the active mineral because of the extensive past research conducted on aluminum based adsorbents for fluoride removal. However, bauxite is comprised of various additional minerals including oxides of Fe (hematite and goethite), Ti (anatase, rutile), Si (kaolinite), and other Al oxides (boehmite, gibbsite, and diaspore). Additional batch studies are needed to characterize the relative fluoride adsorption kinetics, affinities, and capacities of each individual component. These findings can help us predict the likely effectiveness of globally diverse ores with varying chemical composition so we can more selectively choose which locations to source ore from for further testing.

It is important to conduct additional fieldwork to determine if any non-alkaline bauxite deposits are present in fluorosis affected countries like India other trace alkaline or acidic minerals potentially present in bauxite ores[52] (e.g., $MgCO_3$, $CaMg(CO_3)_2$, humic materials, silicates) could negatively affect the ore's fluoride removal performance. To determine the long-term durability of bauxite's applicability as a fluoride adsorbent in the field, bauxite ores of

varying composition can be exposed to various influent water compositions and processing conditions as these factors could potentially influence the leaching of metals, total dissolved solids (TDS) and desorption of fluoride into product water. As an example, in Chapter 3 we found that Cr dissolution was more prevalent in cases using heated Indian bauxite and Al and Mn dissolution were more prevalent in cases using acidified groundwater. To confirm the hypothesis that Cr dissolution increases with temperature due an increase in the rate of oxidation of Cr(III) to its more soluble Cr(VI) form, further tests can be conducted to characterize the leachate of Indian bauxite that has been burned in an anoxic gas such as Argon or Nitrogen. If this scenario were confirmed to be true, bauxite could be heated in an anoxic atmosphere to retard Cr oxidation and prevent dissolution. Alternatively, Fe(II) could also be added to product water containing excess dissolved Cr to reduce Cr(VI) back to its less toxic and less soluble Cr(III) form.[103]

5.2. Practical Considerations for Field Implementation

5.2.1. Summary of Results

To confirm that locally sourced bauxite ore can be realistically used in field applications as a low-cost, practical adsorbent material for remediating inorganic fluoride contaminated groundwater, we conducted some preliminary tests to measure impact of particle size on fluoride removal and settling and we conducted desorption studies. In our range of tested particle sizes (35 μm-250 μm), we found that particle size had an impact on adsorption kinetics but did not dramatically impact overall fluoride removal. We also found that fluoride did not desorb from the bauxite even after 1 hour of settling, which is a good sign for field implementation.

5.2.2. Future Work: Field Reactor Design

In order for our proposed scalable and affordable fluoride removal (SAFR) process to become a mature technology, several remaining unknowns must still be addressed. Prior to implementing this water treatment process in the field, we suggest that a rigorous demonstration of the entire bauxite-based defluoridation process, from processing raw bauxite ore to producing potable water be conducted. To achieve this goal, low-cost solid-separation methods (e.g., addition of a coagulant (e.g., alum or polyaluminum chloride), using a rapid sand filter, or tube settler) can be tested to reduce the post-settling turbidity to drinking water standards.

To design an optimal reactor that utilizes bauxite's maximum adsoprtion capacity and that remains easy to operate and maintain in a rural setting, we can first refer to existing applications of common adsorbents such as activated carbon or activated alumina. These adsorbents are typically deployed as either granular filter bed media (particle size ~ 1mm) or powdered batch dispersive media (particle size < 50 μm).[104] In our system, we have demonstrated the successful use of bauxite as powdered dispersive batch media (particle sizes 1 μm < 250 μm). Despite working well with a finely powdered media, a continuous fluow stirred tank reactor (CFSTR) design may be challenging to operate in a rural setting with intermittent power and unreliable groundwater sources. Alternatively, bauxite could also be tested as a dispersive batch media in a sequential countercurrent batch reactor to progressively treat multiple batches of fluoride contaminated water until the bauxite media has been saturated.

Another option is to using bauxite as a coarser granular media in a plug flow reactor (PFR) where the adsorbent interacts and equilibrates with a higher influent contaminant concentration (in our case, 10 ppm F^-) rather than with a lower effluent concentration (which in our case is set at < 1.5 ppm F) as in a CFSTR. It is expected that bauxite's adsorption density (mg F^-/g adsorbent) described by the adsorption isotherms in Section 2.3.3 will be greater in the more efficient PFR filter reactor design. Furthermore, the use of bauxite in a column filter bed could also be studied by using larger grain sizes to avoid clogging of the filter media and to reduce the large energy requirement of pushing water through packed media. However, it is important to keep in mind that using bauxite as a coarser granular medium could also decrease the available surface area for adsorption and reduce its effectiveness as a fluoride adsorbent. Testing if the bauxite media could be reused till saturation or regenerated chemically is important because it would alter the cost (and perhaps complexity) of the overall treatment process. Researchers have successfully regenerated other defluoridation adsorbents (e.g., magnesium incorporated bentonite clay[65] and nano-magnesium oxide[105]) with 95-97% recovery using 1M NaOH or 1M HCl.

5.2.3. Future Work: Resource Recovery and Detailed Cost Analysis

To address potential disposal problems and to lower operational costs, the use of bauxite for other resource recovery applications should also be investigated. It would be worthwhile to explore the potential resale of fluoride-laden bauxite sludge to aluminum manufacturing companies to further reduce the fiscal and environmental impact of implementing this technology. Studies attempting to recycle red mud, the toxic, highly alkaline (pH 10.5-12.5)[106], metal-laden waste byproduct of the Bayer process used to extract aluminum from bauxite, can teach us about the potential options for reuse of bauxite in various industries (e.g., metallurgy, construction, glass/ceramics, chemical, agriculture, and water/wastewater treatment).[107] The Aluminum Company of America (commonly known as ALCOA) proposed that carbonating the highly alkaline red mud using industrial CO_2 streams can allow for easier storage and handling so red mud residue can later be reused for a variety of useful purposes including cement and concrete manufacturing, brick and tile making[51,106–108], road construction[109], and as a soil amendment or fertilizer[107]. Other researchers have demonstrated that sulfidizing red mud (i.e., treating it with Na_2S, $(NH_4)_2S$, or H_2S to bind sulfur to metal atoms to prevent leaching) enables its use as an adsorbent for heavy metals (e.g., Cd, Cr, Pb, Hg, As, Mn, Sr) and other inorganic and organic contaminants (e.g., P, bacteria, DOC (tannin, lignin)).[109] Given the many proposed uses of red mud- a waste product from activated alumina and aluminum production-, the fluoride-laden bauxite sludge produced by our defluoridation process could also be used for similar purposes after it is dried and concentrated.

In the future, our lab prototype for the SAFR process needs to be scaled up from our 10-200 mL beaker study to a 600 L tank field study, and eventually a full-scale 1000 L water treatment plant. Testing our bauxite based defluoridation process in a field setting will allow us to establish some key supply chain logistics (e.g., sourcing and processing bauxite in rural India) and to assess the capital and operational costs for full treatment process. If proof of concept of a working field pilot is successfully demonstrated in rural India, our proposed SAFR technology could eventually be expanded to other parts of the world where high fluoride concentrations have also been detected such as the East African Rift Valley. In the long run, it would also be

beneficial to compare the environmental, greenhouse gas, energy, material, waste disposal, and transportation cost tradeoffs associated with using different bauxite ores and necessary processing scenarios. Consideration of these factors through a more comprehensive cost model could help important stakeholders (e.g., local governments and community operators around the world) answer tough questions such as: What are the tradeoffs of remediating fluoride using a lower grade, cheaper bauxite that is less efficient, produces more sludge, and require more pre-treatment versus? What are the benefits and disadvantages of using a higher-grade bauxite that is slightly higher in material cost and has added transportation cost, but requires fewer activation steps and is more effective (i.e., requires lower doses and produces less sludge)? Is it better (financially, operationally, and environmentally) to discard bauxite media after saturation or to regenerate it using caustic chemicals?

5.2.4. Future Work: Technology Adoption and User Behavior

To address societal problems in resource-constrained regions, engineers and scientists have long suggested the implementation of a myriad of technical solutions. Academic, corporate, and nonprofit groups have innovated numerous technologies with the intention of providing disaster relief, adequate healthcare, education, and water and sanitation in developing countries. However, we are often left with failed technological interventions because lasting solutions to these deep-rooted issues must be accompanied by parallel infrastructural and institutional changes.[110] Some infamous examples of such failed technologies implemented without institutional support in some cases include the PlayPump, LifeStraw, Unmanned-Aerial-Vehicles (volunteer drone pilots in Nepal)[110], One-Laptop-Per-Child[111], and malaria bed nets.[112] There are various lessons to be learned from the challenges faced by these entities.

PlayPump was initially implemented in sub-Saharan Africa under assumptions that playing children could generate enough power to pump water to meet a community's daily need and post-pumping stored water would be easily accessible and potable.[113] In reality, PlayPumps were installed in large communities facing water shortages/scarcity and they required a lot more energy and time to pump the groundwater than initially expected. PlayPumps did not produce the community's required daily water supply, had a larger upfront cost than conventional hand pumps, and were difficult to repair and maintain if damaged.[113]

Another technology focused on water provision is LifeStraw, which was developed by the Swiss company Vestergaad. Initially advertised as an affordable, portable filter for individual point of use water purification, LifeStraw was later rebranded as an emergency survival tool for use during natural disasters like earthquakes and floods.[114] Based on lab tests of their initial prototype, LifeStraw met the WHO standards for removing bacteria (but not viruses, giardia, or cryptosporidium) and was estimated to cost $3.50 per unit. If used properly, one filter could also treat approximately 700L of water in its lifetime, sufficient to meet the drinking water needs of one person for one year.[115] Despite these advantages demonstrated in lab studies, field studies in Sudan[115] and Ethiopia[116] indicated no significant improvement in LifeStraw consumers' gastrointestinal health due to inconsistent use, and low levels of adoption. LifeStraw could have also unintentionally encouraged poor hygiene habits and exposed users to higher risk of illness by instructing them to use the treatment device on contaminated water bodies near sewers and fecal ponds.

These two examples illustrate the importance of conducting field trials, needs assessments, and baseline social surveys prior to scaling up and widely distributing a new technology. Furthermore, understanding key social factors influencing adoption and retention of a technology including the local cultural context, user behavior, peoples' willingness to pay for water, peoples' preferences for water taste, and potential unintended consequences is pertinent to the long-term success of an intervention like SAFR in a community.

REFERENCES

(1) Saxena, V.; Ahmed, S. Inferring the chemical parameters for the dissolution of fluoride in groundwater. *Environ. Geol.* **2003**, *43* (6), 731–736 DOI: 10.1007/s00254-002-0672-2.

(2) Edmunds, W. M.; Smedley, P. L. Chapter 12: Fluoride in Natural Waters. In *Essentials of Medical Geology*; Selinus, O., Ed.; Springer Netherlands: Dordrecht, 2013; pp 311–336.

(3) Chilton, J. Dahi, E. Lennon, M. Jackson, P.; Fawell, J.; Bailey, K. . *WHO Water Series: Fluoride in Drinking Water*; Fawell, J. K., Bailey, K., Eds.; WHO drinking water quality series; World Health Organization: Geneva, 2006; Vol. 408.

(4) Ozsvath, D. L. Fluoride and environmental health: A review. *Rev. Environ. Sci. Biotechnol.* **2009**, *8* (1), 59–79 DOI: 10.1007/s11157-008-9136-9.

(5) Jagtap, S.; Yenkie, M. K.; Labhsetwar, N.; Rayalu, S. Fluoride in Drinking Water and Defluoridation of Water. *Chem. Rev.* **2012**, *112* (4), 2454–2466 DOI: 10.1021/cr2002855.

(6) Habuda-Stanić, M.; Ravančić, M. E.; Flanagan, A. A Review on Adsorption of Fluoride from Aqueous Solution. *Materials (Basel).* **2014**, *7* (9), 6317–6366 DOI: 10.3390/ma7096317.

(7) Madhukar, M.; Murthy, B. M. S.; Udayashankara, T. H. A Review on Conventional and Alternative Methods for Defluoridation of Water. *J. Water Pollut. Purif. Res.* **2014**, *1* (2), 1–12.

(8) Meenakshi; Maheshwari, R. C. Fluoride in drinking water and its removal. *J. Hazard. Mater.* **2006**, *137* (1), 456–463 DOI: 10.1016/j.jhazmat.2006.02.024.

(9) Featherstone, J. D. Prevention and reversal of dental caries: role of low level fluoride. *Community Dent. Oral Epidemiol.* **1999**, *27* (1), 31–40 DOI: 10.1111/j.1600-0528.1999.tb01989.

(10) Rocha-Amador, D.; Navarro, M. E.; Carrizales, L.; Morales, R.; Calderón, J. Decreased intelligence in children and exposure to fluoride and arsenic in drinking water. *Cad. Saude Publica* **2007**, *23* (4), S579–S587 DOI: 10.1590/S0102-311X2007001600018.

(11) Fluorosis Research and Rural Development Foundation. *State of Art Report on Extent of Fluoride In Drinking Water and the Resulting Endemicty in India*; New Delhi, India, 1999.

(12) *Backward Regions Grant Fund Programme Guidelines*; 2007.

(13) *District Census Handbook Nalgonda: Village and Town Directory*; 2011.

(14) Rao, N.V, Ramamohana, Rao, N., Rao, K. S. P.; , Schuiling, R. D.; Ramamohana Rao, N. V.; Rao, N.; Surya Prakash Rao, K.; Schuiling, R. D. Fluorine distribution in waters of Nalgonda District, Andhra Pradesh, India. *Environ. Geol.* **1993**, *21* (1–2), 84–89 DOI: 10.1007/BF00775055.

(15) Kingshuk, N. *Battleground Telangana: Chronicle of an Agitation*; Harper Collins, 2011.

(16) Osterwalder, L.; Johnson, C. A.; Yang, H.; Johnston, R. B. Multi-criteria assessment of community-based fluoride-removal technologies for rural Ethiopia. *Sci. Total Environ.* **2014**, *488–489* (1), 532–538 DOI: 10.1016/j.scitotenv.2013.10.072.

(17) Mwenge Kahinda, J.; Taigbenu, A. E.; Boroto, J. R. Domestic rainwater harvesting to improve water supply in rural South Africa. *Phys. Chem. Earth, Parts A/B/C* **2007**, *32* (15–18), 1050–1057 DOI: 10.1016/j.pce.2007.07.007.

(18) UCLA. First Demonstration Of Reverse Osmosis http://engineering.ucla.edu/first-demonstration-of-reverse-osmosis/ (accessed Aug 1, 2017).

(19) Mohapatra, M.; Anand, S.; Mishra, B. K. K.; Giles, D. E.; Singh, P. Review of fluoride

removal from drinking water. *J. Environ. Manage.* **2009**, *91* (1), 67–77 DOI: 10.1016/j.jenvman.2009.08.015.
(20) Bhatnagar, A.; Kumar, E.; Sillanpää, M. Fluoride removal from water by adsorption-A review. *Chem. Eng. J.* **2011**, *171* (3), 811–840 DOI: 10.1016/j.cej.2011.05.028.
(21) Khairnar, M. R.; Dodamani, A. S.; Jadhav, H. C.; Naik, R. G.; Deshmukh, M. A. Mitigation of Fluorosis - A Review. *J. Clin. Diagnostic Res.* **2015**, *9* (6), ZE05-ZE09 DOI: 10.7860/JCDR/2015/13261.6085.
(22) Reisner, D.; Pradeep, T. *Aquananotechnology: Global Prospects*, 1st ed.; CRC Press: Taylor & Francis Group: Boca Raton, FL, 2014.
(23) Johnson, C. A.; Bretzler, A. *EAWAG WRQ Geogenic Contamination Handbook*; 2015.
(24) Tomar, V.; Kumar, D. A critical study on efficiency of different materials for fluoride removal from aqueous media. *Chem. Cent. J.* **2013**, *7* (1), 51 DOI: 10.1186/1752-153X-7-51.
(25) Sundaram, C. S.; Viswanathan, N.; Meenakshi, S. Defluoridation of water using magnesia/chitosan composite. *J. Hazard. Mater.* **2009**, *163* (2–3), 618–624 DOI: 10.1016/j.jhazmat.2008.07.009.
(26) Dahi, E. The State of Art of Small Community Defluoridation of Drinking Water. In *Proceedings of the 3rd International Workshop on Fluorosis Prevention and Defluoridation of Water*; Chiang Mai, Thailand, 2000.
(27) Chen, W.-Q.; Graedel, T. E. Dynamic analysis of aluminum stocks and flows in the United States: 1900–2009. *Ecol. Econ.* **2012**, *81*, 92–102 DOI: 10.1016/j.ecolecon.2012.06.008.
(28) Teng, S. X.; Wang, S. G.; Gong, W. X.; Liu, X. W.; Gao, B. Y. Removal of fluoride by hydrous manganese oxide-coated alumina: Performance and mechanism. *J. Hazard. Mater.* **2009**, *168* (2–3), 1004–1011 DOI: 10.1016/j.jhazmat.2009.02.133.
(29) Maliyekkal, S. M.; Shukla, S.; Philip, L.; Nambi, I. M. Enhanced fluoride removal from drinking water by magnesia-amended activated alumina granules. *Chem. Eng. J.* **2008**, *140* (1–3), 183–192 DOI: 10.1016/j.cej.2007.09.049.
(30) Maliyekkal, S. M.; Sharma, A. K.; Philip, L. Manganese-oxide-coated alumina: A promising sorbent for defluoridation of water. *Water Res.* **2006**, *40* (19), 3497–3506 DOI: 10.1016/j.watres.2006.08.007.
(31) Bansiwal, A.; Pillewan, P.; Biniwale, R. B.; Rayalu, S. S. Copper oxide incorporated mesoporous alumina for defluoridation of drinking water. *Microporous Mesoporous Mater.* **2010**, *129* (1–2), 54–61 DOI: 10.1016/j.micromeso.2009.08.032.
(32) Wasay, S. A.; Tokunaga, S.; Park, S.-W. Removal of Hazardous Anions from Aqueous Solutions by La(lll)- and Y(lll)-lmpregnated Alumina. *Sep. Sci. Technol.* **1996**, *31* (10), 1501–1514 DOI: 10.1080/01496399608001409.
(33) Gwala, P.; Andey, S.; Mhaisalkar, V.; Labhasetwar, P.; Pimpalkar, S.; Kshirsagar, C. Lab scale study on electrocoagulation defluoridation process optimization along with aluminium leaching in the process and comparison with full scale plant operation. *Water Sci. Technol.* **2011**, *63* (12), 2788–2795 DOI: 10.2166/wst.2011.475.
(34) Choi, W.-W.; Chen, K. Y. The Removal of Fluoride From Waters by Adsorption. *J. Am. Water Works Assoc.* **2012**, *71* (10), 562–570.
(35) Farrah, H.; Slavek, J.; Pickering, W. Fluoride interactions with hydrous aluminium oxides and alumina. *Aust. J. Soil Res.* **1987**, *25* (1), 55–69 DOI: 101071/SR9870055.
(36) Bray, L. *USGS Mineral Commodities Summaries 2015: Bauxite and Alumina*; United

States Geologic Survey: Reston, Virginia, 2016.
(37) Sorg, T. *Removal of Fluoride from Drinking Water Supplies by Activated Alumina*; US EPA: Cincinnati, Ohio, 2014.
(38) Vithanage, M.; Rajapaksha, A. U.; Bootharaju, M. S.; Pradeep, T. Surface complexation of fluoride at the activated nano-gibbsite water interface. *Colloids Surfaces A Physicochem. Eng. Asp.* **2014**, *462*, 124–130 DOI: 10.1016/j.colsurfa.2014.09.003.
(39) Gomoro, K.; Zewge, F.; Hundhammer, B.; Megersa, N. Fluoride removal by adsorption on thermally treated lateritic soils. *Bull. Chem. Soc. Ethiop.* **2012**, *26* (3), 361–372 DOI: 10.4314/bcse.v26i3.5.
(40) Buamah, R.; Mensah, R. A.; Salifu, A. Adsorption of fluoride from aqueous solution using low cost adsorbent. *Water Sci. Technol. Water Supply* **2013**, *13* (2), 238–248 DOI: 10.2166/ws.2013.016.
(41) Craig, L., Stillings, L., Decker, D., Thomas, M. J. Comparing activated alumina with indigenous laterite and bauxite as potential sorbents for removing fluoride from drinking water in Ghana. *Appl. Geochemistry* **2015**, *56*, 50–66 DOI: 10.1016/j.apgeochem.2015.02.004.
(42) Kalista, P. H. Defluoridation of High Fluoride Waters from Natural Water Sources by Using Soils Rich in Bauxite and Kaolinite. *J. Eng. Appl. Sci.* **2009**, *4* (4), 240–246.
(43) Kayira, C.; Sajidu, S.; Masamba, W.; Mwatseteza, J. Defluoridation of Groundwater Using Raw Bauxite: Kinetics and Thermodynamics. *CLEAN - Soil, Air, Water* **2014**, *42* (5), 546–551 DOI: 10.1002/clen.201200488.
(44) Lavecchia, R., Medici, F., Piga, L., Rinaldi, G., Zuorro, A. Fluoride removal from water by adsorption on a high alumina content bauxite. *Chem. Eng. Trans.* **2012**, *26*, 225–230 DOI: 10.3303/CET1226038.
(45) Mohapatra, D.; Mishra, D.; Mishra, S. P.; Chaudhury, G. R.; Das, R. P. Use of oxide minerals to abate fluoride from water. *J. Colloid Interface Sci.* **2004**, *275* (2), 355–359 DOI: 10.1016/j.jcis.2004.02.051.
(46) Sajidu, S.; Kayira, C.; Masamba, W.; Mwatseteza, J. Defluoridation of Groundwater Using Raw Bauxite: Rural Domestic Defluoridation Technology. *Environ. Nat. Resour. Res.* **2012**, *2* (3), 1–9 DOI: 10.5539/enrr.v2n3p1.
(47) Sujana, M. G. G.; Anand, S. Fluoride removal studies from contaminated ground water by using bauxite. *Desalination* **2011**, *267* (2–3), 222–227 DOI: 10.1016/j.desal.2010.09.030.
(48) Thole, B.; Mtalo, F.; Masamba, W. Groundwater Defluoridation with Raw Bauxite, Gypsum, Magnesite, and Their Composites. *CLEAN - Soil, Air, Water* **2012**, *40* (11), 1222–1228 DOI: 10.1002/clen.201100111.
(49) Dzombak, D. A., and Karamalidis, A. K. *Surface Complexation Modeling: Gibbsite*; Wiley: New York, 2010.
(50) Geologic Survey of India. *Detailed Information of Bauxite in India*; Hyderabad, India, 1994; Vol. 211.
(51) Dodoo-Arhin, D.; Konadu, D. S.; Annan, E.; Buabeng, F. P.; Yaya, A. Fabrication and Characterisation of Ghanaian Bauxite Red Mud-Clay Composite Bricks for Construction Applications. *Am. J. Mater. Sci.* **2013**, *3* (5), 110–119 DOI: 10.5923/j.materials.20130305.02.
(52) Authier-Martin, M.; Forte, G.; Ostap, S.; See, J. The mineralogy of bauxite for producing smelter-grade alumina. *J. Miner. Met. Mater. Soc.* **2001**, *53* (12), 36–40 DOI: 10.1007/s11837-001-0011-1.

(53) Gorchev, H. G.; Ozolins, G.; World Health Organization. *Guidelines for drinking-water quality, 4th ed.*, 4th ed.; World Health Organization: Geneva, 2011; Vol. 38.
(54) Chemistry, T.; Sposito, G. *The chemistry of soils*, 2nd ed.; Oxford University Press: Oxford ; New York, 2008.
(55) Quast, K. Some Surface Characteristics of Six Hematite Ores from the Middleback Range Area, South Australia. *Int. J. Min. Eng. Miner. Process.* **2012**, *1* (2), 73–83 DOI: 10.5923/j.mining.20120102.09.
(56) Phillips, B. L.; Tossell, J. A.; Casey, W. H. Experimental and theoretical treatment of elementary ligand exchange reactions in aluminum complexes. *Environ. Sci. Technol.* **1998**, *32* (19), 2865–2870 DOI: 10.1021/es9802246.
(57) Prakash, S. , Das, B., and Venugopal, R. Surface Properties of Indian Hematite and Bauxite and Their Coating Mechanism with Colloidal Magnetite. *J. Sci. Ind. Res. (India).* **1999**, *58* (6), 436–442.
(58) Shrivastava, B. . .; Vani, A. Comparative Study of Defluoridation Technologies in India. *Asian J. Exp. Sci.* **2009**, *23* (1), 269–274.
(59) Hagvall, K.; Persson, P.; Karlsson, T. T. T. Speciation of aluminum in soils and stream waters: The importance of organic matter. *Chem. Geol.* **2015**, *417*, 32–43 DOI: 10.1016/j.chemgeo.2015.09.012.
(60) Cherukumilli, K.; Delaire, C.; Amrose, S.; Gadgil, A. J. Factors Governing the Performance of Bauxite for Fluoride Remediation of Groundwater. *Environ. Sci. Technol.* **2017**, *51* (4), 2321–2328 DOI: 10.1021/acs.est.6b04601.
(61) Das, N.; Pattanaik, P.; Das, R. Defluoridation of drinking water using activated titanium rich bauxite. *J. Colloid Interface Sci.* **2005**, *292*, 1–10 DOI: 10.1016/j.jcis.2005.06.045.
(62) Ayoob, S.; Gupta, A. K. Fluoride in Drinking Water: A Review on the Status and Stress Effects. *Crit. Rev. Environ. Sci. Technol.* **2006**, *36* (6), 433–487 DOI: 10.1080/10643380600678112.
(63) Central Groundwater Board Ministry of Water Resources Government of India. *Ground water quality in shallow aquifers of India*; Faridabad, 2010.
(64) Atasoy, A. D.; Yesilnacar, M. I.; Sahin, M. O. Removal of fluoride from contaminated ground water using raw and modified bauxite. *Bull. Environ. Contam. Toxicol.* **2013**, *91* (5), 595–599 DOI: 10.1007/s00128-013-1099-z.
(65) Thakre, D.; Rayalu, S.; Kawade, R.; Meshram, S.; Subrt, J.; Labhsetwar, N. Magnesium incorporated bentonite clay for defluoridation of drinking water. *J. Hazard. Mater.* **2010**, *180* (1–3), 122–130 DOI: 10.1016/j.jhazmat.2010.04.001.
(66) US-EPA. Drinking Water Contaminants – Standards and Regulations https://www.epa.gov/dwstandardsregulations (accessed Mar 18, 2017).
(67) Fluorosis Research & Rural Development Foundation (FR&RDF). Districts Endemic for Fluorosis http://www.fluorideandfluorosis.com/fluorosis/districts.html (accessed Dec 4, 2017).
(68) Singh, A.; Chakraborty, S.; Roy, T. K. Vilage Size in India. *Asian Popul. Stud.* **2008**, *4* (2), 111–134 DOI: 10.1080/17441730802246630.
(69) The Registrar General and Census Commissioner of India. India State Census http://www.census2011.co.in/states.php.
(70) Gadgil, A. J.; Roy, J. *IUSSTF project final report*; 2017.
(71) Amrose, S. E.; Bandaru, S. R. S.; Delaire, C.; van Genuchten, C. M.; Dutta, A.; DebSarkar, A.; Orr, C.; Roy, J.; Das, A.; Gadgil, A. J. Electro-chemical arsenic

remediation: Field trials in West Bengal. *Sci. Total Environ.* **2014**, *488–489* (1), 539–546 DOI: 10.1016/j.scitotenv.2013.11.074.
(72) Sajidu; I, S. M.; Masamba; L, W. R.; Thole; B; Mwatseteza; F, J. Groundwater fluoride levels in villages of Southern Malawi and removal studies using bauxite. *Int. J. Phys. Sci.* **2008**, *3* (1), 1–11.
(73) Baranyai, V. Z.; Kristály, F.; Szűcs, I. Influence of grain and crystallite size on the gibbsite to boehmite thermal transformation. *Stud. Univ. Babeș-Bolyai. Chem.* **2015**, *60* (2), 27–44.
(74) Ayoob, S.; Gupta, A. K.; Bhakat, P. B.; Bhat, V. T. Investigations on the kinetics and mechanisms of sorptive removal of fluoride from water using alumina cement granules. *Chem. Eng. J.* **2008**, *140* (1–3), 6–14 DOI: 10.1016/j.cej.2007.08.029.
(75) Peryea, F.J., Kittrick, J. A. Relative solubilities of corundum, gibbsite, boehmite, and diaspore at standard state conditions. An addendum. *Clays Clay Miner.* **1988**, *36* (5), 391–396 DOI: 10.1346/CCMN.1989.0370611.
(76) Valeev, D. V.; Mansurova, E. R.; Bychinskii, V. A.; Chudnenko, K. V. Extraction of Alumina from high-silica bauxite by hydrochloric acid leaching using preliminary roasting method. *IOP Conf. Ser. Mater. Sci. Eng.* **2016**, *110* (1), 1–6 DOI: 10.1088/1757-899X/110/1/012049.
(77) Nasrabadi, T.; Ruegner, H.; Sirdari, Z. Z.; Schwientek, M.; Grathwohl, P. Using total suspended solids (TSS) and turbidity as proxies for evaluation of metal transport in river water. *Appl. Geochemistry* **2016**, *68*, 1–9 DOI: 10.1016/j.apgeochem.2016.03.003.
(78) Hannouche, A.; Ghassan, C.; Ruban, G.¨el; Tassin, B.; Lemaire, B.; Joannis, C. Relationship between turbidity and total suspended solids concentration within a combined sewer system. *Water Sci. Technol.* **2011**, *64* (12), 2445–2452.
(79) Rügner, H.; Schwientek, M.; Beckingham, B.; Kuch, B.; Grathwohl, P. Turbidity as a proxy for total suspended solids (TSS) and particle facilitated pollutant transport in catchments. *Environ. Earth Sci.* **2013**, *69* (2), 373–380 DOI: 10.1007/s12665-013-2307-1.
(80) Najm, I.; Snoeyink, V.; Suidan, M.; Lee, C.; Richard, Y.; Najm, N. I.; Snoeyink, L. V.; Suidan, T. M.; Lee, H. C.; Richard, Y. Effect of Particle Size and Background Natural Organics on the Adsorption Efficiency of PAC. *Am. Water Work. Assoc.* **1990**, *82* (1), 65–72.
(81) Suneetha, M.; Sundar, B. S.; Ravindhranath, K. Removal of fluoride from polluted waters using active carbon derived from barks of Vitex negundo plant. *J. Anal. Sci. Technol.* **2015**, *6* (15) DOI: 10.1186/s40543-014-0042-1.
(82) Schoeman, J. J.; MacLeod, H. Effect of Particle Size and Interfering Ions on Fluoride Removal By Activated Alumina. *Water SA* **1987**, *13* (4), 229–234.
(83) Muller, K. (EAWAG). *CDN's Experiences in Producing Bone Char*; 2007.
(84) Yean, S.; Cong, L.; Yavuz, T. C.; Tomson, M. B. Effect of Magnetite Particle Size on Adsorption and Desorption of Arsenite and Arsenate. *J. Mater. Res. 2* **2005**, *20* (12), 3255–3264 DOI: 10.1557/jmr.2005.0403.
(85) Qiu, H.; Lv, L.; Pan, B.; Zhang, Q. Q.; Zhang, W.; Zhang, Q. Q. Critical review in adsorption kinetic models. *J. Zhejiang Univ. Sci. A* **2009**, *10* (5), 716–724 DOI: 10.1631/jzus.A0820524.
(86) L. Candela, D. D. P.; Candela, L.; Perlmutter, D. D. Kinetics of Boehmite Formation by Thermal Decomposition of Gibbsite. *Ind. Eng. Chem. Res* **1992**, *31* (3), 694–700 DOI: 10.1021/ie00003a007.

(87) Ojo, O. I.; Otieno, F. A. O.; Ochieng, G. M. Groundwater: Characteristics, qualities, pollutions and treatments: An overview. *Int. J. Water Resour. Environ. Eng.* **2012**, *4* (6), 162–170 DOI: 10.5897/IJWREE12.038.
(88) MacDonald, L. H. An Integrated Approach to Address Endemic Fluorosis in Jharkhand, India. *J. Water Resour. Prot.* **2011**, *3* (7), 457–472 DOI: 10.4236/jwarp.2011.37056.
(89) Churchill, H. V. Occurrence of fluorides in some waters of the United States. *Ind. Eng. Chem. Res* **1931**, *23*, 996–998.
(90) Smith, M. C. and; Lantz, E. The Cause Of Mottled Enamel, A Defect Of Human Teeth. *Tech. Bull. Univ. Arizona* **1931**, *32*, 253–282.
(91) Dean, H. T. Classification of mottled enamel diagnosis. *J. Am. Dent. Assoc.* **1934**, *21*, 1421–1426.
(92) Shortt, H. E.; Mcrobert, G. R.; Barnard, T. .; Nayar, A. S. Endemic Fluorosis in the Madras Presidency. *Indian J. Med. Res.* **1937**, *25* (2), 533–564.
(93) Khairnar, M. R.; Dodamani, A. S.; Jadhav, H. C.; Naik, R. G.; Deshmukh, M. A. Mitigation of Fluorosis - A Review. *J. Clin. DIAGNOSTIC Res.* **2015**, *9* (6), 5–9 DOI: 10.7860/JCDR/2015/13261.6085.
(94) Dzombak, D. A.; Morel, F. M. M. *Surface Complexation Modeling: Hydrous Ferric Oxide*; John Wiley & Sons, Inc., 1990.
(95) Huang, C.-P.; Stumm, W. Specific adsorption of cations on hydrous γ-Al2O3. *J. Colloid Interface Sci.* **1973**, *43* (2), 409–420 DOI: 10.1016/0021-9797(73)90387-1.
(96) Stumm, W.; Huang, C. P.; Jenkins, S. R. Specific chemical interaction affecting the stability of dispersed systems. *Croat. Chem. Acta* **1970**, *42*, 223–245.
(97) Davis, J. A.; Coston, J. A.; Kent, D. B.; Fuller, C. C. Application of the Surface Complexation Concept to Complex Mineral Assemblages. *Environ. Sci. Technol.* **1998**, *32* (19), 2820–2828 DOI: 10.1021/es980312q.
(98) Schroeder, S. L. M.; Weiher, N. F K-edge X-ray absorption near-edge structure (XANES) of AlF3 polymorphs: combining ab initio calculations with Walsh correlation diagrams. *Phys. Chem. Chem. Phys.* **2006**, *8* (15), 1807–1811 DOI: 10.1039/b518124k.
(99) Shimizu, K.; Kato, Y.; Yoshida, H.; Satsuma, A.; Hattori, T.; Yoshida, T. Al K-edge XANES study for the quantification of aluminium coordinations in alumina. *Chem. Commun.* **1999**, No. 17, 1681–1682 DOI: 10.1039/a904286e.
(100) Ildefonse, P.; Cabaret, D.; Sainctavit, P.; Calas, G.; Flank, A.-M. a. M.; Lagarde, P.; . Aluminium X-ray absorption near edge structure in model compounds and Earth's surface minerals. *Phys. Chem. Miner.* **1998**, *25* (2), 112–121 DOI: 10.1007/s002690050093.
(101) Martinez, E. J.; Girardet, J.-L.; Morat, C. Multinuclear NMR Study of Fluoroaluminate Complexes in Aqueous Solution. *Inorg. Chem.* **1996**, *35* (3), 706–710 DOI: 10.1021/ic9507575.
(102) Hay, M. B.; Myneni, S. C. B. X-ray absorption spectroscopy of aqueous aluminum-organic complexes. *J. Phys. Chem. A* **2010**, *114* (20), 6138–6148 DOI: 10.1021/jp909656q.
(103) Prasad, P. V. V. V.; Das, C.; Golder, A. K. Reduction of Cr(VI) to Cr(III) and removal of total chromium from wastewater using scrap iron in the form of zerovalent iron(ZVI): Batch and column studies. *Can. J. Chem. Eng.* **2011**, *89* (6), 1575–1582 DOI: 10.1002/cjce.20590.
(104) Chowdhury, Z. K.; Summers, R. S.; Westerhoff, G. P.; Leto, B. J.; Nowack, K. O.; Corwin, C. J. Activated Carbon Adsorption Technologies. In *Activated Carbon: Solutions*

for Improving Water Quality; Passantino, L. B., Ed.; American Water Works Association, 2013; pp 3–13.
(105) Devi, R. R.; Umlong, I. M.; Raul, P. K.; Das, B.; Banerjee, S.; Singh, L. Defluoridation of water using nano-magnesium oxide. *J. Exp. Nanosci.* **2014**, *9* (5), 512–524 DOI: 10.1080/17458080.2012.675522.
(106) Rai, S.; Lataye, D. H.; Chaddha, M. J.; Mishra, R. S.; Mahendiran, P.; Mukhopadhyay, J.; Yoo, C.; Wasewar, K. L. Methodology, An Alternative to Clay in Building Materials: Red Mud Sintering Using Fly Ash via Taguchi's. *Adv. Mater. Sci. Eng.* **2013**, *2013* DOI: http://dx.doi.org/10.1155/2013/757923.
(107) Schwarz, M.; Lalík, V. Possibilities of Exploitation of Bauxite Residue from Alumina Production,. In *From Extraction to Forming*; Nusheh, M., Ed.; InTech, 2012; pp 1–22.
(108) Cooling, D. A red mud remedy. *ECOS Magazine*. 2005, p 127.
(109) Ritter, S. K. Making The Most Of Red Mud. *Chemical & Engineering News (ACS)*. July 2014, pp 33–35.
(110) Bellman, E. Epic Fail: Tech Tricks Are No Fix for Developing-World Problems https://blogs.wsj.com/indiarealtime/2015/09/04/epic-fail-tech-tricks-are-no-fix-for-developing-world-problems/ (accessed Apr 7, 2017).
(111) Warschauer, M.; Ames, M. Can One Laptop Per Child Save the World's Poor. *J. Int. Aff.* **2010**, *64* (1), 33–51.
(112) Pulford, J.; Hetzel, M. W.; Bryant, M.; Siba, P. M.; Mueller, I. Reported reasons for not using a mosquito net when one is available: a review of the published literature. *Malar. J.* **2011**, *10* (83) DOI: 10.1186/1475-2875-10-83.
(113) Borland, R. Radical Plumbers and PlayPumps – Objects in development, Trinity College, Dublin, 2011.
(114) LifeStraw by Vestergaard http://www.vestergaard.com/lifestraw-personal (accessed Apr 7, 2017).
(115) Elsanousi, S.; Abdelrahman, S.; Elshiekh, I.; Elhadi, M.; Mohamadani, A.; Habour, A.; ElAmin, S. E.; Elnoury, A.; Ahmed, E. A.; Hunter, P. R. A study of the use and impacts of LifeStraw in a settlement camp in southern Gezira, Sudan. *J. Water Health* **2009**, *7* (3), 478–483 DOI: 10.2166/wh.2009.050.
(116) Boisson, S.; Kiyombo, M.; Sthreshley, L.; Tumba, S.; Makambo, J.; Clasen, T. Field Assessment of a Novel Household-Based Water Filtration Device: A Randomised, Placebo-Controlled Trial in the Democratic Republic of Congo. *PLoS One* **2010**, *5* (9), e12613 DOI: 10.1371/journal.pone.0012613.
(117) Amini, M.; Mueller, K.; Abbaspour, K. C.; Rosenberg, T.; Afyuni, M.; Møller, K. N.; Sarr, M.; Johnson, C. A. Statistical Modeling of Global Geogenic Fluoride Contamination in Groundwaters. *Environ. Sci. Technol.* **2008**, *42* (10), 3662–3668 DOI: 10.1021/es071958y.
(118) World Rural Population (% Total Population) http://data.worldbank.org/indicator/SP.RUR.TOTL.ZS (accessed May 6, 2017).
(119) Alfredo, K. A. Drinking Water Treatment by Alum Coagulation: Competition Among Fluoride, Natural Organic Matter, and Aluminum, The University of Texas Austin, 2012.
(120) Edmunds, M.; Smedley, P. Chapter 12: Fluoride in Natural Waters; Academic Press, 2005; pp 301–329.
(121) Hunt, J. R. *Partial Lecture Notes for Environmental Physical-Chemical Processes (Civil and Environmental Engineering 211A)*; Berkeley, CA, 2013.